

**STRUCTURAL DETERMINATION OF TRICLOSAN DERIVATIVES AS  
INHIBITORS OF *Plasmodium falciparum* ENOYL REDUCTASE (PfENR)**

A Thesis

by

EDINSON LUCUMI MORENO

Submitted to the Office of Graduate Studies of  
Texas A&M University  
in partial fulfillment of the requirements for the degree of

MASTER OF SCIENCE

December 2005

Major Subject: Biochemistry

**STRUCTURAL DETERMINATION OF TRICLOSAN DERIVATIVES AS  
INHIBITORS OF *Plasmodium falciparum* ENOYL REDUCTASE (PfENR)**

A Thesis

by

EDINSON LUCUMI MORENO

Submitted to the Office of Graduate Studies of  
Texas A&M University  
in partial fulfillment of the requirements for the degree of

MASTER OF SCIENCE

Approved by

Chair of Committee,  
Committee Members,

Head of Department,

James C. Sacchettini  
James C. Hu  
J. Martin Scholtz  
David P. Giedroc  
Gregory Reinhart

December 2005

Major Subject: Biochemistry

**ABSTRACT**

Structural Determination of Triclosan Derivatives as Inhibitors of *Plasmodium falciparum* Enoyl Reductase (PfENR). (December 2005)

Edinson Lucumi Moreno, B.S., Universidad Del Valle (Colombia);

M.S., Universidad de Barcelona (Spain)

Chair of Advisory Committee: Dr. James C. Sacchettini

Malaria is a disease that causes more than 1 million deaths per year world wide and more than 400 million clinical cases. Due to the acquired resistance of *Plasmodium falciparum* to the drugs used to control the infection, searching for new anti-malaria drugs is necessary in modern days. Recent studies have shown that the parasite synthesizes fatty acids using a fatty acid synthase type II (FAS-II) instead of a type-I fatty acid synthase (FAS-I) that is present in other eukaryotes. *Plasmodium falciparum* enoyl reductase (PfENR) is responsible for the last step of fatty acid biosynthesis in the parasite. This enzyme is located within the apicoplast, a plastid-like organelle that is responsible for several important metabolic pathways, including fatty acid biosynthesis. It is known that triclosan is an inhibitor of ENR in bacteria and we and others have shown that it is also effective against ENR in apicomplexan organisms such as *P. falciparum*. However triclosan cannot be used to treat malaria in humans because it has metabolic liability (glucoronidation) which limits its inhibitory potency. We have used X-ray

crystallography and a Structural Activity Relationship (SAR) strategy to design and co-crystallize a tertiary complex of PfENR with  $\text{NAD}^+$  and triclosan derivatives to improve their properties as drugs to treat malaria. More than five hundred triclosan derivatives were synthesized, and their *in vitro* and *in vivo* inhibitory activity evaluated. Furthermore, structural studies were made of their affinity to interact with residues in PfENR active sites, as well as with the cofactor  $\text{NAD}^+$ . A total of six PfENR- $\text{NAD}^+$ -triclosan analog/complexes structures were determined. Analogs which had replacements of chloride groups at position 5 of ring A and 4' of ring B were determined, allowing the structural analysis of the binding of these triclosan analogs to PfENR. In addition, the urea derivatives (modification at position 1) as well as phenylsulphonamides (modification at position 2') have shown to be more potent inhibitors than triclosan in the *in vivo* assay. The analysis of the inhibitory properties and the structure of these analogs bound to PfENR will provide novel compounds in the search for new anti-malarial drugs.

## **DEDICATION**

To my family

## ACKNOWLEDGMENTS

I express my thanks to Dr. Jim C. Sacchetti, Mack Kuo, the Medicines for Malaria Venture (MMV) and all the members of the Sacchetti Lab.

## TABLE OF CONTENTS

	Page
ABSTRACT .....	iii
DEDICATION .....	v
ACKNOWLEDGMENTS .....	vi
TABLE OF CONTENTS.....	vii
LIST OF FIGURES .....	ix
LIST OF TABLES.....	x
 CHAPTER	
I INTRODUCTION.....	1
1.1. General Description about Malaria.....	1
1.2. Malaria Transmission.....	4
1.3. The Vector Mosquito ( <i>Anopheles gambiae</i> ).....	6
1.4. The Parasite ( <i>P. falciparum</i> ).....	6
1.5. The Apicoplast.....	7
1.6. Fatty Acid Biosynthesis.....	8
1.7. <i>Plasmodium falciparum</i> enoyl Reductase (PfENR).....	16
1.8. Triclosan .....	19
1.9. Dose Response Curves of Enzyme Inhibition.....	21
II EXPERIMENTAL SECTION .....	24
2.1. Preliminary Studies.....	24
2.2. Synthesis of Triclosan Derivatives .....	27
2.3. <i>In Vivo</i> Whole Cell Evaluation .....	30
2.4. PfENR Expression and Purification.....	30
2.5. <i>In Vitro</i> PfENR Evaluation .....	31
2.6. Crystallization Condition.....	31
III STRUCTURAL ANALYSIS OF TRICLOSAN BINDING TO PfENR .....	33
3.1. Introduction.....	33
3.1.1. Mode of Binding of Triclosan to (PfENR).....	33
3.2. Results.....	37
3.2.1. Structural Determination of Triclosan Derivatives (Position 1).....	37

## CHAPTER

3.2.2 Structural Determination of Triclosan Derivatives (Linker (Ether) Position) .	44
3.2.3 Structural Determination of Triclosan Derivatives (Positions 2' and 4') .....	49
3.2.4 Structural Determination of Triclosan Derivatives (Position 5 and 4') .....	55
3.2.5 Structural Determination of Triclosan Derivatives in Every Position .....	72
3.2.6 Structural Determination of Miscellaneous Triclosan Derivatives.....	74
3.3 Discussion .....	78
IV CONCLUSIONS AND FUTURE WORK.....	87
REFERENCES .....	90
VITA.....	99



**LIST OF FIGURES**

	Page
Figure 1. Aminoacid Sequence of PfENR. ....	17
Figure 2. Structure of PfENR.....	18
Figure 3. Structure of Triclosan.....	19
Figure 4. Structures of Known PfENR Inhibitors.....	26
Figure 5. Structures of Possible Triclosan Analogs.....	29
Figure 6. PfENR Crystals, Space Group P4 <sub>3</sub> 2 <sub>1</sub> 2.....	32
Figure 7. X-Ray Structure of Triclosan Bound to PfENR.....	35
Figure 8. Fractional Velocities as Function of Inhibitor Concentration. ....	36
Figure 9. X-Ray Structure of (JPC-2136-A1) and (JPC-2137-A1) Bound to PfENR.....	60
Figure 10. X-Ray Structure of (JPC-2141-A1) Bound to PfENR. ....	63
Figure 11. X-Ray Structure of (JPC-2166-A1) Bound to PfENR. ....	65
Figure 12. X-Ray Structure of (JPC-2153-A1) Bound to PfENR. ....	67
Figure 13. X-Ray Structure of (JPC-2305-A1) Bound to PfENR. ....	71

**LIST OF TABLES**

	Page
Table 1. Triclosan Analogs at Position 1 ( $R_1$ ) .....	39
Table 2. Triclosan Analogs at Position 1 Urea Class ( $R_1$ ) .....	40
Table 3. Triclosan Analogs at Position 1H Substitution ( $R_1$ ) .....	42
Table 4. Triclosan Analogs at Linker Position ( $R_1$ and $R_2$ ) .....	46
Table 5. Triclosan Analogs at Linker Position (Linker Miscellaneous) .....	48
Table 6. Triclosan Analogs at Position 2' ( $R_2$ ) .....	50
Table 7. Triclosan Analogs at Position 2' ( $R_2$ ) and 4' ( $R_3$ ) .....	53
Table 8. Triclosan Analogs at Position 4' ( $R_3$ ) and 5 ( $R_4$ ) .....	56
Table 9. Triclosan Analogs at Position 5 ( $R_4$ ) .....	69
Table 10. Triclosan Analogs at All Positions .....	73
Table 11. Miscellaneous Triclosan Analogs .....	75

## CHAPTER I

### INTRODUCTION

#### 1.1. General Description about Malaria

Malaria is a parasitic disease transmitted by infected mosquitos of the genus *Anopheles*, and caused by parasites of the genus *Plasmodium*. It is an illness that has been part of human society since ancient times. For instance, it was common in the boggy realm surrounding the city of Rome in the times of the Roman Empire, acquiring its name from the Latin (mal-aria) that means “bad-air”; it was also known as the Roman fever.<sup>1</sup>

Even though malaria originated in Africa, it is nowadays a worldwide problem. Malaria is common in all tropical regions in the globe. This means that it affects many communities in the poorest countries of the developing world. For instance, in south Saharan countries, malaria in addition to HIV are generating an epidemic (there is a death from malaria worldwide every 30 seconds) that has plunged Africa in a health and economic crisis, because the fact that these countries are losing high percentage of their young population.<sup>1,2,3</sup>

The fight against malaria has led the scientific community worldwide to approach its control from different directions. For example, many scientists in different institutions and some pharmaceutical companies are researching the development of an effective vaccine against the parasite. However, due to the complexity of this disease, the degree of protection offered by these vaccines have shown to be very limited.<sup>3</sup>

---

This thesis follows the format of the Journal of Medicinal Chemistry.

Another strategy has been to focus on controlling the vector (mosquito of the genus *Anopheles*) responsible of malaria transmission: First, by creating physical barriers in the house such as bed nets impregnated with insecticide (pyrethroid emulsion) to avoid bites from the mosquito. Second, by spraying the inside of the walls and roof of the houses with a residual insecticide, and Third by controlling breeding water places where development of the larva mosquito take place. Even though people located in rural regions of countries where malaria is a health problem follow these methods to prevent the disease, high percentage of the population still get infected.<sup>4</sup>

The control of malaria using antimalarial drugs has mainly been focused in the use of quinine, an alkaloid found in the bark of plants of the genus *Cinchona* (used for more than three centuries, but now used only in severe *falciparum* malaria by reason of its side effects) and its derivatives chloroquine, mefloquine and more recently sulphadoxine-pyrimethamine. Chloroquine has been used since the 1940's, it has scant side effects and low cost, making possible its use by many rural communities in developing countries. Other drugs that have been used in the treatment of malaria are: Atebrin, proguanil, malarone, maloprim, fansidar, halofantrin, and artemisinin. However, these drugs have induced the emergence of new resistant strains of *Plasmodium*. Therefore, malaria control is day by day a more difficult challenge for the scientist researching this disease.<sup>1,2,4,5</sup>

As part of this fight against malaria, the determination of the genome sequence of *P. falciparum* generated the possibility to identify critical enzymes (drug targets) involved in various metabolic pathways within the parasite's metabolism. One of these new enzymes is the *P. falciparum* enoyl reductase (PfENR) which is involved in the last

step of fatty acid biosynthesis, a pathway essential for the survival of apicomplexan parasites.<sup>5,6,7,8</sup>

PfENR is located within the apicoplast, a recently discovered organelle in *P. falciparum* that has a bacterial origin, where several metabolic processes take place. The parasite uses for the biosynthesis of fatty acids a so called type II fatty acid biosynthetic pathway, in which several enzymes are responsible for different steps in the biosynthesis of these essential metabolites. This differs from type I fatty acid biosynthesis that takes place in other eukaryotic organisms, where one multi-functional enzyme complex is responsible for the process.<sup>8,9,10</sup>

One of the inhibitors of bacterial ENR is 5-chloro-2-(2,4-dichlorophenoxy) phenol (triclosan).<sup>11</sup> This is used as an antibacterial in hospital hygiene and cleaning products, among other applications.<sup>11,12,13</sup> Surolia and Surolia in 2001 found that triclosan inhibits *P. falciparum* ENR, making possible its evaluation as a potential inhibitor of this enzyme and its study as a potential candidate for the treatment of malaria.<sup>14</sup> However, the phenol group of triclosan has a metabolic liability (glucuronidation) making it susceptible to modification in human metabolism.<sup>10,15,16</sup> Our research has focused on the synthesis, *in vivo* (whole cell) and *in vitro* (enzyme) inhibitory evaluation, and structural elucidation of triclosan derivatives less prone to modifications that could act as inhibitors responsible of increasing the inhibitory potency of these new types of possible anti malarial drugs. The development of this project has been a joint effort among private industry (Jacobus Pharmaceutical Company) and several Universities (Department of Microbiology and Immunology at Albert Einstein College of Medicine, and the Department of Biochemistry and Biophysics at Texas A&M University).

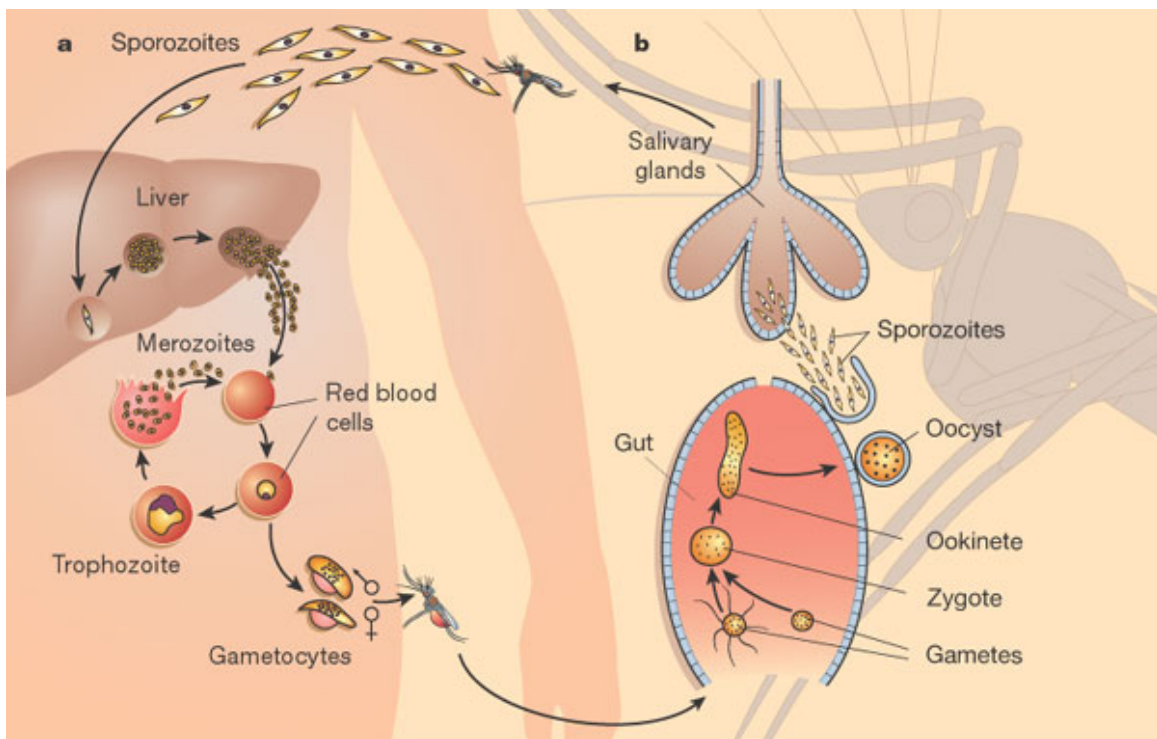
## 1.2. Malaria Transmission

The United Nations tried to eradicate malaria in the early 50's by reducing infecting vectors population feeding on humans, as well as making malaria prophylactic drugs available to anyone anywhere. However, in this century malaria still claims the lives of more than 2 million people per year and, there are 300-500 million clinical cases every year.<sup>2,4,5,17</sup>

Malaria is transmitted by the bite of the female *Anopheles* mosquitoes that has bitten an infected host (human).<sup>18</sup> The vector is carrying the sporozoites stage of the parasite (Scheme 1) which enters the bloodstream and localizes in the liver of the infected human. The division of these sporozoites produces the merozoites which are the stage of the parasite that infects red blood cells. These merozoites differentiate into special cells called gametocytes that are ingested by the mosquito. These cells then combine in the gut with other gametes (sperm and egg) to form a zygote that, in turn, after division, gives rise to the sporozoites which then migrate to the mosquito salivary glands to start the cycle over again (Scheme 1).<sup>13,19,20</sup>

After transmission, clinical manifestation of malaria depends upon immune state of the host and the degree of parasitemia. Children with no immunity endure serious manifestations while those with immunity have fewer symptoms regardless of massive parasitemia. There is more mortality of children under the age of 5 years than in adults due to malaria. The incubation period for *Plasmodium vivax* is 10-18 days, 11-16 days for *P.ovale* and *P.malariae* and 7-14 days for *P.falciparum*.<sup>20</sup>

Symptoms related with malaria infection are: Headache, nausea, general weakness, body ache, loss of appetite, and vomiting. Fever is one of the main symptoms of malaria; it is described as convulsive high fever with chills. Malaria produced by *P.falciparum* frequently renders with consecutive fever complications, which include cerebral malaria related with convulsion, delirium, altered consciousness and deep coma.<sup>20</sup>



### Scheme 1 Life Cycle of *P. falciparum*

Sporozoites enter the bloodstream of the infected host and then localize in the liver, where they divide and produce the merozoites that goes to infest the erythrocytes, gametocytes are produced from these merozoites to further be ingested by the mosquito and by combination with the other gametes form a zygote from which sporozoites are produced to allow the cycle to continue<sup>6</sup>.

### 1.3. The Vector Mosquito (*Anopheles gambiae*)

“There are around 3200 species of mosquitoes belonging to 42 genera, and only one genus, *Anopheles*, is able to transmit human malaria. The genus *Anopheles* contains around 430 known species of which approximately 70 are malaria vectors, but only 40 of these are thought to be of any major importance. *Anopheles* mosquitoes have an almost world wide distribution, although they typically are not found at altitudes above 2500m. During growth and metamorphosis, the mosquito passes through four distinct stages: egg, larva, pupa and adult. The immature stages are aquatic, depending on free water for their survival and development.”<sup>18</sup>

The genus is divided into six subgenera, four of which include disease vectors. Among the species of *Anopheles* is *A. gambiae* that predominates in humid areas, prefers feeding on humans resting indoors being a highly efficient malaria vector. *A. arabiensis* is found in savannah regions, readily bites humans, may rest indoors, often feeds on cattle and rats, and is the second most important vector in malaria transmission. Other species include *A. quadriannulatus*, *A. melas*, *A. merus*, and *A. bwambae*”.<sup>18</sup>

### 1.4. The Parasite (*P. falciparum*)

“Protozoa of the genus *Plasmodium* are responsible of causing malaria. The 120 or so species of *Plasmodium* are found in the blood of mammals, reptiles and birds, and are recognized taxonomically by the presence of two types of asexual division: schizogony, in the vertebrate host; and sporogony, in the insect vector. Within the



vertebrate host schizogony is found within erythrocytes (erythrocytic schizogony).<sup>18</sup> Two subgenera of the parasites are found in humans, *Laverania* and *Plasmodium*. The subgenera *Plasmodium* include the most pathogenic form of malaria *Plasmodium falciparum*, and the closely related *P. reichenowi*.<sup>18</sup> The subgenera *Laverania* include the remaining parasites of humans, namely *P. vivax*, *P. malarie* and *P. ovale*. Three malaria parasites are found exclusively in humans: *P. falciparum*, *P. vivax* and *P. ovale*.<sup>18</sup>

### 1.5. The Apicoplast

The apicoplast is an organelle similar to plastids in plants that contains a 35 kb circular genome that encodes components of a prokaryotic transcriptional and translation system. The apicoplast is surrounded by four membranes and contains its own genome, this being a characteristic cellular feature of apicomplexan parasites.<sup>8,9</sup>

Apicoplast functions include fatty acid and isoprenoid synthesis. Studies of plastid inhibitors and apicoplast mis-segregation mutants confirmed the essential requirement of this organelle for normal parasite development, indicating that inhibition or loss of apicoplast function resulted in parasite death accompanied by reinvasion of host cells.

The apicoplast localization of *de novo* fatty acid biosynthetic enzymes renders, by analogy with the plant plastid, the first argument for the endosymbiosis (algal cell which had previously incorporated a cyanobacterium) origin of the pathway.<sup>14,21,26</sup>

The multi-subunit type II fatty acid synthase (FAS II) found in bacteria and plant plastids is also present in the apicoplast of *Plasmodium* and *Toxoplasma*. Proteins involved in these pathways are often the products of nuclear genes that encode N-terminal signal and transit peptide sequences for apicoplast localization. On the other hand the *fas*

*I* gene, which encodes a multi-domain protein, the FAS I enzyme, found in the cytosol of animal cells has not been found in apicomplexan genomes.<sup>8-11,22-26</sup>

## 1.6. Fatty Acid Biosynthesis

Fatty acids are important metabolites for supplying precursors to make part of biological membranes as well as an essential mode of storage metabolic energy. Therefore, biosynthesis of fatty acids is a common process in biological systems.<sup>10,11,21,25</sup>

One of the most complex multifunctional polypeptide structures in animals is the fatty acid synthase. It is a single polypeptide that contains all the catalytic components responsible for the reactions that lead to the formation of, for example, palmitic acid from acetyl-CoA and malonyl-CoA. Formation of these products involve seven enzymatic reactions that were first studied in *E.coli* (where the reactions are catalyzed by independent enzymes)<sup>25-32</sup>

In some mycobacteria, higher eukaryotes, and yeast the biosynthetic enzymes are embodied into a large multifunctional polypeptide in which different reactions in the pathway are catalyzed by different domains of this elaborated enzyme. It is commonly referred to as type I fatty acid synthase (FAS-I), and the pathway is also called associated pathway. The fatty acid synthase found in yeast is a 2500 kDa  $\alpha_6 \beta_6$  multifunctional enzyme, while in animals  $\alpha_2$  is a 534 kDa multifunctional enzyme consisting of two very similar polypeptides chains.<sup>10,21,25-32</sup>

The fatty acid biosynthesis pathway is a cyclic process in which an acetyl primer originally linked as a thioester in acetyl-CoA experiences a series of decarboxylative condensations with seven malonyl moieties. Each condensation reaction generates a 3-

ketoacyl moiety that goes through the same three-step  $\beta$ -carbon reduction to create an entirely saturated acyl moiety two carbons longer than that in the previous cycle. Thus, after conclusion of seven cycles of elongation and reduction, the final product is the saturated C<sub>16</sub> fatty acid, palmitic acid.<sup>10,27</sup>

A dissociated pathway mainly found in bacteria, plants (chloroplast), algae plastids and recently discovered in apicomplexan parasites (*P. falciparum*) is responsible for fatty acid biosynthesis in steps performed by separate distinct enzymes. This pathway is referred to as fatty acid synthase II (FAS-II) system. The enzymes involved in this type II FAS in *E. coli* are:

ACP transacylase (FabD) responsible of producing malonyl-ACP from malonyl CoA and ACP,  $\beta$ -ketoacyl-ACP synthase III (FabH) that catalyzes the condensation of malonyl-ACP and acyl CoA (acetyl-CoA) forming a  $\beta$ -ketoacyl-ACP product,  $\beta$ -ketoacyl-ACP reductase (FabG) which reduces the  $\beta$ -ketoacyl-ACP to  $\beta$ -hydroxyacyl-ACP by the sequential action of  $\beta$ -hydroxyacyl-ACP dehydrase (FabA or FabZ) and enoyl-ACP reductase (FabI).

In *E. coli* ACP is a 10 kDa polypeptide and the elongation cycle to produce the  $\beta$ -ketoacyl-ACP product is catalyzed by two enzymes: acyl-malonyl-ACP ( $\beta$ -ketoacyl-ACP synthase I (FabB)) or  $\beta$ -ketoacyl-ACP synthase II (FabF) depending on the chain length of the acyl-ACP substrate. The product of FabF or FabB is then exposed to another round of reduction catalyzed by FabG, FabZ and FabI. In each cycle that the elongation takes place the acyl-ACP product is amplified by two carbons (Scheme 2).<sup>10,11,21,26,33</sup>

The general reaction for the conversion of the substrate crotonoyl CoA to butyryl CoA is shown in Scheme 3. ENR is the enzyme responsible of completing cycles of fatty acid elongation *in vivo*. ACP thioesters are utilized by the enzymes of fatty acid biosynthesis.<sup>34,35</sup> The enzymes responsible of fatty acid biosynthesis in *P. falciparum* are:  
*Acetyl-CoA Carboxylase*

The source of carbon units in FAS II system is derived from acetyl-CoA. In *P. falciparum* a pyruvate dehydrogenase complex is the source of acetyl CoA for fatty acid biosynthesis and it is localized within the apicoplast. In addition, acetyl CoA carboxylase (ACCase) form malonyl-CoA from acetyl CoA and bicarbonate that is required for FAS II. Interestingly, ACCase from *P. falciparum* is similar to a multi-domain ACCase found in the cytosol of plants. The maturation of *P. falciparum* in red blood cells can be reduced likely toward the inhibition of ACCase by the action of inhibitors like aryloxyphenoxypropionate (fops and dims) herbicides with IC<sub>50</sub> values of 100-200 μM.<sup>21,36-43</sup>

#### *Acyl Carrier Protein*

One of the fundamental enzymes involve in type II FAS is acyl carrier protein (ACP). The acyl intermediates are covalently attached to ACP through a thioester linkage in every phase of the pathway. PfACP is a protein of 137 amino acids encoded by the *pfacp* gene located in chromosome 2. This enzyme is thought to target the apicoplast. Participation of ACP in fatty acid biosynthesis depends on the addition of 4'-phosphopantetheine prosthetic group to ACP, which is responsible for the attachment of the acyl groups during fatty acid biosynthesis. The transfer of this prosthetic group from

coenzyme A to a conserved serine found in all ACP proteins is made by holo-ACP synthase (in *E.coli* it is called EcAcpS). On the other hand, the *P. falciparum* ACP synthase enzyme is 29% identical to EcAcpS and it is called PfAcpS, it may target the apicoplast. However this enzyme remains to be studied to open the possibility to be a good target for antimalarial drugs evaluation.<sup>21,44-46</sup>

#### *Malonyl-CoA ACP Transferase*

The first step to start the chain elongation in type II FAS is catalyzed by malonyl-CoA: ACP transacylase (MCAT), this enzyme is found in *P. falciparum* (PfMCAT). It is thought that this enzyme targets the apicoplast. However, there is a lack of relevant studies to confirm this. The catalytic domain of PfMCAT shares 28% sequence identity with EcFabD. Even though its crystal structure is not defined yet, it is hypothesized to expose an overall fold similar to that seen in the structure of its similar found in *E. coli* homolog. The active side residues are well conserved in PfMCAT and MCATs from different organisms.<sup>47-49</sup>

There have been several mutagenesis studies that revealed some non catalytic residues in the active side of MCAT and present in PfMCAT that are involved in maintaining the turnover rate of this enzyme, conferring substrate specificity for malonyl-CoA. Knowing these, structural and mechanistic characteristics of this enzyme together with rational design of inhibitors that target this enzyme can be accomplished, because MCATs and, particularly PfMCAT can be an interesting target to explore antimalarial drugs development, due to the essentiality of this enzyme for the survival of the parasite.<sup>49-51</sup>

### *$\beta$ -Ketoacyl-ACP Synthase III*

This enzyme catalyzes the second step of chain initiation and elongation in type II FAS, and the gene that encodes this enzyme (*pfkasIII*) was one of the first to be identified in *P. falciparum* genome project, indicating the presence of FAS II system in this organism. The enzyme responsible for this function in *E. coli* is EcFabH, its catalytic domain shares 35 % identity with PfKASIII being C-H and N common residues in these proteins active side. Some studies also have shown that PfKASIII catalyzes two reaction: acyl CoA:ACP trans acylase (ACAT) activity and  $\beta$ -ketoacyl-ACP synthase (KAS) activity useful for the implementation of PfKASIII inhibitory screen assay.<sup>52-54</sup>

Due to the particular function of this enzyme as a condensation enzyme there have been significant efforts to find inhibitors of this enzyme as antibacterial agents. For example, the use of cerulenin an inhibitor of KAS in type I and II FAS, being this disadvantageous to be used in humans. On the other hand, thiolactomycin inhibits *P. falciparum*, probably by binding to other condensing enzymes PfKASI/II also found in *P. falciparum* but not being characterized yet. Currently, thiolactomycin derivatives as well as indole analogs are the main scaffold used in high throughput screening for the design of drugs that target PfKASIII.<sup>21,55-57</sup>

### *$\beta$ -Ketoacyl-ACP Reductase*

This enzyme (PfKAR) catalyzes the NADPH dependent reduction of  $\beta$ -ketoacyl-ACP to  $\beta$ -hydroxyacyl-ACP product. There are no studies demonstrating the apicoplast localization of this protein (PfKAR). This enzyme belongs to the short-chain

dehydrogenase/reductase (SDR) family of enzymes, sharing 47% sequence identity with *E. coli* FabG (EcFabG) and has the typical catalytic triad motif S-Y-K. Additionally, KAR is found as a single isozyme in bacteria making it an ideal antibacterial drug target. However there are no reports of specific inhibitors of KAR in *P. falciparum*.<sup>21,58-64</sup>

### *$\beta$ -Hydroxyacyl-ACP Dehydratase*

This enzyme (PfHAD) is responsible of the dehydration of  $\beta$ -Hydroxyacyl-ACP to *trans*-2-acyl-ACP. The localization of this enzyme into the apicoplast is still a matter of study. However, it seems likely that 76 amino acids in the amino-terminal region comprise an apicoplast leader peptide, in addition to a 154 amino acid enzymatic domain that shares 21% identity with EcFabA and 42% sequence identity with EcFabZ. These two enzymes catalyze the dehydration of  $\beta$ -hydroxyacyl-ACP in *E. coli*, and EcFabA also catalyzes the isomerization of *trans*-2-acyl-ACP to *cis*-3-acyl-ACP. The determination of the crystal structure of EcFabA has been done with and without inhibitor bound to the enzyme, allowing the determination of an aspartic acid residue in the active side (glutamate in EcFabZ) that is likely to be important for the additional *trans/cis* isomerase activity of EcFabA. PfHAD lacks the presence of the aspartic acid residue; however, it has the glutamate present in EcFabZ, and considering its high sequence identity this indicates that PfHAD does not have isomerase activity and that it is a monofunctional dehydratase.<sup>65-68</sup>

PfHAD is currently the subject of inhibition studies. More than 400 compounds have been tested and their inhibitory activities have been shown to be less than 1 $\mu$ M and the IC<sub>50</sub> for *P. falciparum* around 100 $\mu$ M for some specific compounds. The structure of

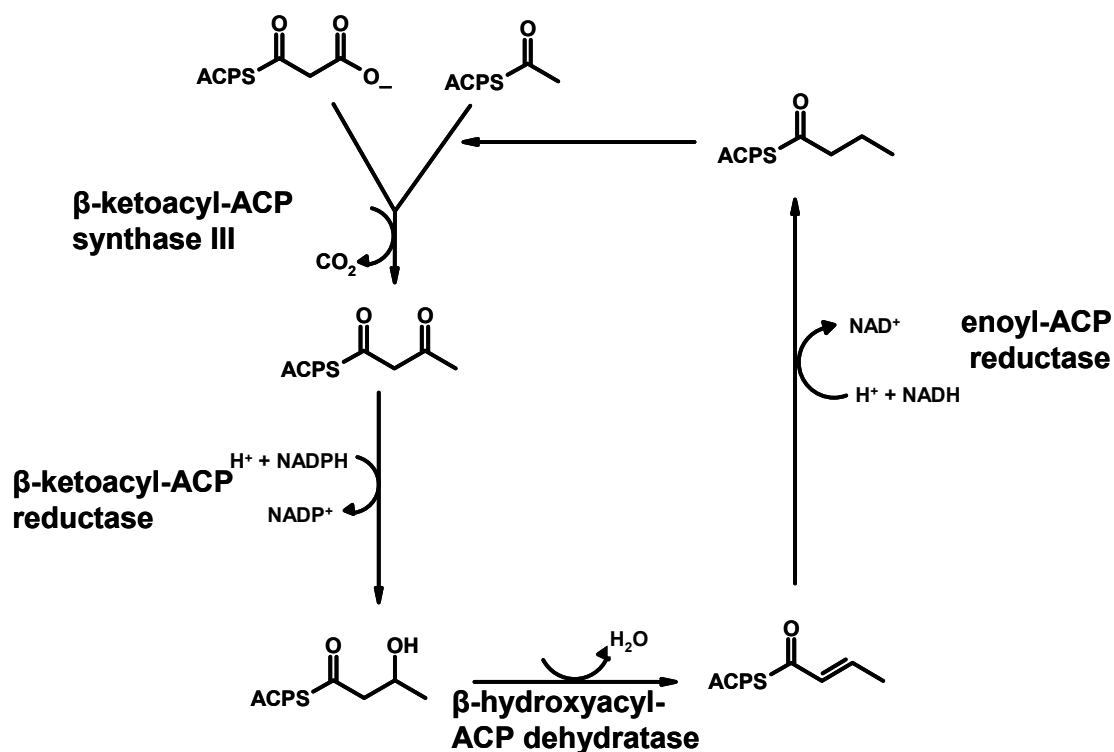
PfHAD awaits to be determined and it will offer a clearer understanding of the design of more potent inhibitors that target this important enzyme in *P. falciparum* fatty acid biosynthesis.<sup>21,69</sup>

### *Enoyl-ACP Reductase*

One of the most important enzymes in the FAS II system and responsible for the last step in the pathway, is enoyl-ACP reductase (ENR). This enzyme is responsible of the limiting step (conversion of *trans*-2-acyl-ACP to acyl-ACP) in fatty acid chain elongation cycle. In *P. falciparum* apicoplast localization of this enzyme still has to be determined, however there is a 77 amino acid sequence in the N-terminal region of PfENR that appears to target the apicoplast. PfENR shares 16% sequence identity with *E. coli* FabI, 47 % with its similar in the plant *Brassica napus*. Its homolog in *M. tuberculosis* is called InhA. Several studies have shown that PfENR uses NADH as a cofactor for the catalytic reaction in which crotonoyl-CoA is transformed into the product butyryl-CoA, being the detection of the depletion of NADH to NAD<sup>+</sup> followed at 340nm.  
11,70-72

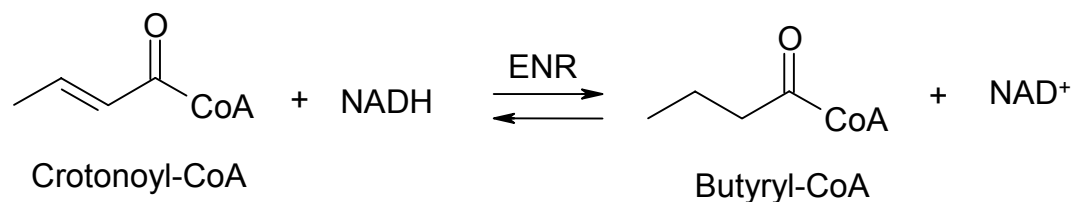
Recently, PfENR is the subject of the search for different types of inhibitors that target this enzyme. However, these studies are based on the previous knowledge of several bacterial ENR inhibitors such as diazaborine, isoniazid, ethionamide and triclosan, being this last one very effective inhibitor of PfENR. In addition, several studies report the x-ray crystal structure of PfENR-NAD<sup>+</sup>-triclosan tertiary complex, conferring structural information of triclosan mode of inhibition. However, use of triclosan in malaria medical treatment is restrained by its metabolic liability.<sup>21,73,74</sup>





### Scheme 2 Enzymes of Fatty Acid Elongation

Reactions in fatty acid biosynthesis are initiated by  $\beta$ -ketoacyl-ACP synthase III, which condense malonyl ACP with acetyl-CoA, followed by a reduction of the  $\beta$ -ketoester by  $\beta$ -ketoacyl-ACP reductase.  $\beta$ -hydroxyacyl-ACP dehydratase catalyzes the elimination reaction and the final conversion of trans-2-enoyl-ACP to acyl-ACP is catalyzed by the single NADH-dependent enoyl-ACP reductase (FabI) starting the elongation cycle over again<sup>11</sup>.



**Scheme 3** Reaction Catalyze by ENR

Reduction of crotonoyl-CoA into butyryl-CoA, wherein NADH acts as the coenzyme catalyzed by ENR<sup>16</sup>

**1.7. *Plasmodium falciparum* Enoyl Reductase (PfENR)**

The parasite responsible of producing malaria in humans (*Plasmodium falciparum*) synthesizes fatty acids using a type II pathway that is absent in humans. The enoyl reductase gene in this organism (*pfenr*) encodes an anticipated protein of 432 amino acids with an expected molecular weight of 49.8 kDa, enoyl acyl carrier protein reductase or *Plasmodium falciparum* enoyl reductase (Figure 1 and 2).<sup>10,11</sup>

PfENR is a tetramer, and is responsible for the final step in fatty acid elongation. This enzyme targets the apicoplast and is a validated antimicrobial drug target.<sup>11</sup> PfENR shows 47% sequence similarity to enoyl reductases from *Brassica napus* as is illustrated in Figure 1. The PfENR sequence differs from those other ENRs in that it contains a 43 amino-acid insert in a loop which in the ENRs from other species is known to experience appreciable conformational change on inhibitor (and likely substrate) binding (Figure 2) This enzyme also has a particular low complexity region between residues 325-367 (underline red region in Figure 1) enriched in polar residues like asparagines, lysine glutamine and serine. Even though it has been found that this insertion have been reported in other *P. falciparum* enzymes, they have minimal impact on the enzyme functionality<sup>11</sup>

As it is described in Figure 2 each subunit of PfENR is composed of seven  $\beta$ -strands ( $\beta$ 1-  $\beta$ 7) that form a parallel  $\beta$ -sheet and nine  $\alpha$  helices ( $\alpha$ 1 –  $\alpha$ 9) that are connected to the  $\beta$ -strands by a number of loops of varying length. The parallel  $\beta$ -sheet is bordered by helices  $\alpha$ 1,  $\alpha$ 2,  $\alpha$ 4,  $\alpha$ 5,  $\alpha$ 6, and  $\alpha$ 9, with  $\alpha$ 3 arranged along the top of  $\alpha$ 2 and  $\alpha$ 4. Helix  $\alpha$ 8 is located at the C termini of strands  $\beta$ 6 and  $\beta$ 7. The loop regions between  $\alpha$ 2-  $\beta$ 3,  $\beta$ 3 -  $\alpha$ 3-  $\alpha$ 4, and  $\beta$ 4 -  $\alpha$ 5 of PfENR are longer due to insertions in the sequence, and helix  $\alpha$ 2 was shifted away from the protein, toward the solvent, relative to the bacterial ENRs.<sup>11</sup> (Figure 2).

```

PbENR 1 MNKE-----NYWKNKILR-----KKKNE-----NLRINRVESNQDKID
pfenr 1 MNKISQRLLFLFLHFYTIVCFIQNNTQKTFHNVLQNEQIRGKEKAFYRKEKRENIFIGNKMKH--LNNMNNTHNNHYMEKEEQDASNIN
pvenr 1 MHVRRVQLATLLLYIASVSAMLRSAKLG-GGQPKWEIER-----RGNsREMqFITSKAIKGVAHKRKSQHSSPAHEMVSSEQSGQAE
bnapus 1 -----SESSSEKASSGGLP
ecoli 1 -----G
mtb 1 -----MTG

PbENR 35 NIKKNENENEICPIAGVGDsNGYWGIAKELSKRNKVKVIFGVWPPVYNIFIKNLESgKfDKDMIINNDNSKRMQILDVLPDAGFDNYD
pfenr 89 KIKEENKNE-DICPIAGIGDTNGYWGIAKELSKRNKVKIIFGVWPPVYNIFMKNYKNGKFDNDMIIDKD--KMMNILDMLPPDASFDTAN
pvenr 83 GINGKGEPLGDICPIAGVGDtNGYWGIAKELSKRNKVKIILGVWPPVYNIFMKNLQSGKFPDSDMIIGEG--KkMELLDILPFDAAPDSAS
bnapus 14 -IDLKGRK-----AFIAGIADdNGYGWAVAKSLAAAGAEILVGTWVPALNIFPETSLSRRGKFPDQSRVLPDG--SLMEIKKVVYPLDAVPDNP
ecoli 2 FLSGKR-----ILVTGVASKLSIAYGIAQAMHREGAEIAP-----TYQNDKLGK-----RVEFPAAQLGSDIVLQC--
mtb 4 LLDGKR-----ILVSGIITDSSIAEHIARVAQEQAQLVLTG-----FDRLR-----LIQRITDRLPKAKAPL----

PbENR 125 DIDEDETKNNKRYNNLKNYSIEEVANLIYNKYGKISMLVHSLANGREVQKSLDTSRDGYLDAISKSSYSLSLCKHFCKFMNSGGSVVSL
pfenr 176 DIDEETKNNKRYNMLQNYTIEDVANLIHQKYGKINMLVHSLANAKEVQKDLLNTRKGYLDALSKSSYSLSLCKYFVNMKFPQSSIISL
pvenr 171 DVDEETKNNKRYASLDSYSIEEVANLVYKKYGKINMLVHSLANGREVERSLLETSGGYLDALSKSSYSLSLALCKHFCKIMHPQSSVISL
bnapus 97 DVPEdVKANKRYAGSSNWTVQEAAEcVRQDFGSDILVHSLANGPEVSKPLETEsRKGYLAASASSYsFVSLLSHFIPIMNPPGGASISL
ecoli 63 DVAEDASIDTMFAELG-----KVNPKEDGFVHSIGFAPGQDLGDGYVNAVTRREGKIAHDISsYsFVAMAKACRSMLNPPGSALLTL
mtb 61 -LELDVQNEEHLASLAGRVTEAIG--AGNKLDGVVHsIGFMPQTGMGINPFPDAPYADVSKGIHISAYsYASMAKALLPIMNPPGGSIVGM

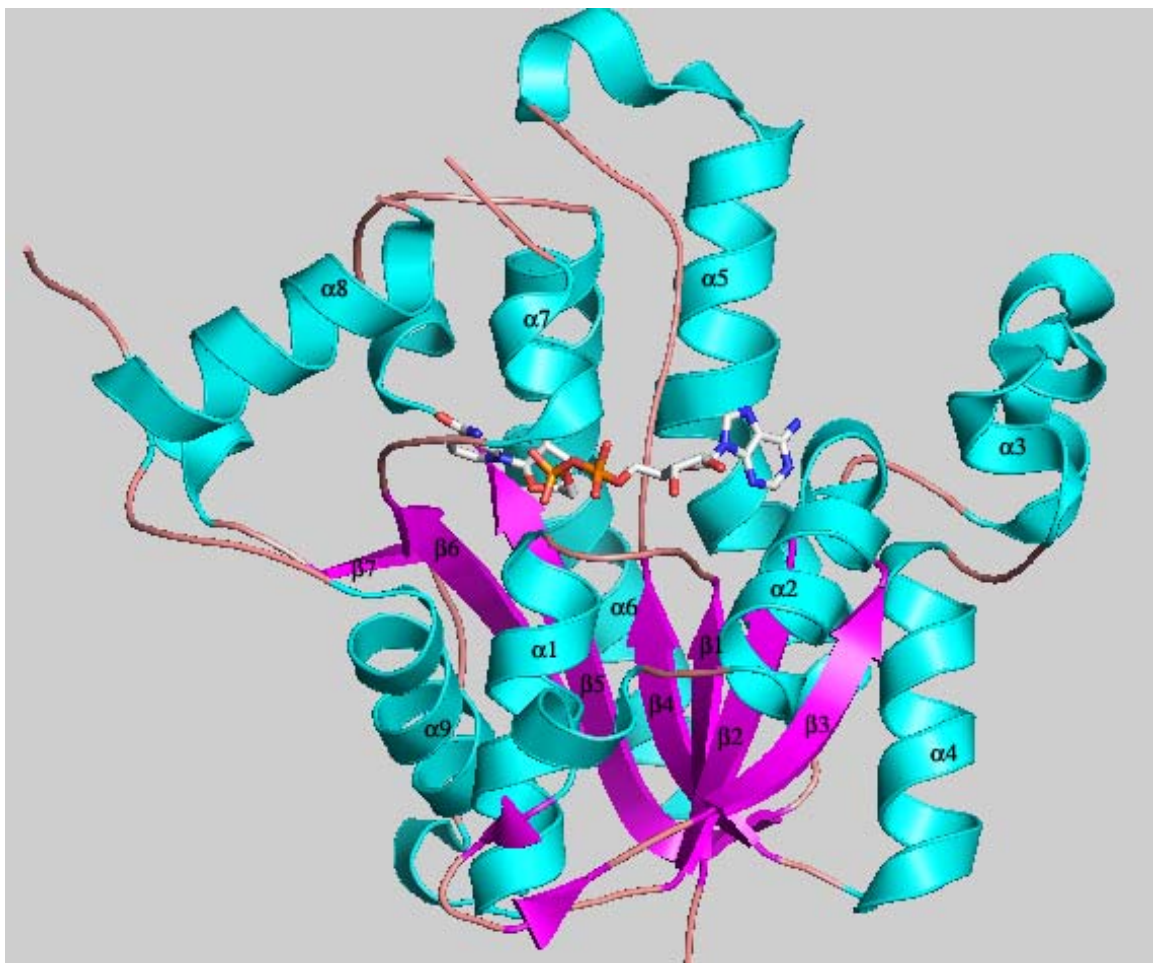
PbENR 215 TYQASQKVVFPQGGGSSAKAALESdTRVLAyHLGRNYNIRINTISAGPLKSRAATAINKFNNNQKNN-----MNSsGET
pfenr 266 TYHASQKVVFPYGGGSSAKAALESdTRVLAyHLGRNYNIRINTISAGPLKSRAATAINKLNNTYENNTNQKNRNSHDVHNIMNNSGEK
pvenr 261 SYIASQKVVFPYGGGSSAKAALESdTRVLAyHLGRKHKIRVNTISAGPLKSRAATAIKKATPQSGGN-----EGEK
bnapus 187 TYIASERIIPGYGGGSSAKAALESdTRVLAyEAGRKQNIrVNTISAGPLGSRAAKAIG-----
ecoli 144 SYLSAERAIPNYN-VMGLAKASLEANVRMANAMGPE-GVRVNAISAGPIRTLAASGIKD-----
mtb 148 FDFP-SRAMPAYN-WMTVAKSALESVNRFPVAREAG-KYGVRSNLVAAGPIRTLAASATVGGALGEEAG-----

PbENR 290 DK-----QNYsFIDYAI DYSEKYAPLKKLL-STDVGSVASPFLLSKESsAVTgQTiYVDNGLNIMfGPDD--LFQSSDS
pfenr 356 EEKNSASQNYTFIDYAI EYSEKYAPLRQKLL-STDIGVASPFLLSRESRAITGQTiYVDNGLNIMfLPDD--IYRNESE
pvenr 333 -----KNLAFIDYAI DYSEKYAPLQKLL-STDVGAVAAPFLLSKESRAVtGQTiYVDNGLNIMfGPDD--LFQGGAA
bnapus 246 -----FIDTMIEYSYNNAPIQKTLT-ADEVGNAAAPLVSPLASAITGATiYVDNGLNSMGVALDSPVFKDLDK
ecoli 202 -----FRKMLAHCEAVTPIERTVT-IEDVGNsAAFPcSDLSAGISGEVHVHVGgFPIAAMNLELk-----
mtb 213 -----AQIQLLEEgWDQRAPIGWNNMDATFVAKTVCALLSDWLPATTGDILYAGGGHARTQL-----

```

**Figure 1.** Aminoacid Sequence of PfENR.

Sequence alignment representation of PfENR aligned with sequences of homologues ENR's from *Plasmodium bergeri* (pbENR), *Plasmodium vivax* (pvenr) *Brassica napus* (bnapus), *Escherichia coli* (ecoli), and *Mycobacterium tuberculosis* (mtb). Green (complete conserved residues) yellow (two or more highly conserved residues) grey (at least one similar amino acid residue), the catalytic important residues are marked by (\*) and the low complexity region by the red line.<sup>11</sup>

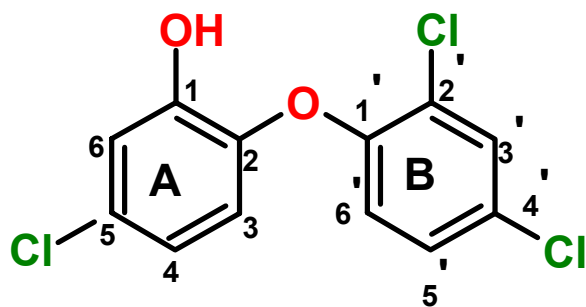


**Figure 2.**Structure of PfENR.

Representation of PfENR monomer with NADH bound at the active site, it is composed of seven  $\beta$ -strands and nine  $\alpha$  helices.

### 1.8. Triclosan

5-chloro-2-(2',4'-dichlorophenoxy) phenol (triclosan) (Figure 3 ) is a chemical that has been used since the 60's as an antibacterial and an antifungal agent, it was invented by Ciba more than 40 years ago. Since then, it has been incorporated in many common use products for humans such as, soaps, toothpastes, cosmetics, toys etc.<sup>75</sup> It is suggested that triclosan blocks lipid biosynthesis by specifically inhibiting the *fabI* gene product of *E. coli*, the InhA product of *M. smegmatis*, and the enzyme enoyl-acyl carrier protein reductase (ENR) by mimicking its natural substrate.<sup>12</sup> *E. coli* enoyl reductase is also known to be inhibited by the antibacterial diazaborines, and the enoyl reductase of *mycobacterium* is a target of the antitubercular drug isoniazid.<sup>76-90,91</sup>



**Figure 3.**Structure of Triclosan.

Structure of triclosan specifying the location of each possible substitution in the molecule, the hydroxyl group (red) at ring A, the chloride groups at position 2',4' and 5 (green) as well as the ether group at the linker position (red)

There have been limited studies of triclosan metabolism. As a hydroxylated compound, it should be expected that glucuronidation and sulfonation would be the main pathways of triclosan metabolism.<sup>10,77</sup> One study showed that triclosan was excreted primarily as the glucuronide following application of a 1% formulation to guinea pig or rat skin. Another study showed that topically applied triclosan formed sulfate and glucuronide conjugates in human as well as rat skin.<sup>10,77,80-86</sup> The human hepatic biotransformation of triclosan has not been reported in the open literature. There have been no studies of the possible interactions of triclosan with Type II fatty acid biosynthesis enzymes.<sup>77</sup> Wang *et al*<sup>77</sup> reported that triclosan was metabolized to glucuronide or sulfate conjugates in the presence of human liver microsomes or cytosol, respectively. Exposure to concentrations of triclosan higher than 20  $\mu\text{M}$  should have resulted in glucuronidation being the predominant pathway in the liver.<sup>77,82,83</sup>

On the other hand, several studies report triclosan resistance in *E.coli*, being this the same point mutation (A217V) that affects the affinity of triclosan to PfENR. In addition, triclosan presents poor bioavailability indicating a potential limitation in the use of this compound in the field. Recent research suggested the use of arginine oligomers to overcome this problem. In this study triclosan was attached to octaarginine via a hydrolysable ester linkage, proving that triclosan modified in this manner has *in vitro* therapeutic activity.<sup>10, 78,79,91</sup>

### 1.9. Dose Response Curves of Enzyme Inhibition

Biological assays are defined as tools to determine a property of a specific system of study. It is done by measuring a specific signal as a function of the concentration of some exogenous compound. The results of these types of measurements are presented as plots of the signal obtained as a function of the concentration of the exogenous substance. These graphs are referred to as dose response plots; the representation of the change in signal with change in concentration of substance is known as a dose response curve. The resulting plots have the form of a Langmuir isotherm; they can be used to follow protein-ligand binding equilibrium to further track the inhibitory effect of a particular compound on the initial velocity of an enzymatic reaction at an adjusted concentration of substrate.<sup>87</sup>

The  $IC_{50}$  value is defined as the concentration of inhibitor essential to achieve a half-maximal level of inhibition. Thus the equation that represents the effect of the inhibitor concentration on the velocity of the reaction is associated to the Langmuir Isotherm equation as follows:

**Equation 1**

$$\frac{V_i}{V_0} = \frac{1}{1 + \frac{[I]}{IC_{50}}}$$

Where:

$V_i$  is defined as the initial velocity in the presence of inhibitor at concentration  $[I]$

$V_0$  is defined as the initial velocity in the absence of inhibitor

$V_i/V_o$  is defined as the fractional net effect of the inhibitor on enzyme activity.

The real term to define the effectiveness of a compound is the dissociation constant of that compound for the enzyme. However,  $V_i/V_o$  gives an acceptable estimation of the inhibitory activity of the compound being studied.<sup>87</sup>

Changes in solution conditions have an effect in the  $IC_{50}$  value of a particular inhibitor. As a result, when we compare different types of competitive inhibitors, it has to be taken into account that the  $IC_{50}$  values must be measured at the same concentration of substrate, there will be different variation in  $IC_{50}$  values of a non competitive and a competitive inhibitor when we vary the substrate concentration.

Accordingly, the effectiveness observed *in vitro* under a particular set of solution conditions may not be the same effectiveness observed *in vivo*, where the conditions are different. It is more acceptable to use the  $K_i$  values to compare the inhibitory potency of different compounds.<sup>87</sup>

By derivation of velocity equations we can determine the relationship between  $K_i$ ,  $[S]$ ,  $K_m$  and  $IC_{50}$  for competitive, non competitive and uncompetitive inhibitors, giving as a result equations 2 and 3

For noncompetitive inhibitors:

**Equation 2**

$$IC_{50} = \frac{[S] + K_m}{\frac{K_m}{K_i} + \frac{[S]}{\alpha K_i}}$$

If  $\alpha = 1$  then  $K_i = IC_{50}$



For uncompetitive inhibitors:

**Equation 3**       $\alpha K_i = \frac{IC_{50}}{1 + \frac{K_m}{[S]}}$

If  $[S] \gg K_m$ , then  $\alpha K_i \sim IC_{50}$

The  $IC_{50}$  values can be converted to  $K_i$  values using the above equations, however we must know the mode of inhibition of the compound being analyzed.

A common strategy used in developing structure-activity relationships is to determine important variations in the inhibitory mechanism shared by a series of related compounds, assuming that all the derivative molecules share the same mode of inhibition as the parent molecule. In this way, it can be determined the mode of inhibition for the parent molecule only, and then apply equations 2 and 3 to the rest of the type of molecules been studied<sup>87</sup>

## CHAPTER II

### EXPERIMENTAL SECTION

#### 2.1. Preliminary Studies

After the discovery of triclosan as an inhibitor of ENR in *P. falciparum* by Surolia and Surolia,<sup>14</sup> several studies have focused in the design of antimalarial drugs that target fatty acid biosynthesis. Perozzo et al.<sup>11</sup>, defined the structure of PfENR in a binary complex with NAD<sup>+</sup> and as a tertiary complex with NAD<sup>+</sup> and triclosan, giving insights to the mode of binding of triclosan to PfENR as well as the characteristics of the active site of the protein, allowing the design of different kinds of triclosan derivatives that could inhibit PfENR.<sup>11,73,92</sup>

Triclosan (Figure 3) binds forming a non covalent complex with NAD<sup>+</sup>(NADH) and with PfENR mainly forming hydrogen bonds. This mode of binding exhibit  $\pi$ - $\pi$  stacking interaction between the nicotinamide ring of NAD<sup>+</sup>(NADH) and the phenol ring (A) of triclosan. This same ring formed additional van der Waals interactions with the side chains of Tyr267, Tyr277, Pro314, Phe368, and Ile369. In addition to hydrogen-bonding with the 2'-hydroxyl group of the nicotinamide ribose and with Tyr277.<sup>11</sup>

Studies on inhibitors of *E. coli* FabI reported the use of compound 4 (Figure 4)<sup>73</sup> In this study it was shown that this naphthyridinones display similar binding interactions with NAD<sup>+</sup> and the active site of FabI to those found for triclosan; the linking amide carbonyl is positioned for an H-bond interaction with the 2'-hydroxyl of NAD<sup>+</sup> and the hydroxyl of tyrosine156. The central *cis*-amide fragment of compound 4 (Figure 4) appears to participate in a  $\pi$ - $\pi$  stacking interaction with the nicotinamide portion of

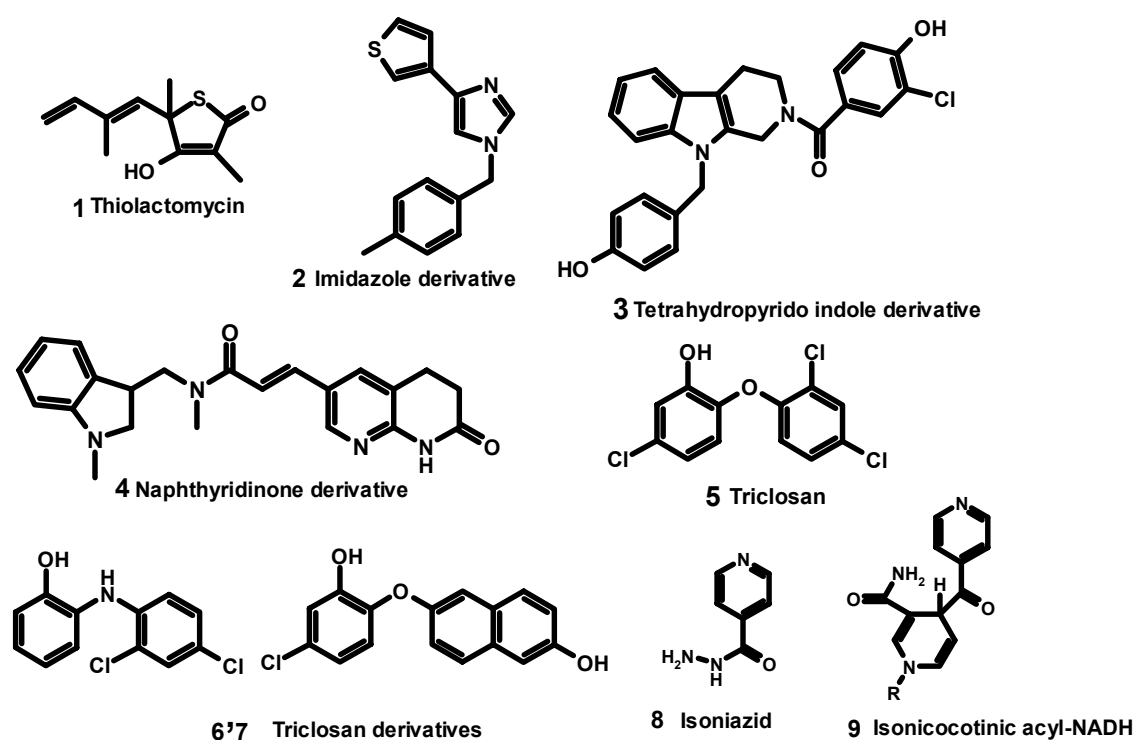
NAD<sup>+</sup>. Alanine95 is involved in H-bond interactions that bind both the pyridylamine and the *N*-acyl hydrogen of the naphthyridinone moiety.<sup>73</sup>

InhA is the ACP in *M. tuberculosis*. It is inhibited by isonicotinic acyl-NADH compound 9 (Figure 4), an adduct molecule that is the product of the activation of isoniazid compound 8 (Figure 4) (a pro-drug that is activated in the active site of several ACPs in presence of KatG which catalyzes the oxidation of Mn<sup>+2</sup> to Mn<sup>+3</sup>) and NADH, to form the adduct.<sup>76,88</sup> This isonicotinic acyl-NADH binds to the active site of PfENR producing a conformational change in the residue Tyr267 whose side chain rotates ~30° and forms an aromatic ring-stacking interaction with the pyridine ring of the isonicotinic acyl group. The nitrogen of the isonicotinic acyl group, the oxygen of Tyr267 hydroxyl group and an ordered water molecule form a hydrogen-bonding network. The carbonyl oxygen of the isonicotinic acyl group, the 2'-hydroxyl oxygen of the nicotinamide ring, the oxygen of Tyr277 hydroxyl group and a highly ordered water molecule form another hydrogen-bonding network. (Wang et al. personal communication)

Perozzo et al.<sup>11</sup> reported two triclosan derivatives, compounds 6 and 7 (Figure 4), where modifications were made mainly on the linker, OH group and substituents in the A and B ring of the molecule. These substitutions did not increase the inhibitory activity of those inhibitors compared to triclosan. Therefore, more studies in the possible substituents that will increase triclosan derivatives affinity for the enzyme will be necessary.

In this study, we have synthesized and evaluated *in vivo* and *in vitro* inhibitory activity of more than 500 triclosan derivatives as PfENR inhibitors, as well as co-crystallized those that have an effective inhibition of the enzyme. The purpose of this is

to gain information for the design of more potent PfENR inhibitors where a gain in suppression of PfENR activity could facilitate substitution or removal of the phenol group in ring A of triclosan that is susceptible to metabolic liability (glucuronidation) in human metabolism producing clearance of triclosan.<sup>10</sup>



**Figure 4.** Structures of Known PfENR Inhibitors.

Structures of different kind of PfENR inhibitors including triclosan (5) and triclosan analogs (6,7)

## 2.2. Synthesis of Triclosan Derivatives

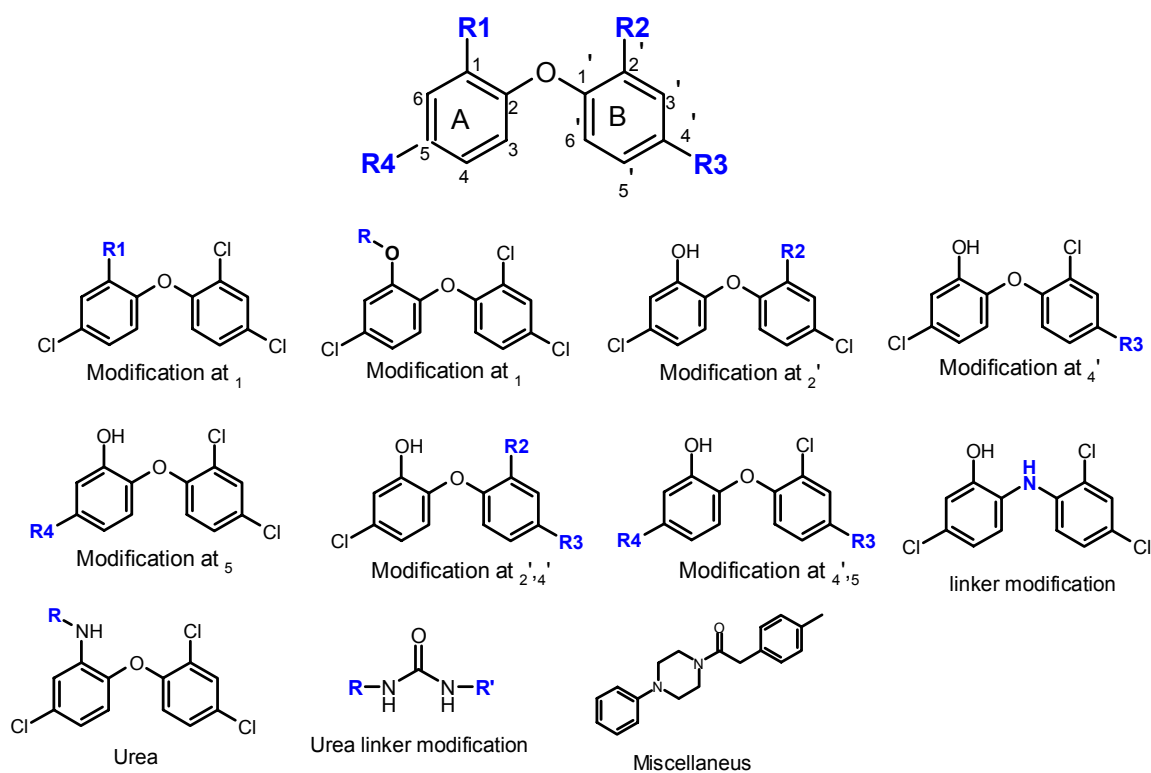
The synthesis of triclosan derivatives was accomplished by Jacobus Pharmaceutical Company. The synthesis strategy focused mainly on substituents at position 1, 5 of ring A and 2' and 4' on ring B, as well as some miscellaneous compounds (Figure 5). These analogs allow us to acquire information about the interaction among those particular substituents on triclosan with the amino acids located in the active site that might increase the binding capacity of those inhibitors, and therefore, their potential as possible drug candidates to treat malaria.

2'-substituted triclosan derivatives were prepared via standard reductive amination protocols using  $\text{NaBH}(\text{OAc})_3$  from the corresponding benzaldehyde and aminomethyl precursors. The benzaldehyde precursor was synthesized from 4-chloro-2-methoxyphenol and the appropriate *o*-fluorobenzaldehyde via nucleophilic aromatic substitution ( $\text{S}_{\text{N}}\text{Ar}$ ) chemistry. The aminomethyl derivatives were afforded by a two step procedure:  $\text{S}_{\text{N}}\text{Ar}$  reaction of 4-chloro-2-methoxyphenol with the appropriate *o*-fluorobenzonitrile and then lithium aluminum hydride reduction of the nitrile. In the case of the  $\alpha$ - $\alpha$ -dimethylated aminomethyl derivatives, reaction of the corresponding aryl nitrile with  $\text{CeCl}_3/\text{MeLi}$  in tetrahydrofuran furnished the amine derivative (Figure 5).

The synthesized 5-substituted triclosan derivatives were prepared via a range of synthetic strategies. Synthesis of the 5-aryl triclosan subclass began with a Suzuki reaction between 4-bromo-2-methoxyphenol and the appropriate arylboronic acid or boronate ester. This *m*-arylphenol was then reacted with the appropriate aryl fluoride in a nucleophilic aromatic substitution ( $\text{S}_{\text{N}}\text{Ar}$ ) reaction. Cleavage of the remaining methoxy group was achieved by stirring with an excess of boron (III) bromide. The 5-alkyl and 5-

alkylaryl subclasses were prepared from the corresponding 5-aldehyde triclosan 1-methyl ether intermediate (itself prepared via  $S_NAr$  reaction of the necessary phenol and aryl fluoride pieces) via a three step protocol: reaction with the appropriate alkyl- or aryl-Grignard reagent, ionic dehydroxylation of the benzylic alcohol with trifluoroacetic acid/triethylsilane, and methyl ether cleavage with boron (III) bromide (Figure 5).

The urea derivatives were prepared using classical methods for urea synthesis. In some cases, the isocyanate was condensed with the appropriate amine precursor to afford the desired urea which was isolated via precipitation from the reaction mixture. Otherwise, a solution of one amine was stirred with phosgene or triphosgene in the presence of base to afford an intermediate isocyanate that was then condensed with the second amine to afford the urea product (Figure 5).



**Figure 5.** Structures of Possible Triclosan Analogs.

Types of triclosan derivatives generated in this study by modification of position 1, 2', 4' and 5' as well as modification in the linker ether atom and some miscellaneous compounds.

### **2.3. *In Vivo* Whole Cell Evaluation**

The inhibitory activities of triclosan and its analogs against *P. falciparum* asexual blood stages were performed by our collaborators at the department of Microbiology and Immunology at Albert Einstein College of Medicine. A 72-h *in vitro* assay that measures decreases in [<sup>3</sup>H] hypoxanthine uptake as a marker of growth inhibition was used. Two strains of *P. falciparum* were used in this study, strain 3D7 is chloroquine sensitive and strain Dd2 that is chloroquine resistant, and the values for this results are reported as two different measurements of IC<sub>50</sub>/IC<sub>90</sub>.

### **2.4. PfENR Expression and Purification**

The expression and purification of PfENR was performed as is described by Perozzo et al.<sup>11</sup> A BL21 (DE3) Codon<sup>+</sup>-RIL cells (Novagen) harboring the expression plasmids were grown in terrific broth. The cells were induced with 1 mM isopropyl-1-thio-β-D-galactopyranoside when the optical density reached 1.6 (*A*<sub>600</sub>) for 5 hours at 37 °C. Cell pellets were resuspended in lyses buffer (20 mM Tris/HCl, pH 8.0, 500 mM NaCl, 50 mM imidazole) and disrupted using a French press. The filtered supernatant was applied to a metal chelate (Pharmacia) affinity column loaded with nickel. The column was washed with buffer B (20 mM Tris/HCl, pH 8.0, 500 mM NaCl, 150 mM imidazole) and eluted with buffer C (20 mM Tris/HCl, pH 8.0, 500 mM NaCl, 400 mM imidazole). The protein was concentrated using Amicon ultra Millipore and applied to a



Superdex 200 size-exclusion column equilibrated with buffer D (20 mM Tris/HCl, pH 7.5, 150 mM NaCl).<sup>11</sup>

## 2.5. *In Vitro* PfENR Evaluation

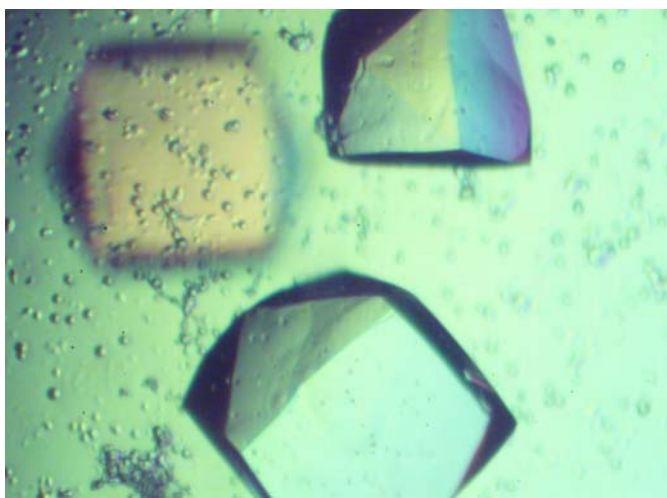
For the *in vitro* determination of triclosan analogs as PfENR inhibitors we developed a reliable assay. The experiments were carried out on a BMG LABTECH FLUOstar OPTIMA multifunctional microplate reader at 25 °C in 20 mM Tris pH 8.0, 150 mM NaCl, 10 mM EDTA, 1 mM DTT (buffer D) in a total volume of 200  $\mu$ L, using 50 nM PfENR, 400  $\mu$ M NADH, and 40  $\mu$ M NAD<sup>+</sup>. The reaction was started with Crotonoyl Coenzyme A (C<sub>4</sub>CoA) to a final concentration of 300  $\mu$ M C<sub>4</sub>CoA per well and, detection of the oxidation of NADH to NAD<sup>+</sup> was followed at  $\lambda$ = 340 nm using Constar 96 well plates.

The dose response curves of enzyme inhibition were followed by measuring the effect of an inhibitor on the initial velocity of the enzyme reaction at a fixed concentration of substrate. All the inhibitors IC<sub>50</sub>s (concentration of inhibitor required to achieve a half-maximal degree of inhibition) were evaluated from 10  $\mu$ M to 10 nM, Langmuir curves were determined using the program Kaleidagraph 3.5 by fitting the data to the equation  $v_i/v_0=1/(1+([I]/IC_{50}))$  and obtaining the final IC<sub>50</sub> value for each inhibitor that has a  $V_i/V_0$  value less than 0.3  $\mu$ M.

## 2.6. Crystallization Condition

The hanging drop vapor diffusion method was used for the crystallization condition, in which 24 mg/mL of PfENR was incubated with 4 mM NADH in buffer D

and 2  $\mu\text{L}$  of this mixture was mixed with 2  $\mu\text{L}$  of the well solution consisting of 2.5 M  $(\text{NH}_4)_2\text{SO}_4$ , 100 mM NaOAc, and 270 mM tris pH 7.7, and equilibrated at 17  $^\circ\text{C}$ , to get the binary complex of PfENR-NAD<sup>+</sup>. Those crystals were used in inhibitor soaking experiments, where 2  $\mu\text{L}$  of inhibitor dissolved in 100% acetonitrile were directly added to the crystallization drop containing crystals of binary complex with a space group  $P4_32_12$  (cell dimension  $a = b = 132.05 \text{ \AA}$ ,  $c = 82.84$ ) (Figure 6) to a final concentration of 2.1 mM. After 7 to 10 days of incubation, crystals soaked with the inhibitor were exposed at room temperature in a Rigaku X-ray generator utilizing a copper rotating anode (CuK $\alpha$  wavelength = 1.54  $\text{\AA}$ ). Diffraction data was collected from 2.4- $\text{\AA}$  to 3.1- $\text{\AA}$  resolution from single crystals using a MacScience DIP2030 image plate detector with double-focusing mirrors. The data were processed and scaled using DENZO/SCALEPACK.<sup>11</sup>



**Figure 6.** PfENR Crystals, Space Group  $P4_32_12$ .

## CHAPTER III

### STRUCTURAL ANALYSIS OF TRICLOSAN BINDING TO PfENR

#### 3.1. Introduction

##### 3.1.1. Mode of Binding of Triclosan to (PfENR)

Taking into account information derived from the crystal structure of PfENR it is known that the active side of this enzyme is mainly constituted by hydrophobic residues: Val222, Tyr277, Tyr267, Phe368, Pro314, Gly315, Leu315, His214, Ala217, Asn218, Ala219, Lys220, Met231, and Lys285, as is described in Figure 7a and 7b. The  $\alpha$ 8-Helix that forms part of this NAD<sup>+</sup>-TCL binding pocket is formed by Ala319, Ala320, Ala322, Ile323, Ala372, and is represented as lines in some of the figures for better visualization of the triclosan and triclosan analogs mode of binding.

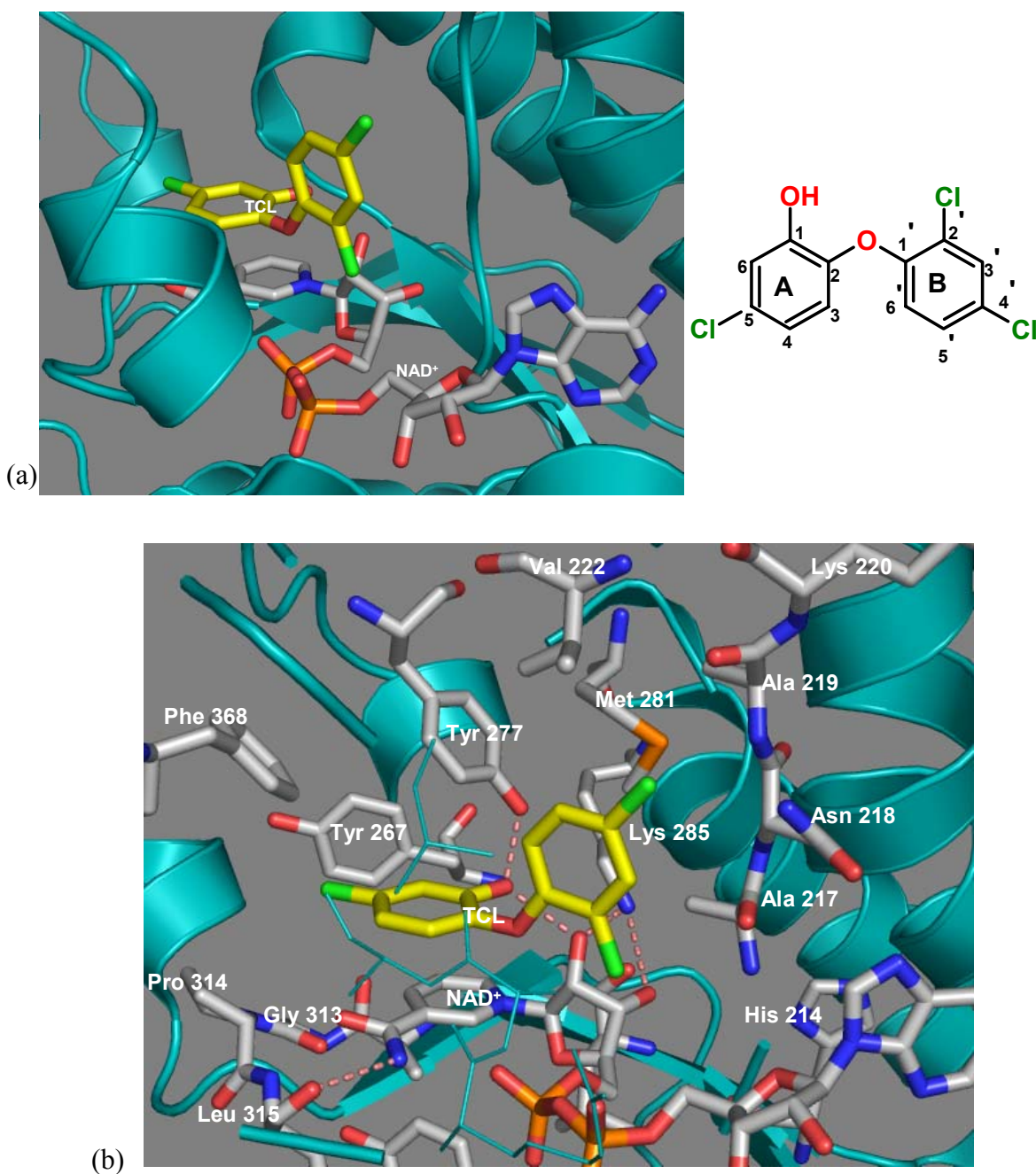
Using the crystal structure obtained for PfENR-NAD<sup>+</sup>-triclosan complex we have found that the phenol ring (ring A) of the inhibitor interacts in an opposite orientation with the nicotinamide ring of NAD<sup>+</sup> allowing  $\pi$ -cation interactions<sup>11</sup>. The same ring forms additional van der Waals interactions with the side chains of Tyr267, Tyr277, Pro314, Phe368, and Ile369. In addition, the phenolic hydroxyl hydrogen-bonds to the 2'-hydroxyl moiety of the nicotinamide ribose, the oxygen atom of Tyr277, and the amino nitrogen of Lys285 is located within 4.65 Å (Figure 7a and 7b). These residues are completely conserved in all known ENRs and are thought to have implication in the enzyme's catalytic mechanism.<sup>11</sup> On the other hand, the ether oxygen atom of triclosan interacts with the 2'-hydroxyl group of the nicotinamide ribose, and is located within

3.49 Å of one of the oxygen atoms of the nicotinamide ribose phosphate, forming a weak hydrogen bond with this group.

Ring B (2,4-dichlorophenoxy ring) of triclosan is located in a pocket bounded by the pyrophosphate and nicotinamide moieties of NAD<sup>+</sup>, by the peptide backbone residues 217-231 and by the side chains of Asn218, Val222, Tyr277, and Met281. The 4-chloro atom of ring B is placed adjacent to the side chains of Val222 and Met281 and residues 218-219, the 2-chloro atom is surrounded by the  $\alpha$ -carbon atom, the side chain of Ala217, and atoms of the nicotinamide ribose pyrophosphate moiety.<sup>11</sup>

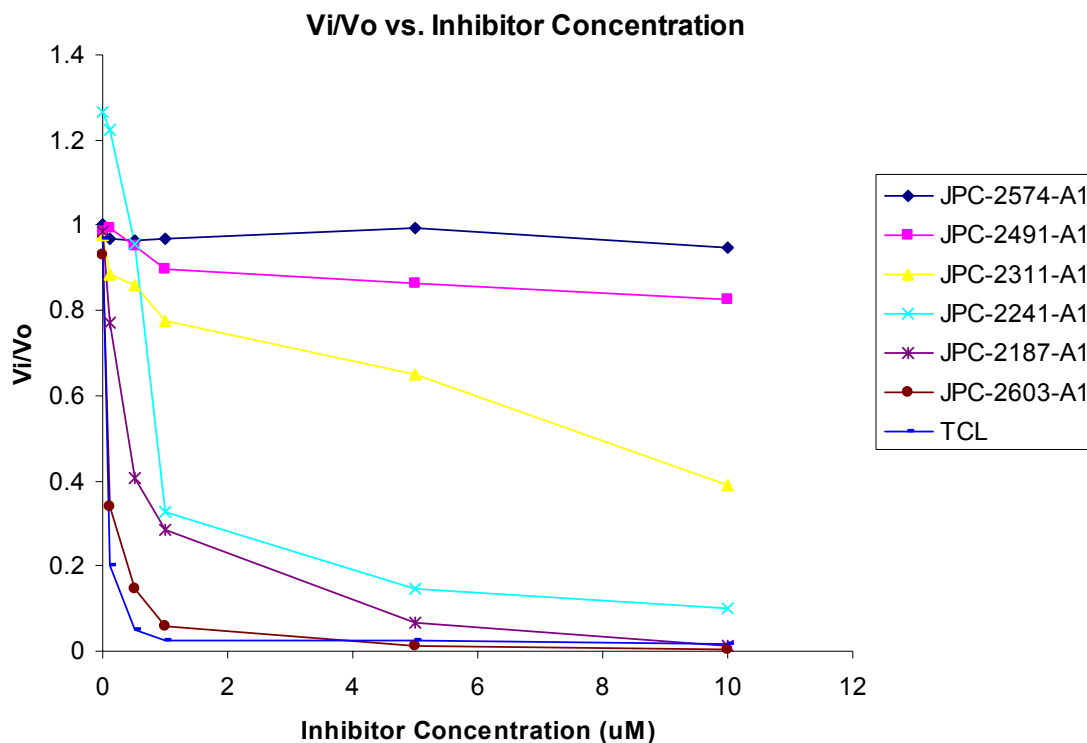
The chloride atom of ring A at position 5 is surrounded by mainly hydrophobic residues making van der Waals contacts with the side chains of Tyr267, Pro314, and Phe368. For this study several types of triclosan derivatives were synthesized, mainly to make substitutions at positions 1, and 5 of ring A, and 2' and 4' of ring B, as well as the linker ether group, and some miscellaneous compounds that should resemble the triclosan mode of binding to PfENR.

This chapter describes the results, discussion and implication of the data obtained in the whole cell assay, and the enzymatic assays of the different triclosan derivatives evaluated in this study. In addition, we describe the crystallographic structure obtained for those compounds for which determination of the tertiary complexes bound to PfENR-NADH crystal structure were possible to obtain.<sup>11</sup>



**Figure 7.** X-Ray Structure of Triclosan Bound to PfENR.

(a) Structural representation of triclosan (yellow sticks) and NAD<sup>+</sup> (white sticks) bound to the active site of PfENR. (b) Structural representation of triclosan and NAD<sup>+</sup> showing the location of the amino acids (white sticks) at the active side of PfENR and some of the interactions that define the mode of binding of triclosan and NAD<sup>+</sup>, helix  $\alpha 7$  is represented as lines (green) for better visualization of triclosan and NAD<sup>+</sup>.



**Figure 8.** Fractional Velocities as Function of Inhibitor Concentration.

$V_i/V_o$  variation for triclosan and some triclosan derivatives in the PfENR *in vitro* assay, inhibitor JPC-2574-A1 (◆)  $IC_{50} > 100 \mu\text{M}$  has no inhibitory capacity against PfENR, JPC-2491-A1 (■)  $IC_{50} 41.5 \mu\text{M}$  and JPC-2311-A1 (▲)  $IC_{50} 22.5 \mu\text{M}$  have a moderate inhibition of PfENR, JPC-2241-A1 (×)  $IC_{50} 4.26 \mu\text{M}$  is an acceptable inhibitor, JPC-2187-A1 (\*)  $IC_{50} 0.36 \mu\text{M}$  shows to be potent inhibitors and JPC-2603-A1 (●)  $IC_{50} 0.063 \mu\text{M}$  was as good as triclosan (-)  $IC_{50} 0.034 \mu\text{M}$

To better understand the reported enzymatic data (*in vitro* evaluation) Figure 8 represent the variation in inhibitor capacity as function of inhibitor concentration for triclosan and some triclosan derivatives, allowing this to further classifies the inhibitors as no inhibition, moderate inhibition and potent inhibitory activity against PfENR

## 3.2. Results

### 3.2.1. Structural Determination of Triclosan Derivatives (Position 1)

The hydroxyl group of the phenol ring is essential for triclosan binding; it forms hydrogen-bonds with the 2'-hydroxyl group of the nicotinamide ribose and with Tyr277 (Figure 7a and 7b). Given the metabolic liability *in vivo* by glucuronidation of triclosan,<sup>84</sup> analogs capable of maintaining or improving these interactions but without the liability problem needed to be synthesized. A total of ninety-six triclosan analogs introducing hydrophobic (dichlorobenzanilide, naphthyl anilide, trifluoromethyl-phenyl-urea, benzo[d][1,3]dioxol-6-yl-urea, chlorobenzyl ether and propan-1-ol, among others) and hydrophilic (aniline, nitro, trifluoromethyl, or methoxy among others) characteristics at position one of triclosan, targeting total or partial replacement of the hydroxyl group of ring A, were evaluated for their PfENR inhibitory potency. The objective of this evaluation was to seek for hydrogen bonding formation or van der Waals interactions between the synthetic analogs and residues in this region of the protein.

The structure for some of these triclosan derivatives at position one of the A ring, the results of whole cell assays (*in vivo* activity) presented as IC<sub>50</sub>/IC<sub>90</sub> values for the two parasite strains 3D7<sup>a</sup> (drug-sensitive) and Dd2<sup>a</sup> (resistant to the antimalarials chloroquine, pyrimethamine/sulfadoxine), and the enzymatic assays values (*in vitro* activity) are shown in Tables 1,2 and 3. The values obtained were compared with the *in vivo* (IC<sub>50</sub>/IC<sub>90</sub> = 0.4/0.7 µg/mL for strain 3D7<sup>a</sup> and 0.9/1.8µg/mL for strain Dd2<sup>a</sup>) and *in vitro* activities (0.034 µM in the PfENR inhibition assay) measured for triclosan.

The inhibitors shown in Table 1 are those containing mainly polar group replacements for the hydroxyl group of triclosan. Even though no crystallographic data were obtained for these types of triclosan derivatives to show the type of interactions of this type of molecule with PfENR-NAD<sup>+</sup> binary complex, the poor IC<sub>50</sub> values obtained for this type of analogs in the enzymatic assay (higher than 50μM), demonstrate that replacement of this hydroxyl group have a considerable effect in the inhibition of PfENR as consequence there is low or non inhibitory activity of the resulting analogs compared with 0.034μM obtained for triclosan. On the other hand, with the exception of **JPC-2574-A1** (0.7/1.4μg/mL and 1.3/3μg/mL) none of the others analogs shows a considerable *in vivo* inhibitory activity against the two strains of the parasite 3D7<sup>a</sup> and Dd2<sup>a</sup>.

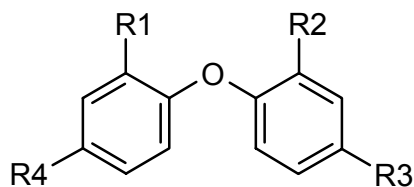
Among the ninety-six triclosan analogs evaluated, some had the hydroxyl group replaced with an urea group (Table 2). No crystallographic data were obtained for this kind of triclosan derivative. However, we inferred that the urea group replacement did not generate or maintain the hydrogen bonds with Tyr277 and the 2'-hydroxyl group of the nicotinamide ribose in NAD<sup>+</sup> required for binding (Figure 7b). These urea derivatives could not form any interactions with Tyr267 and Lys285, which are located within 5.33Å and 4.41Å of the hydroxyl group of triclosan in the direction which will be occupied by this substitution.

Triclosan derivatives that result from modification of position one with a urea group, which we have called urea derivatives, show considerable inhibitory activity in the whole cell assay for the two strains of the parasites used (3D7<sup>a</sup> and Dd2<sup>a</sup>). The inhibition extends from a minimum of 0.02/0.025 μg/mL for strain 3D7<sup>a</sup> and 0.03/0.05 μg/mL for strain Dd2<sup>a</sup>, (**JPC-2201-A1** Table 2) to a maximum of 65.5 μg/mL for strain 3D7<sup>a</sup> and

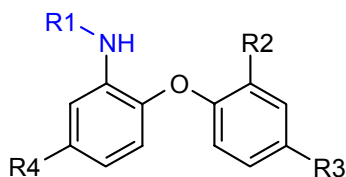


39.2  $\mu\text{g/mL}$  for strain Dd2<sup>a</sup> (JPC-1095-A1 Table 3). In addition, compounds like JPC-2236-A1 also showed a potent parasite inhibitory activity with an  $\text{IC}_{50}/\text{IC}_{90}$  value of 0.04/0.05  $\mu\text{g/mL}$  for strain 3D7<sup>a</sup> and 0.05/0.05  $\mu\text{g/mL}$  for strain Dd2<sup>a</sup>

**Table 1.** Triclosan Analogs at Position 1 (R<sub>1</sub>)

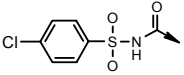
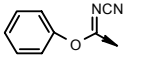
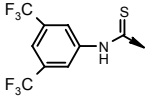
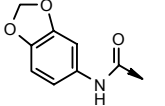
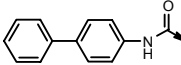
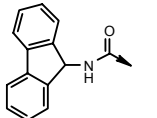
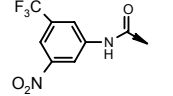
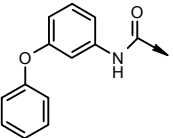
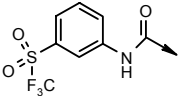
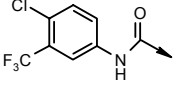
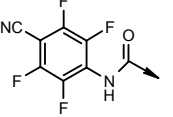


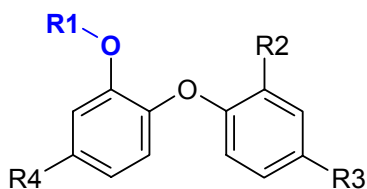
Compound	R <sub>1</sub>	R <sub>2</sub>	R <sub>3</sub>	R <sub>4</sub>	3D7 <sup>a</sup> EC <sub>50</sub> / EC <sub>90</sub> ( $\mu\text{g/mL}$ )	Dd2 <sup>a</sup> EC <sub>50</sub> / EC <sub>90</sub> ( $\mu\text{g/mL}$ )	PfENR <sup>b</sup> IC <sub>50</sub> ( $\mu\text{M}$ )
triclosan	OH	Cl	Cl	Cl	0.4 / 0.7	0.9 / 1.8	0.034
JPC-2063-A-1	NH <sub>2</sub>	Cl	Cl	Cl	15 / 27.6	16.4 / 24.6	>50
JPC-2064-A-1	NO <sub>2</sub>	Cl	Cl	Cl	9.6 / 21	16.5 / 24	>50
JPC-2130-A1	NH-CH <sub>3</sub>	Cl	Cl	Cl	13/23.4	11.6/22.7	>50
JPC-2132-A1	COOH 	Cl	Cl	Cl	23/45.6	19/43	>50
JPC-2133-A1	CONH <sub>2</sub> 	Cl	Cl	Cl	>50/>50	>50/>50	>50
JPC-2548-A-1	F <sub>3</sub> C	Cl	Cl	Cl	36/48.6	34.5/48.6	>50
JPC-2574-A-1	H <sub>2</sub> N   CH <sub>2</sub> -CH <sub>3</sub>	Cl	Cl	Cl	0.7/1.4	1/3	>50
JPC-2577-A-1	CH <sub>3</sub> -O-CH <sub>2</sub> -O- 	Cl	Cl	Cl	17.5/38.5	16.6/41	>50

**Table 2.** Triclosan Analogs at Position 1 Urea Class (R<sub>1</sub>)

Compound	R <sub>1</sub>	R <sub>2</sub>	R <sub>3</sub>	R <sub>4</sub>	3D7 <sup>a</sup> EC <sub>50</sub> / EC <sub>90</sub> (μg/mL)	Dd2 <sup>a</sup> EC <sub>50</sub> / EC <sub>90</sub> (μg/mL)	PfENR <sup>b</sup> IC <sub>50</sub> (μM)
triclosan	OH	Cl	Cl	Cl	0.4 / 0.7	0.9 / 1.8	0.034
JPC-2069-A1		Cl	Cl	Cl	1.2 / 2.7	1.9 / 4.6	>50
JPC-2070-A1		Cl	Cl	Cl	14 / 41.6	22 / 46	>50
JPC-2077-A1		Cl	Cl	Cl	2.2 / 3.4	2.5 / 4.4	>50
JPC-2080-A1		Cl	Cl	Cl	0.3 / 1	0.5 / 1	>50
JPC-2081-A1		Cl	Cl	Cl	3.3 / 6	4 / 6	>50
JPC-2107-A1		Cl	Cl	Cl	17.5 / 29	11.6 / 23	>50
JPC-2201-A1		Cl	Cl	F <sub>3</sub> C	0.02/0.025	0.03/0.05	>50
JPC-2215-A1		OH	Cl	F <sub>3</sub> C	0.2/0.2	0.1/0.2	8.7
JPC-2219-A1		Cl	Cl	F <sub>3</sub> C	0.13/0.19	0.16/0.20	>50
JPC-2236-A1		Cl	Cl	F <sub>3</sub> C	0.04/0.05	0.05/0.05	>50
JPC-2284-A1		OMe	Cl	F <sub>3</sub> C	0.08/0.1	0.04/0.09	>50

Table 2. Continued

Compound	R <sub>1</sub>	R <sub>2</sub>	R <sub>3</sub>	R <sub>4</sub>	3D7 <sup>a</sup> EC <sub>50</sub> / EC <sub>90</sub> (μg/mL)	Dd2 <sup>a</sup> EC <sub>50</sub> / EC <sub>90</sub> (μg/mL)	PfENR <sup>b</sup> IC <sub>50</sub> (μM)
JPC-2289-A1		Cl	Cl	F <sub>3</sub> C	18.0/32.0	13.2/25.6	>50
JPC-2290-A1		H	F <sub>3</sub> C	F <sub>3</sub> C	1.2/2.0	1.2/3.0	>50
JPC-2314-A1		Cl	Cl	F <sub>3</sub> C	0.13/0.19	0.1/0.2	>50
JPC-2320-A1		Cl	Cl	F <sub>3</sub> C	0.8/1.46	1/1.5	>50
JPC-2323-A1		Cl	Cl	F <sub>3</sub> C	0.3/0.4	0.3/0.4	>50
JPC-2342-A1		Cl	Cl	F <sub>3</sub> C	0.8/1.5	1.4/ 3	>50
JPC-2396-A1		Cl	Cl	F <sub>3</sub> C	0.04/0.05	0.04/0.05	>50
JPC-2478-A1		Cl	Cl	F <sub>3</sub> C	0.3/0.4	0.2/0.3	>50
JPC-2479-A1		Cl	Cl	F <sub>3</sub> C	0.078/0.1	0.08/0.1	>50
JPC-2485-A1		Cl	F <sub>3</sub> C	OF <sub>3</sub> C	0.04/0.08	0.07/0.1	>50
JPC-2559-A1		Cl	Cl	F <sub>3</sub> C	0.1/0.2	<0.1/0.2	>50

**Table 3.** Triclosan Analogs at Position 1H Substitution (R<sub>1</sub>)

Compound	R <sub>1</sub>	R <sub>2</sub>	R <sub>3</sub>	R <sub>4</sub>	3D7 <sup>a</sup> EC <sub>50</sub> / EC <sub>90</sub> (μg/mL)	Dd2 <sup>a</sup> EC <sub>50</sub> / EC <sub>90</sub> (μg/mL)	PfENR <sub>b</sub> IC <sub>50</sub> (μM)
triclosan	H	Cl	Cl	Cl	0.4±0.1 / 0.7±0.1	0.9±0.1 / 1.8±0.3	0.034
JPC-1093-A-1	HOOC	Cl	Cl	Cl	>20 / >20	>20 / >20	38
JPC-1095-A-1	H <sub>2</sub> NOC	Cl	Cl	Cl	65.5 / > 50	39.2 / > 50	16.3
JPC-2001-A-1		Cl	Cl	Cl	34.4 / >50	36.9 / >50	5.3
JPC-2002-A-1		Cl	Cl	Cl	20/ 39	20/ 46	10.8
JPC-2019-A-1		Cl	Cl	Cl	4/ 7	2.8±/ 5.6	>10
JPC-2026-A-1		Cl	Cl	Cl	21/ 38	11/ 37	>50
JPC-2138-A1	HO	Cl	Cl	Cl	5.7/11	5.6/12.6	>50
JPC-2139-A1	H <sub>3</sub> C	Cl	Cl	Cl	11.1/24.5	9.8/22	>50
JPC-2577-A-1		Cl	Cl	Cl	17.5/38.5	16.6/41.4	>50

For the *in vitro* inhibitory activity assay, the same number of compounds was evaluated, and the inhibitory activity ranged from a minimum  $IC_{50}$  of 5.3  $\mu\text{M}$  for compound **JPC-2001-A1** where a morpholino carbamate replaced the hydroxyl group of triclosan (Table 3), to a maximum of 50  $\mu\text{M}$  for most of the compounds where transformation of the hydroxyl group at position one of triclosan was made (Tables 1, 2 and 3). Modifications at this position dramatically decreased the inhibitory activity ( $IC_{50}$ ) of most of these triclosan analogs to PfENR, since this data suggest that any major group at this position affects the hydrogen bonding of hydroxyl group at position one of triclosan with the 2' hydroxyl group of the nicotinamide ribose and Tyr277 (Figure 7b), as well as the van der Waals interactions of ring A of triclosan with the side chains of Tyr267, Tyr277 Pro314, Phe368 and Ile369. We were unable to obtain crystallographic data for all of the triclosan analogs at position one, to determine their structure and the characteristics of the interactions that can take place among PfENR,  $\text{NAD}^+$  and the triclosan analog.

### 3.2.2 Structural Determination of Triclosan Derivatives (Linker (Ether) Position)

The ether oxygen atom of triclosan (linker position) interacts with the 2'-hydroxyl group of the nicotinamide ribose and approaches it within 3.49 Å of one of the oxygen atoms of the nicotinamide ribose phosphate group. A total of one hundred-and-thirty triclosan analogs at this position were evaluated with the whole cell assay (*in vivo* activity) as well as with the enzymatic assay (*in vitro* activity). Parts of the results obtained are shown in Tables 4 and 5.

In one-hundred-and-nine of those analogues, (some of them shown in Table 4), the ether group of triclosan was substituted by a urea group in addition to some modification on rings A and B, introducing new characteristics to the nature of the molecule. These compounds showed an efficient *in vivo* inhibitory activity in the two parasite strains (3D7<sup>a</sup> and Dd2<sup>a</sup>) used in the assay. The inhibition ranges from a minimum IC<sub>50</sub>/ IC<sub>90</sub> of 0.04/0.05 µg/mL and 0.03/0.05 µg/mL, respectively, for compound **JPC-2417-A1** up to 50 µM for most of the compounds where transformation of the ether group at the linker position of triclosan was made, hence, it is approximately ten times more potent than triclosan, for which the whole cell activity was 0.4/0.7 µg/mL for strain 3D7<sup>a</sup> and 0.9/1.8 µg/mL for strain Dd2<sup>a</sup>. In this group of inhibitors the maximum value attained was greater than 50/50 µg/mL and 50/50 µg/mL for compound **JPC-2358-A1** for both parasite strains. Moreover, the IC<sub>50</sub> values collected in the PfENR assay were higher than 50 µM. Therefore, these modifications did not introduce any improvement in the inhibitory potential of these analogs compared with an IC<sub>50</sub> value of 0.034 µM obtained for triclosan.

When substituting the ether linkage of triclosan by amino or urea groups, in addition to some changes in the structure of rings A and B, there was no significant improvement in the inhibitory ability of those derivatives to PfENR, possible due to the essential interaction of this ether group with the 2'-hydroxyl group of nicotinamide ribose, and one of the oxygen atoms of the nicotinamide ribose phosphate group that could not be maintained by this urea linkage group (Figure 7b).

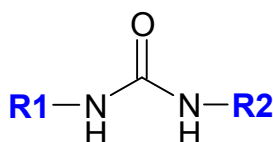
In twenty-one of the linker analogs where the ether group of triclosan was substituted by an amino group and the main characteristic groups in ring A and B of triclosan were maintained intact (Table 5), we found satisfactory *in vivo* inhibitory activity in the two strains of the parasite 3D7<sup>a</sup> and Dd2<sup>a</sup> used in this study. The *in vivo* inhibitory activity ranges from a minimum IC<sub>50</sub>/IC<sub>90</sub> of 0.15/0.4 µg/mL and 0.1/0.4 µg/mL, respectively, for compound **JPC-2578-A1**, this value is slightly better than triclosan, to a maximum of 30/>50 µg/mL and 24/38 µg/mL for compound **JPC-2579-A1** in both strains of the parasite (Table 5). In the case of the enzymatic inhibitory activity with these analogs, the minimum IC<sub>50</sub> was 0.046 µM, value as potent as triclosan for inhibitor **JPC-2578-A1** and the maximum was 18.7 µM for compound **JPC-2579-A1**.

These compounds may still be capable of maintaining the interactions of the linker group with 2'-hydroxyl group of the nicotinamide ribose, given the hydrogen bonding characteristics of the amino linker group, in comparison to the miscellaneous linker analogues which most of them presented a value of 50 µM for the enzymatic assay in this series of inhibitors (Table 5).

Considering the result discussed above, it can be suggested that substitutions of the ether atom at this linker position connecting ring A and ring B of triclosan for larger

modifications, such as substitutions with aniline-nitroethylene (**JPC-2533-A1**), thiourea (**JPC-2418-A1**), and cyano guanidine (**JPC-2317-A1**), among others (Table 5), affect the interaction of these derivatives with PfENR. However small modifications, such as an amino group substitution, still maintains some characteristics of the total inhibitory potential of triclosan. None of the triclosan analogs at this position were able to produce the satisfactory result in the soaking experiments, to be able to determine their structure and characteristics of the mode of interactions.

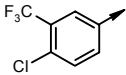
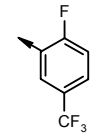
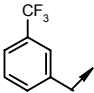
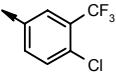
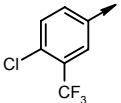
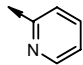
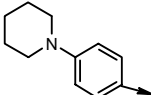
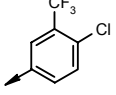
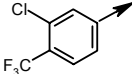
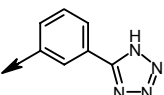
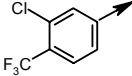
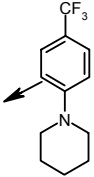
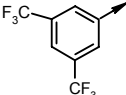
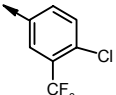
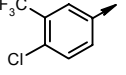
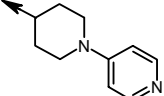
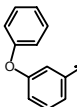
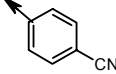
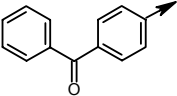
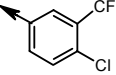
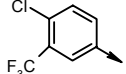
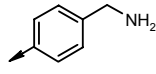
**Table 4.** Triclosan Analogs at Linker Position (R<sub>1</sub> and R<sub>2</sub>)



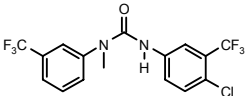
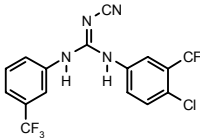
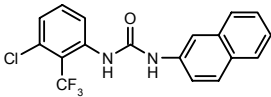
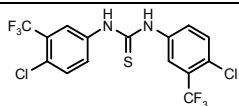
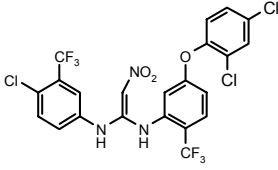
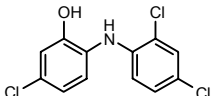
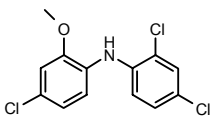
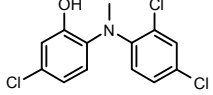
Compound	R <sub>1</sub>	R <sub>2</sub>	3D7 <sup>a</sup> EC <sub>50</sub> / EC <sub>90</sub> (μg/mL)	Dd2 <sup>a</sup> EC <sub>50</sub> / EC <sub>90</sub> (μg/mL)	PfENR <sup>b</sup> IC <sub>50</sub> (μM)
triclosan			0.4±0.1 / 0.7±0.1	0.9±0.1 / 1.8±0.3	0.034
<b>JPC-2065-A1</b>			0.3 / 0.7	0.3 / 0.5	>50
<b>JPC-2220-A1</b>			0.5/0.8	0.5/0.7	>50
<b>JPC-2221-A1</b>			7.4/12	6 / 19	>50
<b>JPC-2230-A1</b>			1.4/ 3	1 / 3	>50
<b>JPC-2250-A1</b>			0.1/0.1	0.1/0.1	>50



Table 4. Continued

Compound	R <sub>1</sub>	R <sub>2</sub>	3D7 <sup>a</sup> EC <sub>50</sub> / EC <sub>90</sub> (μg/mL)	Dd2 <sup>a</sup> EC <sub>50</sub> / EC <sub>90</sub> (μg/mL)	PfENR <sup>b</sup> IC <sub>50</sub> (μM)
JPC-2257-A1			0.2/0.2	0.2/0.2	>50
JPC-2298-A1			1.3/2.6	1.3/2.7	>50
JPC-2358-A1			>50/>50	>50/>50	>50
JPC-2366-A1			4/6	3/6	>50
JPC-2412-A1			15/>50	39/>50	>50
JPC-2414-A1			0.15/0.2	0.1/0.2	>50
JPC-2417-A1			0.04/0.05	0.03/0.05	>50
JPC-2427-A1			0.2/0.3	0.2/0.3	>50
JPC-2430-A1			0.6/0.8	0.4/0.76	>50
JPC-2439-A1			2/3	2/3	>50
JPC-2463-A1			1.7/6	2.5/6.2	>50

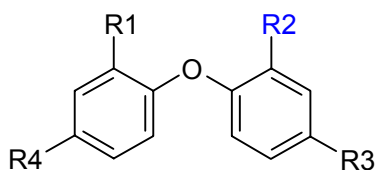
**Table 5.** Triclosan Analogs at Linker Position (Linker Miscellaneous)

Compound	R	3D7 <sup>a</sup> EC <sub>50</sub> / EC <sub>90</sub> (μg/mL)	Dd2 <sup>a</sup> EC <sub>50</sub> / EC <sub>90</sub> (μg/mL)	PfENR <sup>b</sup> IC <sub>50</sub> (nM)
triclosan		0.4±0.1 / 0.7±0.1	0.9±0.1 / 1.8±0.3	0.034
JPC-2266-A1		0.3/0.7	0.3/0.4	>50
JPC-2317-A1		0.6/2.4	0.8/2.7	>50
JPC-2371-A1		0.6/1.0	0.5/0.8	>50
JPC-2418-A3		0.3/0.4	0.3/0.4	>50
JPC-2533-A1		1.2/2.6	1/3	>20
JPC-2578-A1		0.15/0.4	0.1/0.4	0.046
JPC-2579-A1		30/>50	24/38	18.7
JPC-2602-A1				3.7

### 3.2.3 Structural Determination of Triclosan Derivatives (Positions 2' and 4')

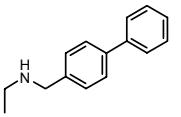
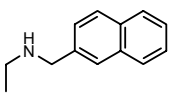
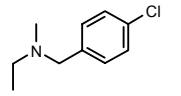
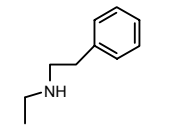
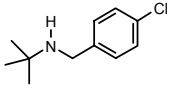
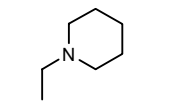
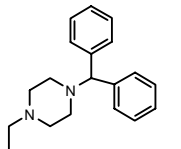
The two chloride atoms in positions 2' and 4' of ring B are located in a pocket bound by the pyrophosphate and nicotinamide moieties of NADH, by the peptide backbone residues 217-231, and by the side chains of Asn218, Val222, Tyr277, and Met281.<sup>11</sup> Although, the 4-chloro atom of ring B was placed adjacent to the side chains of Val222 and Met281 and residues 218-219, the 2-chloro atom was surrounded by the  $\alpha$ -carbon atom, the side chain of Ala217, and atoms of the nicotinamide ribose pyrophosphate moiety (Figure 7).<sup>11</sup>

Tables 6 and 7 show thirty-three triclosan analogs generated by replacement of the chloride group at position 2' of triclosan with hydrophilic moieties (amino, hydroxyl, trifluoromethane, phenylsulfonamide aminomethyl,) capable of forming hydrogen bonding with residues in the active site of PfENR, and with more hydrophobic groups (benzylamino-methyl, phenylpropylamino-methyl, naphthalen-2-yl-methylamino-methyl, benzhydrylpiperazin-1-yl-methyl, naphthalen-2-ylmethylamino-methyl) capable of forming van der Waals or  $\pi$  stacking interactions with PfENR and or NAD<sup>+</sup>.

**Table 6.** Triclosan Analogs at Position 2' (R<sub>2</sub>)

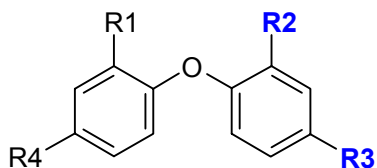
Compound	R <sub>1</sub>	R <sub>2</sub>	R <sub>3</sub>	R <sub>4</sub>	3D7 <sup>a</sup> EC <sub>50</sub> / EC <sub>90</sub> (μg/mL)	Dd2 <sup>a</sup> EC <sub>50</sub> / EC <sub>90</sub> (μg/mL)	PfENR IC <sub>50</sub> (μM)
triclosan	OH	Cl	Cl	Cl	0.4/0.7	0.9/2	0.034
JPC-2205-A1	OH	NH <sub>2</sub>	H	Cl	13/35	22/40	11.4
JPC-2210-A1	OH		H	Cl	2/8	1.5/4	>50
JPC-2239-A1	OH		H	Cl	>0.2/>0.2	0.3/0.4	>50
JPC-2240-A1	OH		H	Cl	0.1/0.2	0.2/0.3	>50
JPC-2242-A1	OH		H	Cl	0.1/0.2	0.2/0.4	>50
JPC-2243-A1	OH		H	Cl	0.2/0.2	0.2/0.4	>50
JPC-2490-A-1	OH		Cl	Cl	9.7/16.3	16.0/26.3	>50
JPC-2292-A-1	OH		CF <sub>3</sub>	Cl	0.1/0.2	0.08/0.1	>50

Table 6. Continued

Compound	R <sub>1</sub>	R <sub>2</sub>	R <sub>3</sub>	R <sub>4</sub>	3D7 <sup>a</sup> EC <sub>50</sub> / EC <sub>90</sub> (μg/mL)	Dd2 <sup>a</sup> EC <sub>50</sub> / EC <sub>90</sub> (μg/mL)	PfENR <sup>b</sup> IC <sub>50</sub> (μM)
JPC-2301-A-1	OH		Cl	Cl	0.1/0.2	0.1/0.2	>50
JPC-2303-A-1	OH		Cl	Cl	0.08/0.18	0.08/0.16	>50
JPC-2308-A-1	OH		Cl	Cl	0.1/0.2	0.1/0.2	>50
JPC-2280-A-1	OH		CF <sub>3</sub>	Cl	0.1/0.3	0.1/0.3	>50
JPC-2333-A-1	OH		Cl	Cl	0.2/0.2	0.1/0.2	>50
JPC-2469-A-1	OH		Cl	Cl	0.1/0.3	<0.1/0.2	>50
JPC-2470-A-1	OH		Cl	Cl	1.1/1.5	0.7/1.4	>50

The *in vitro* and *in vivo* data obtained for these analogs are compared with those for triclosan. For which the inhibitory activity for triclosan in the whole cell assay was 0.4/0.7  $\mu\text{g/mL}$  for strain 3D7<sup>a</sup>, 0.9/1.8  $\mu\text{g/mL}$  for strain Dd2<sup>a</sup>, and for the inhibition assay (PfENR activity) the value was 0.034  $\mu\text{M}$ . In the whole cell assay, the minimum  $\text{IC}_{50}/\text{IC}_{90}$  value was 0.08/0.18  $\mu\text{g/mL}$  for compound **JPC-2303-A1** in strain 3D7<sup>a</sup> and 0.08/0.16  $\mu\text{g/mL}$  for strain Dd2<sup>a</sup>. However, this compound in the assay against PfENR showed no inhibition with an  $\text{IC}_{50}$  value of more than 50  $\mu\text{M}$  whereas in the assay against the parasite, the maximum  $\text{IC}_{50}/\text{IC}_{90}$  value was 9.7/16.3  $\mu\text{g/mL}$  and 16.0/26.3  $\mu\text{g/mL}$  for strains 3D7<sup>a</sup> and Dd2<sup>a</sup> respectively for compound **JPC-2490-A1**, being this compound also not efficient in the enzyme assay with an  $\text{IC}_{50}$  higher than 50  $\mu\text{M}$  (Table 6).

In addition to substitutions at the 2' position, modifications in the 4' position were also studied. A total of seventeen compounds with these characteristics were evaluated, some of which are shown in Table 7. Of these, the minimum  $\text{IC}_{50}$  was found in compound **JPC-2263-A1**, where an isopropyl biguanyl substitution was introduced instead of the usual chloride group of triclosan. This compound has an  $\text{IC}_{50}/\text{IC}_{90}$  of 0.1/1.8  $\mu\text{g/mL}$  for the whole cell assay in strain 3D7<sup>a</sup> and 0.1/1.5  $\mu\text{g/mL}$  for strain Dd2<sup>a</sup>.

**Table 7.** Triclosan Analogs at Position 2' (R<sub>2</sub>) and 4' (R<sub>3</sub>)

Compound	R <sub>1</sub>	R <sub>2</sub>	R <sub>3</sub>	R <sub>4</sub>	3D7 <sup>a</sup> EC <sub>50</sub> / EC <sub>90</sub> (μg/mL)	Dd2 <sup>a</sup> EC <sub>50</sub> / EC <sub>90</sub> (μg/mL)	PfENR <sup>b</sup> IC <sub>50</sub> (μM)
triclosan	OH	Cl	Cl	Cl	0.4 / 0.7	0.9/2	0.034
JPC-2205-A1	OH	NH <sub>2</sub>	H	Cl	13/35	22/>50	11.4
JPC-2214-A-1	OH	NH <sub>2</sub>	CF <sub>3</sub>	Cl	5/7	2.5/5	
JPC-2244-A1	OH	CF <sub>3</sub>	CHO	Cl	1.3/3	0.5/0.6	21
JPC-2263-A1	OH	Cl		Cl	0.1/1.8	0.1/1.5	>50
JPC-2273-A-1	OH	CHO	CF <sub>3</sub>	Cl	2.7/5.6	5/6	3.9
JPC-2288-A-1	OH		CF <sub>3</sub>	Cl	6/12	9/17	0.173
JPC-2334-A-1	OH	CF <sub>3</sub>		Cl	1.5/3	1.5/3	>50
JPC-2335-A-1	OH	CF <sub>3</sub>		Cl	1/2	1/3	>50
JPC-2336-A-1	OH	CF <sub>3</sub>		Cl	3.5/6	4/6	>50
JPC-2343-A-1	OH	CF <sub>3</sub>		Cl	1.1/1.5	0.9/1.5	>50

The maximum IC<sub>50</sub>/IC<sub>90</sub> value of 3.5/6 µg/mL and 4/6 µg/mL for the two strains in this assay, was found in compound **JPC-2336-A-1** where a dimethylamino-phenyl-urea group in position 4' was introduced in addition to a trifluoromethyl group in position 2' (Table 7).

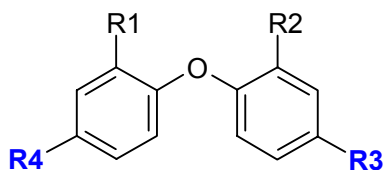
In the case of the enzymatic assay, these analogs do not show any inhibitory activity. The IC<sub>50</sub> value was higher than 50 µM. In addition, replacement of the chloride groups at position 2' and 4' with small polar groups like -CHO, -NH<sub>2</sub>, or -CF<sub>3</sub> caused some effects in the enzymatic assay, in opposition to the value for the whole cell assay found in compounds like **JPC-2273-A1**, IC<sub>50</sub>/IC<sub>90</sub> of 2.7/5.6 µg/mL for strain 3D7<sup>a</sup>, 4.8/6.2 µg/mL for strain Dd2<sup>a</sup> and the IC<sub>50</sub> value in the enzymatic assay was 3.9 µM (Table 7). Therefore, this compound might be targeting PfENR to some degree judging by these *in vivo* and *in vitro* activity results, but no crystallographic data has been collected after the soaking experiments to define the structure of this compound bound to PfENR-NAD<sup>+</sup> complex.



### 3.2.4 Structural Determination of Triclosan Derivatives (Position 5 and 4')

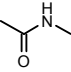
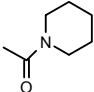
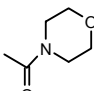
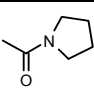
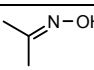
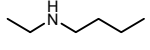
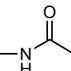
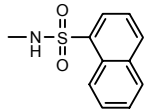
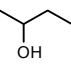
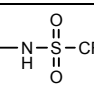
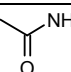
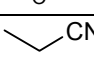
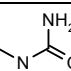
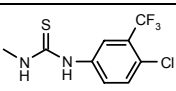
A total of eighty-nine triclosan analogs, which targeted replacement of the chloride atom at 4' and 5 positions with small polar groups such as -NO<sub>2</sub>, -NH<sub>2</sub>, -NHCO, -CN, -OH, -F<sub>3</sub>C, -OCF<sub>3</sub>, as well as nonpolar groups like, -CH<sub>3</sub>, phenyl, phenethyl, tolyl, benzyl, pyridine, isopentyl, methylbutyl, among others, were synthesized. In some of these inhibitors, also the hydroxyl group on position one was modified, resulting in considerable variation of the IC<sub>50</sub> values. Results in the enzymatic assay are presented in Tables 8 and 9 for some of this kind of analogs. Each of these groups introduces possible interesting modes of interactions to the resulting triclosan analogs.

We can divide these eighty-nine analogs in two groups, one group in which forty-three of them had the replacement taking place in position 4' and 5 in addition to some variation in position 1 and 2' (Table 8); and the other group of forty-six inhibitors where the basic replacement took place at position 4', where a urea group was modified (Table 10). Within these eighty-nine analogs, we found the most interesting compounds in the entire study, some of which are shown in (Table 8) together with their *in vivo* and *in vitro* inhibitory activity.

**Table 8.** Triclosan Analogs at Position 4' (R<sub>3</sub>) and 5 (R<sub>4</sub>)

Compound	R <sub>1</sub>	R <sub>2</sub>	R <sub>3</sub>	R <sub>4</sub>	3D7 <sup>a</sup> EC <sub>50</sub> / EC <sub>90</sub> (μg/mL)	Dd2 <sup>a</sup> EC <sub>50</sub> / EC <sub>90</sub> (μg/mL)	PfENR <sup>b</sup> IC <sub>50</sub> (μM)
triclosan	OH	Cl	Cl	Cl	0.4±0.1 / 0.7±0.1	0.9±0.1 / 1.8±0.3	0.034
JPC-2134-A1	OH	Cl	NH <sub>2</sub>	CH <sub>3</sub>	33.3/>50	40.6/>50	1.48
JPC-2135-A1	OH	Cl	NO <sub>2</sub>	CH <sub>3</sub>	1.9/3.5	2.3/4.3	>50
JPC-2136-A1	OH	Cl	NH <sub>2</sub>	Cl	21.7/47	28/>50	0.79
JPC-2137-A1	OH	Cl	NO <sub>2</sub>	Cl	0.6/11	0.6/11	0.099
JPC-2140-A1	OH	H	CN	Cl	2.5/5.	2.5/5	0.230
JPC-2141-A1	OH	H		Cl	22/47	35/50	2.4
JPC-2142-A1	OH	H		Cl	2.7/5	7.7/11	0.548
JPC-2149-A1	OH	Cl	CN	Cl	1.0/1.5	1.7/2.9	0.079
JPC-2150-A1	OH	Cl		Cl	33/41	>50/>50	1.18
JPC-2153-A1	OH	Cl		Cl	13/18	26/39	0.909
JPC-2158-A1	OH	Cl		Cl	20/22	34.6/45	0.760
JPC-2159-A1	OH	Cl		Cl	22/33	48.5/>50	0.044
JPC-2160-A1	OH	Cl		Cl	16/20	25.4/40.7	0.055
JPC-2162-A1	OH	Cl		Cl	10.4/13	22.2/30	0.143

Table 8. Continued

Compound	R <sub>1</sub>	R <sub>2</sub>	R <sub>3</sub>	R <sub>4</sub>	3D7 <sup>a</sup> EC <sub>50</sub> / EC <sub>90</sub> (μg/mL)	Dd2 <sup>a</sup> EC <sub>50</sub> / EC <sub>90</sub> (μg/mL)	PfENR <sup>b</sup> IC <sub>50</sub> (μM)
JPC-2166-A1	OH	Cl		Cl	10/13.7	19.5/27	0.435
JPC-2168-A1	OH	Cl		Cl	2.7/4	9 / 6	0.792
JPC-2169-A1	OH	Cl		Cl	10/16	38/26	0.187
JPC-2171-A1	OH	Cl		Cl	5/7	19/13	0.309
JPC-2178-A1	OH	H		Cl	9/ 19	9/ 19	0.320
JPC-2179-A1	OH	Cl		Cl	1/ 2	1/ 2	1.423
JPC-2181-A1	OH	Cl	OH	Cl	13 / 33	12.7/ 26.6	0.177
JPC-2182-A1	OH	Cl		Cl	6.5/ 19	4 / 14	0.103
JPC-2190-A1	OH	Cl		Cl	10.6/ 21	10 / 22.7	0.665
JPC-2197-A1	OH	H		Cl	9/21	12/23.7	0.230
JPC-2200-A1	OH	Cl		Cl	44.2/>50	>50/>50	0.206
JPC-2212-A1	OH	H		Cl	23/47	21.4/47	0.052
JPC-2283-A1	OH	Cl		Cl	9.6/20	13/24	0.295
JPC-2159-A2	OH	Cl		Cl	47/>50	44.4/>50	0.371
JPC-2431-A1	Cl	H		OCF <sub>3</sub>	0.4/0.7	0.5/0.7	>50
JPC-2545-A1	OH	H	—CF <sub>3</sub>	Cl	0.6/1.5	0.8/2	0.210

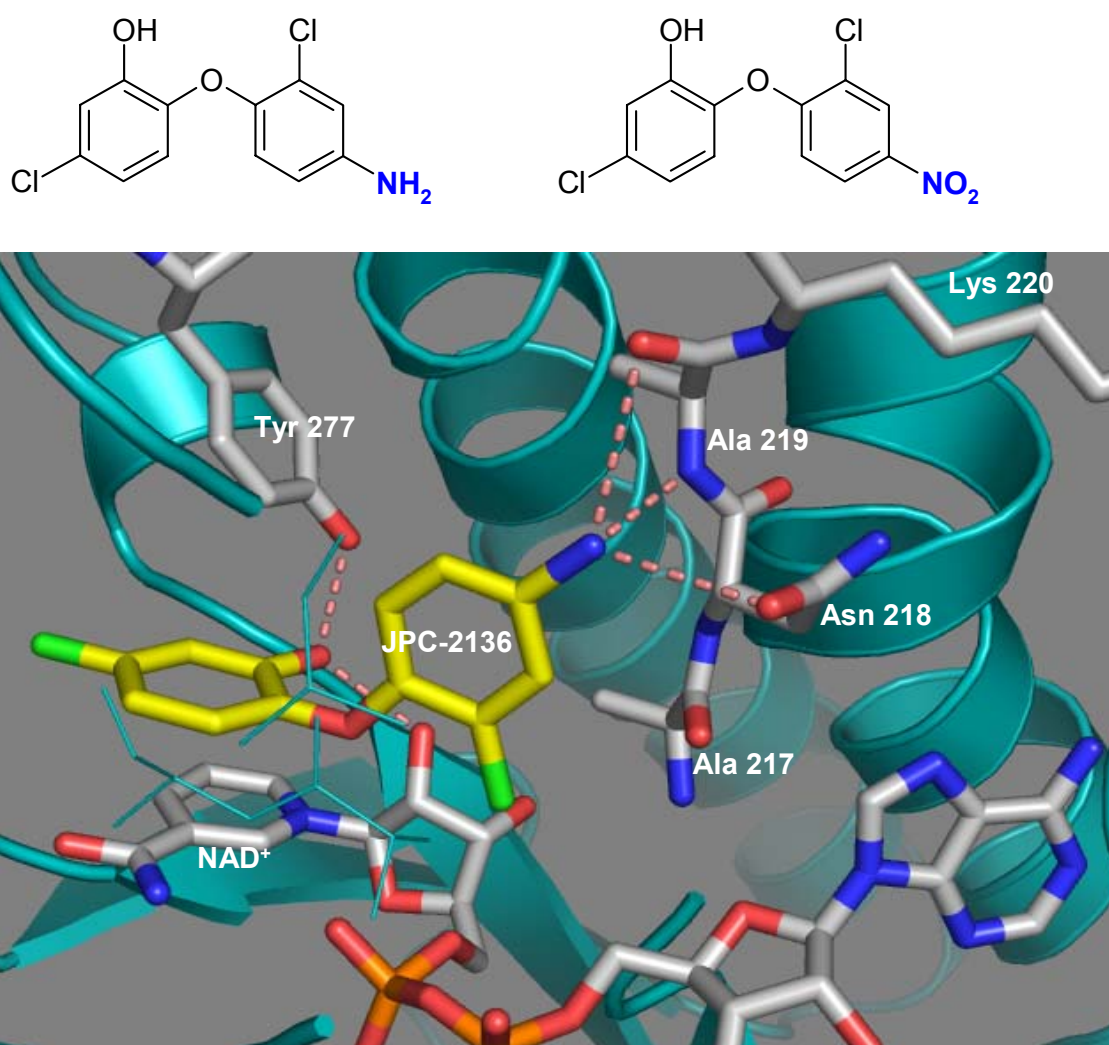
The results have illustrated that, even though the whole cell assay for some of those compounds had a maximum  $IC_{50}/IC_{90}$  value for the inhibition in the two strains of  $>50/>50$   $\mu\text{g}/\text{mL}$  and more than  $50$   $\mu\text{M}$  on the enzymatic assay for most of them, for many of these triclosan analogs at position 5 and 4' the enzymatic inhibitory activity was less than  $1$   $\mu\text{M}$ . For instance, there were values like  $0.044$   $\mu\text{M}$  in the case of compound **JPC-2159-A1** where a urea group substituted the chloride at position 4' almost as potent as triclosan, but has a whole cell  $IC_{50}/IC_{90}$  value of  $22/33$   $\mu\text{g}/\text{mL}$  for strain 3D7<sup>a</sup> (chloroquine sensitive) and  $48.5/>50$   $\mu\text{g}/\text{mL}$  for strain Dd2<sup>a</sup> (chloroquine resistant). Meanwhile, compound **JPC-2305-A1** where a tolyl group was substituted for the chloride at position 5 of triclosan shown a considerable inhibition in both the parasite and the PfENR assay, it display an  $IC_{50}$  of  $0.17$   $\mu\text{M}$  five times less potent than triclosan in the enzyme assay, and a minimum  $IC_{50}/IC_{90}$  value of  $0.7/1.4$   $\mu\text{g}/\text{mL}$  and  $1.3/2.8$   $\mu\text{g}/\text{mL}$  almost as effective as triclosan for the two strains in the whole cell assay (Table 9). One of the minimum values in the enzymatic inhibitory activity was  $0.049$   $\mu\text{M}$  for compound **JPC-2573-A1** where an ethyl group substitutes for the chloride at position 5, with whole cell  $IC_{50}/IC_{90}$  values for the strains used in this study of  $14/3$   $\mu\text{g}/\text{mL}$  and  $1/4.6$   $\mu\text{g}/\text{mL}$ , respectively.

It was only possible to collect crystallographic data for some triclosan analogs modified at the 4' and 5 positions, therefore, crystals of the tertiary complex of PfENR-NAD<sup>+</sup>-inhibitor were obtained. Figures 9-13 show the mode of interactions for six of these inhibitors, where the  $\pi$ - $\pi$  stacking interaction with the nicotinamide ring of NAD<sup>+</sup>, the hydrogen-bonding with the 2'-hydroxyl group of the nicotinamide ribose and with

Tyr277 as well as Van der Waals interactions of ring A with the side chains of Tyr267, Tyr277, Pro314, Phe368, and Ile369 were maintained. Furthermore, depending on the replacement group on position 4' the hydrogen bonds to the residues Asn218, Ala219 were created.

The structure in Figure 9 represents the mode of binding of compound **JPC-2136-A1** and **JPC-2137-A1**, where most of the binding characteristics of triclosan are conserved. In these two compounds, only the 4' chloride group of triclosan was changed for an amino group. Compound **JPC-2136-A1** (Figure 9) had an IC<sub>50</sub>/ IC<sub>90</sub> of 21.7/47.1 µg/mL for strain 3D7<sup>a</sup>, 27.8/>50 µg/mL for strain Dd2<sup>a</sup> in the whole cell assay and, 0.79 µM almost 20 times less active than triclosan in both the whole cell and the PfENR assay.

From Figure 9 we can determine the binding characteristics of compound **JPC-2136-A1**, where there is the typical  $\pi$ - $\pi$  stacking interaction of the analogs with the nicotinamide ring of NAD<sup>+</sup> as well as the van der Waals interactions with the side chains of Tyr267, Tyr277, Pro314, Phe368, and Ile369, besides the interaction of the phenolic hydroxyl that forms hydrogen bonds with the 2'-hydroxyl moiety of the nicotinamide ribose (distance  $O=O = 2.95 \text{ \AA}$ ), the oxygen atom of Tyr277 (distance  $O=O = 2.75 \text{ \AA}$ ) and the amino nitrogen of Lys285. However, the main characteristic for the interaction of this compound with PfENR is that the aniline hydrogen's are hydrogen-bonded with the side chain carbonyl of Asn218 (distance  $C=O-N = 3.34 \text{ \AA}$ ), the main chain carbonyl of Ala219 (distance  $C=O-N = 3.7 \text{ \AA}$ ) and it has favorable interaction with the main chain N-H group of Ala219 (distance  $N-N = 2.7 \text{ \AA}$ ) (Figure 7).



**Figure 9** X-Ray Structure of (JPC-2136-A1) and (JPC-2137-A1) Bound to PfENR.

Stick drawing (yellow) for compound (JPC-2136-A1) and (JPC-2137-A1) in the PfENR (green cartoon representation) –NADH (white sticks) complex and stick format for amino acids at this region, red dots represent the hydrogen bonds interactions. Helix  $\alpha 7$  is represented as green lines for better visualization of JPC-2136 and NAD<sup>+</sup>.

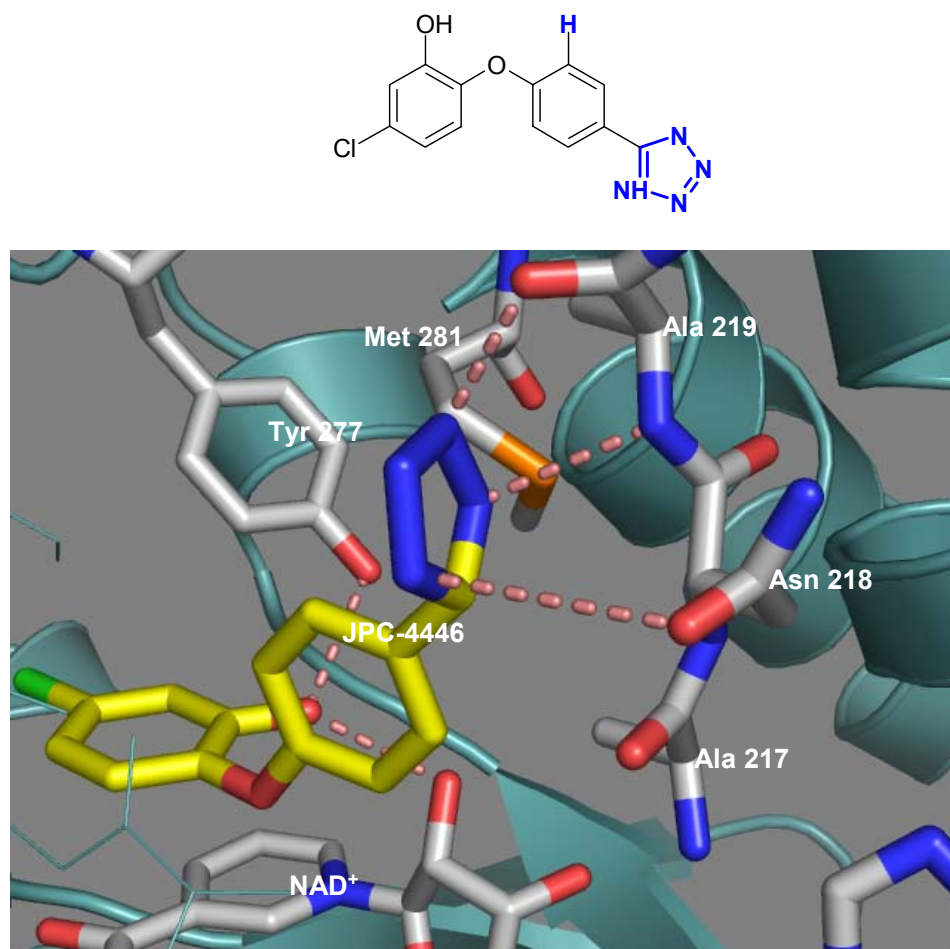
Compound **JPC-2137-A1** has the same binding characteristics that **JPC-2136-A1**. However the crystal structure, in this case, shows that the side chain of Asn218 rotates allowing its carboxamide N-H to interact with one of the nitro oxygen's while the other nitro oxygen forms a hydrogen bond with the main chain N-H group of Ala219 (distance  $N-O = 3.2 \text{ \AA}$ ) (Figure 9). The  $IC_{50}/IC_{90}$  value for this compound was 0.6/11.2  $\mu\text{g/mL}$  for strain 3D7<sup>a</sup>, 0.6/11.3  $\mu\text{g/mL}$  for strain Dd2<sup>a</sup> and 0.099  $\mu\text{M}$  in the enzymatic assay, only three times less active than triclosan (Table 8).

Figure 10 shows the mode of binding of compound **JPC-2141-A1** to PfENR. This compound has an  $IC_{50}$  of 22.3/47.4  $\mu\text{g/mL}$  for strain 3D7<sup>a</sup> and 34.7/>50  $\mu\text{g/mL}$  for strain Dd2<sup>a</sup> in the whole cell assay (almost 50 times less potent than triclosan) in addition to 2.8  $\mu\text{M}$  in the enzymatic assay (10 times less potent than triclosan) (Table 8). It also maintains the same binding characteristics of triclosan, such  $\pi-\pi$  stacking interaction of the analog with the nicotinamide ring of NADH, van der Waals interactions with the side chains of Tyr267, Tyr277, Pro314, Phe368, and Ile369, and the interaction of the phenolic hydroxyl that form hydrogen bonds with the 2'-hydroxyl moiety of the nicotinamide ribose, the oxygen atom of Tyr277, and the amino nitrogen of Lys285. The oxygen linker atom interacts with the 2'-hydroxyl group of the nicotinamide ribose and one of the oxygen atoms of the nicotinamide ribose phosphate. The 2-chloro atom was surrounded by the  $\alpha$ -carbon atom, the side chain of Ala217, and atoms of the nicotinamide ribose pyrophosphate moiety.

This 4' tetrazol position analog is placed adjacent to the side chains of Val222 and Met281 and residues 218-219. The interaction of the phenolic hydroxyl forms hydrogen bonds with the 2'-hydroxyl moiety of the nicotinamide ribose (distance  $O=O = 2.73 \text{ \AA}$ ) and the oxygen atom of Tyr277 (distance  $O=O = 2.79 \text{ \AA}$ ). However, the main characteristics for the interactions in this compound with PfENR is that one of the tetrazol nitrogen's has a weak hydrogen-bonded interaction with the side chain carbonyl of Asn218 (distance  $C=O-N = 4.04 \text{ \AA}$ ), while the others have hydrogen-bonded interaction with the main chain group N-H of Ala219 (distance  $N-N = 2.91 \text{ \AA}$ ) and with the side chain carbonyl of Ala219 (distance  $C=O-N = 2.7 \text{ \AA}$ ). While the  $IC_{50}$  value for this inhibitor in the enzymatic assay shows that it is almost 100 times less active than triclosan, we were still able to determine the characteristics of its interactions with PfENR-NAD<sup>+</sup> complex. (Figure 10)

Compound **JPC-2166-A1** (Table 8) is a derivative where an N-methylamide group is substituted for the chloride group at position 4' in triclosan. This compound has an  $IC_{50}/IC_{90}$  value of 10/13.7  $\mu\text{g/mL}$  for strain 3D7<sup>a</sup>, 19.5/26.8  $\mu\text{g/mL}$  for strain Dd2<sup>a</sup> in the whole cell assay and 0.435  $\mu\text{M}$  in the enzymatic assay (Table 8). Even though the whole cell assay is more than 30 times less effective than triclosan, still the enzyme inhibitory activity is 10 folds less potent than triclosan, despite of this, we were able to determine the mode of binding of this compound (Figure 11) which does not differ much compared to the mode of binding of triclosan and the other inhibitors discussed thus far.

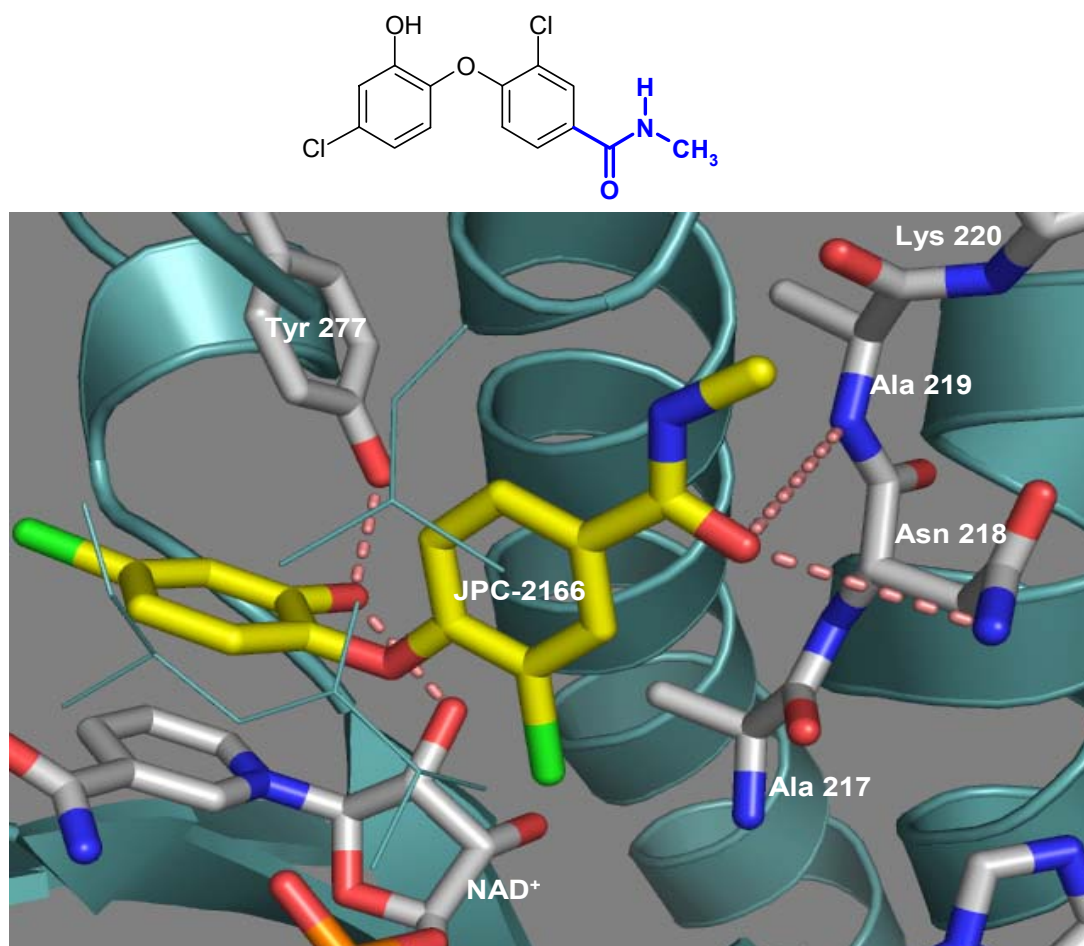




**Figure 10** X-Ray Structure of (JPC-2141-A1) Bound to PfENR.

Stick drawing (yellow) for compound (JPC-2141-A1) in the PfENR (green cartoon representation) –NADH (white sticks) complex and stick format for amino acids at this region, red dots represent the hydrogen bonds interactions, Helix  $\alpha 7$  is represented as green lines for better visualization of the inhibitor and NAD<sup>+</sup>.

The  $\pi$ - $\pi$  stacking interaction of ring A of the analog with the nicotinamide ring of  $\text{NAD}^+$  is maintained as well as the hydrogen bond interaction of the hydroxyl group in ring A of compound **JPC-2166-A1** with Tyr277 (distance  $\text{O}=\text{O} = 2.57 \text{ \AA}$ ) and the 2'-hydroxyl moiety of the nicotinamide ribose (distance  $\text{O}=\text{O} = 2.95 \text{ \AA}$ ). The ether oxygen atom linker of ring A and B still interact with the 2'-hydroxyl group of the nicotinamide ribose, and one of the oxygen atoms of the nicotinamide ribose phosphate (Figure 11). In addition, the carbonyl group of the N-methylamide substitution in position 4' of triclosan makes a weak hydrogen bond with the side chain N-H of Asn218 (distance  $\text{O}=\text{N} = 4.14 \text{ \AA}$ ) and with the backbone N-H of Ala219 (distance  $\text{O}=\text{N} = 3.54 \text{ \AA}$ ). The amide methyl group interacts with the Val222 side chain (Figure 11).

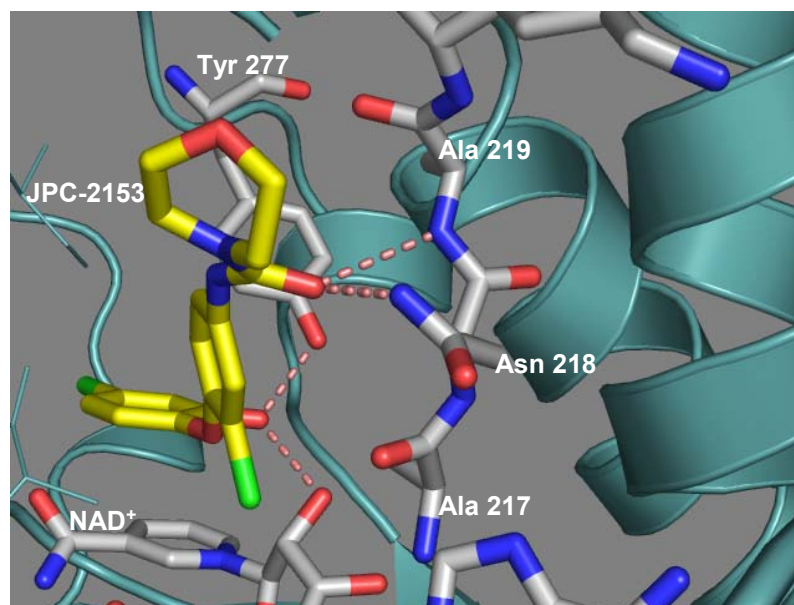
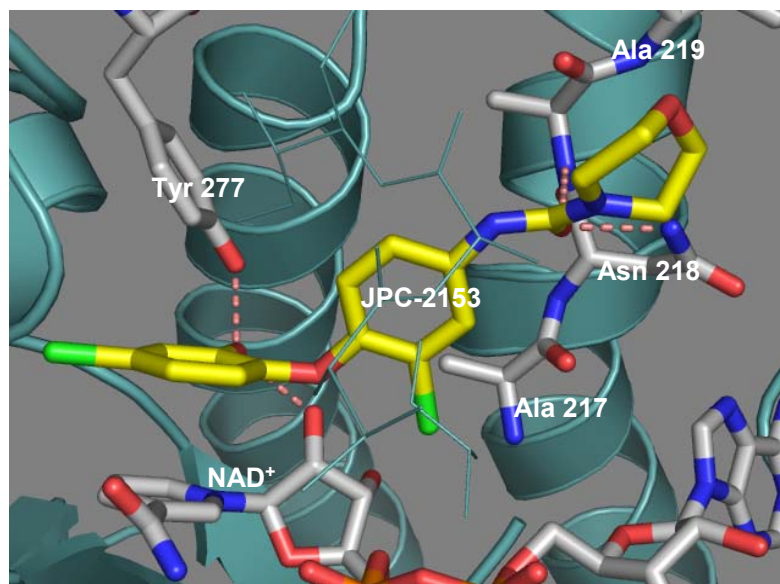
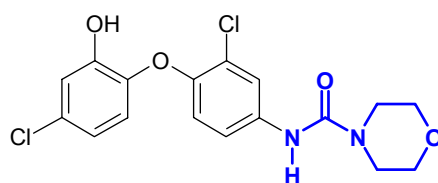


**Figure 11** X-Ray Structure of **(JPC-2166-A1)** Bound to PfENR.

Stick drawing (yellow) for compound **(JPC-2166-A1)** in the PfENR (green cartoon representation) –NADH (white sticks) complex and stick format for amino acids at this region, red dots represent the hydrogen bonds interactions, Helix  $\alpha 7$  is represented as green lines for better visualization of the inhibitor and NAD<sup>+</sup>.

A morpholine-carboxylic acid amide substitution was introduced at position 4' of triclosan to determine the binding capacity and characteristics of this triclosan analog. Compound **JPC-2153-A1** has an  $IC_{50}/IC_{90}$  value of 13.1/18.2  $\mu\text{g/mL}$  for strain 3D7<sup>a</sup> and 26.2/39.3  $\mu\text{g/mL}$  for strain Dd2<sup>a</sup> (50 times less potent than triclosan) in the whole cell assay, even though the  $IC_{50}$  value obtained in the enzymatic assay was 0.91  $\mu\text{M}$  (Table 8) thirty times less active than triclosan. With this molecule, we were able to determine the characteristics of the binding of this triclosan analog to PfENR as it is shown in Figure 12. The  $\pi$ - $\pi$  stacking interaction of ring A of the analog **JPC-2153-A1** with the nicotinamide ring of  $\text{NAD}^+$  is maintained as well as the hydrogen bond interaction of the hydroxyl group in ring A of compound **JPC-2153-A1** with Tyr277 (distance  $\text{O}=\text{O} = 2.55\text{\AA}$ ) and the 2'-hydroxyl moiety of the nicotinamide ribose (distance  $\text{O}=\text{O} = 2.54\text{\AA}$ ). The ether oxygen atom linker of ring A and B still interact with the 2'-hydroxyl group of the nicotinamide ribose and one of the oxygen atoms of the nicotinamide ribose phosphate (Figure 12).

The 4' urea carbonyl group is hydrogen bonded with the side chain N-H of Asn218 (distance  $\text{C}=\text{O}-\text{N} = 2.76\text{\AA}$ ), and the backbone N-H of Ala219 (distance  $\text{C}=\text{O}-\text{N} = 2.98\text{\AA}$ ). Figure 12 shows in two orientations front and side view, the binding of **JPC-2153-A1**. The additional characteristics of the interactions of this molecule compared to those for triclosan to PfENR are that the carboxylic group of the morpholine-carboxylic acid amide forms an additional hydrogen bond with Asn218 and Ala219. Even though compound **JPC-2153-A1** has around 30 times less inhibitory capacity than triclosan, it gives more information about the interaction in the binding pocket of PfENR, being capable of accepting different kind of inhibitors derived from the triclosan scaffold.



**Figure 12** X-Ray Structure of (**JPC-2153-A1**) Bound to PfENR.

Stick drawing (yellow) for compound (**JPC-2153-A1**) in the PfENR (green cartoon representation) –NADH (white sticks) complex and stick format for amino acids at this region, red dots represent the hydrogen bonds interactions, Helix  $\alpha 7$  is represented as green lines for better visualization of the inhibitor and NAD<sup>+</sup>.

One of the most interesting results in this research is the elucidation of the structure of compound **JPC-2305-A1** bound to PfENR-NAD<sup>+</sup> complex. This analog (Figure 13) has an IC<sub>50</sub> five times less active (0.17 μM) than triclosan (0.034 μM) in the enzymatic assay, but in the whole cell assay it is two times as potent as triclosan exhibiting an IC<sub>50</sub>/IC<sub>90</sub> value of 0.7/1.4 μg/mL for the strain 3D7<sup>a</sup>, and 1.3/2.8 μg/mL for strain Dd2<sup>a</sup> (Table 9).

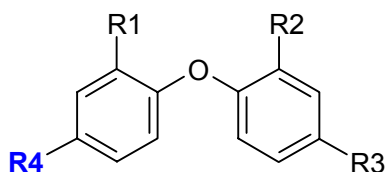
This compound was designed based on the mode of binding of isonicotinic acyl-NAD<sup>+</sup> to the active site of PfENR. This is an adduct molecule that is the product of the activation of isoniazid in the active site of InhA in presence of KatG and NADH. This adduct produces a conformational change on residue Tyr267 in PfENR.<sup>76,88</sup>

We used this information to substitute the chloride group in position 5 of triclosan for an *o*-tolyl group. This substitution in triclosan, in fact, introduced a conformational change in the active site of PfENR, producing a flipping movement of about 45 degrees in residue Tyr267 (Figure 13).

As is shown in Figure 13 the  $\pi$ - $\pi$  stacking interaction of ring A of the analog **JPC-2305-A1** with the nicotinamide ring of NAD<sup>+</sup> is maintained, in addition to a  $\pi$ - $\pi$  stacking interaction of the *o*-tolyl group with Tyr267, Tyr277 still forms the hydrogen bond interaction of the hydroxyl group in ring A of compound **JPC-2305-A1** with Tyr277 (distance  $_{O=O}$  = 2.58Å) and the 2'-hydroxyl moiety of the nicotinamide ribose (distance  $_{O=O}$  = 2.55Å). The ether oxygen atom linker of ring A and B still interacts with the 2'-hydroxyl group of the nicotinamide ribose and one of the oxygen atoms of the nicotinamide ribose phosphate (Figure 13).

The information obtained from the elucidation of the mode of binding of compound (**JPC-2305-A1**) allowed the design of a new series of triclosan analogs that have  $IC_{50}$  values for the *in vitro* assay closer to the  $0.034 \mu\text{M}$  found for triclosan, and introduced a new type of interaction for these types of analogs, some of which are shown in Table 9, where the common characteristics of triclosan binding to PfENR are maintained.

**Table 9.** Triclosan Analogs at Position 5 ( $R_4$ )



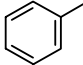
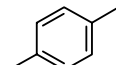
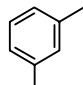
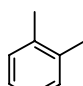
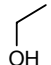
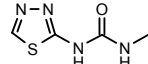
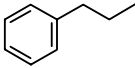
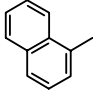
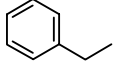
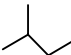
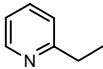
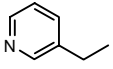
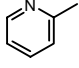
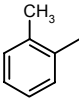
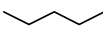
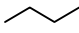
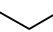
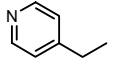
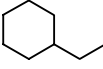
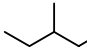
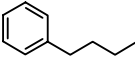
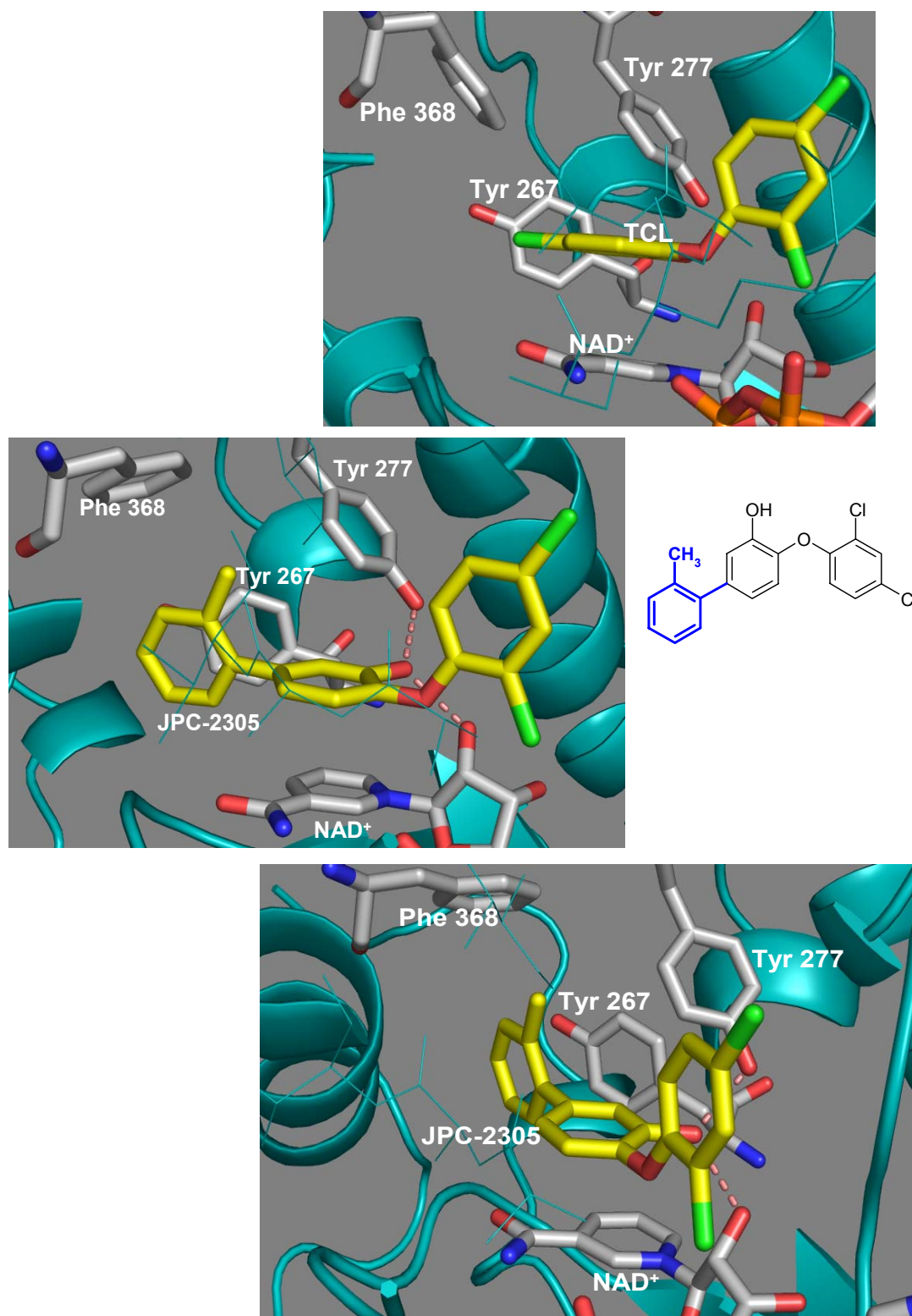
Compound	$R_1$	$R_2$	$R_3$	$R_4$	3D7 <sup>a</sup> $EC_{50} / EC_{90}$ ( $\mu\text{g}/\text{mL}$ )	Dd2 <sup>a</sup> $EC_{50} / EC_{90}$ ( $\mu\text{g}/\text{mL}$ )	PfENR <sup>b</sup> $IC_{50}$ ( $\mu\text{M}$ )
triclosan	OH	Cl	Cl	Cl	$0.4 \pm 0.1 / 0.7 \pm 0.1$	$0.9 \pm 0.1 / 1.8 \pm 0.3$	0.034
JPC-2163-A1	OH	Cl	Cl		1/2	2/3	0.257
JPC-2187-A1	OH	Cl	Cl	$\text{NO}_2$	3 / 4.6	10/ 28	6.77
JPC-2278-A1	OH	Cl	Cl		1.3/3	2.2/3	1.4
JPC-2279-A1	OH	Cl	Cl		1/3	2.8/5.6	4.6
JPC-2305-A1	OH	Cl	Cl		0.7/1.4	1/2.8	0.17
JPC-2315-A1	OH	Cl	Cl		37.7/>50	38.7/>50	1.29
JPC-2380-A1	$\text{CF}_3$	Cl	Cl		1.6/3	1/1.6	>50

Table 9. Continued

Compound	R <sub>1</sub>	R <sub>2</sub>	R <sub>3</sub>	R <sub>4</sub>	3D7 <sup>a</sup> EC <sub>50</sub> / EC <sub>90</sub> (μg/mL)	Dd2 <sup>a</sup> EC <sub>50</sub> / EC <sub>90</sub> (μg/mL)	PfENR <sup>b</sup> IC <sub>50</sub> (μM)
JPC-2448-A1	OH	Cl	Cl		2.5/4	3.7/6	0.139
JPC-2471-A1	OH	H	H		4.6/6	5.6/11	0.232
JPC-2472-A1	OH	Cl	Cl		4/6	5/11	0.132
JPC-2489-A1	OH	Cl	Cl		0.7/2	1/2	0.98
JPC-2492-A1	OH	Cl	Cl		2.7/6	5/10	0.397
JPC-2501-A1	OH	Cl	Cl		2.5/5	4.7/6	0.173
JPC-2530-A1	OH	Cl	CN		3/5	4/6	0.654
JPC-2551-A1	OH	Cl	CN		1/1.6	1 / 1.6	0.24
JPC-2571-A1	OH	Cl	Cl		1 2.8	1/3	0.328
JPC-2572-A1	OH	Cl	Cl		0.9/2	0.8/2.7	0.161
JPC-2573-A1	OH	Cl	Cl		14/3	1/4.6	0.0494
JPC-2575-A1	OH	Cl	CN		2.5/6	3 / 10	0.238
JPC-2589-A1	OH	Cl	Cl		1.4/3	1.8/3	0.269
JPC-2591-A1	OH	Cl	Cl		0.7/1.8	1/2.5	0.268
JPC-2592-A1	OH	Cl	Cl		4/8	5/11	0.662
JPC-2603-A1	OH	Cl	Cl	I			0.063





**Figure 13** X-Ray Structure of (JPC-2305-A1) Bound to PfENR.

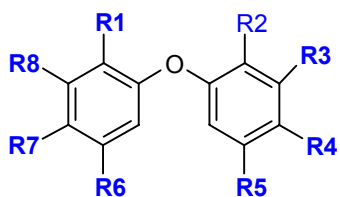
Stick drawing (yellow) for compound (JPC-2305-A1) in the PfENR (green cartoon representation) –NADH (white sticks) complex and stick format for amino acids at this region, red dots represent the hydrogen bonds interactions, Helix  $\alpha 7$  is represented as green lines for better visualization of the inhibitor and NAD<sup>+</sup>.

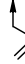

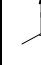
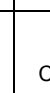
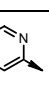
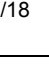
### 3.2.5. Structural Determination of Triclosan Derivatives in Every Position

At this point in the project we were trying to get as many diverse triclosan derivatives as possible. Therefore, Twenty-one analogs, where variations in all positions on both rings were made, can be seen in Table 10. Substitution of the chloride atoms in both rings for small group such as Br, F, H, -CF<sub>3</sub> -NO<sub>2</sub>, -NH<sub>2</sub>, -CH<sub>3</sub> -CN, -OCH<sub>3</sub> were made as well as some phenyl, pyridin and allyl substitutions.

Compound **JPC-2588-A1** displayed the worst IC<sub>50</sub>/ IC<sub>90</sub> value for the whole cell assay 12.5/24.5 µg/mL for strain 3D7<sup>a</sup> and 12.3/23.9 µg/mL for strain Dd2<sup>a</sup>, in which a chloride and iodine group were placed in position 4 and 6 of ring A of triclosan (Table 10). Compound **JPC-2588-A1** shows the poorest IC<sub>50</sub> (>50 µM) for the enzymatic assay in this series of compound. The minimum IC<sub>50</sub>/ IC<sub>90</sub> value for the whole cell assay compound **JPC-2327-A1** was 0.6/1 µg/mL and 0.85/1.5 µg/mL for strains 3D7<sup>a</sup> and Dd2<sup>a</sup> very close to that exhibit by triclosan, with an inhibitory value almost ten times less potent than triclosan in the enzyme assay (0.28 µM) (Table 10). Additionally, we found in the enzymatic assay that compound **JPC-2603-A1** showed a minimum IC<sub>50</sub> value of 0.063 µM, and several others presented a value higher than 50 µM.

As a result, variations in any position of triclosan did not introduce a very significant improvement in the inhibitor efficiency of these analogs (Table 10). This result illustrate that, the compounds described in Table 10 are inhibiting PfENR due to their structure conserve the same characteristics of triclosan scaffold. Unluckily, no crystallographic data was collected after the soaking experiments to define the structure of this compound bound to PfENR-NAD<sup>+</sup> complex.

**Table 10.** Triclosan Analogs at All Positions

Compound	R <sub>1</sub>	R <sub>2</sub>	R <sub>3</sub>	R <sub>4</sub>	R <sub>5</sub>	R <sub>6</sub>	R <sub>7</sub>	R <sub>8</sub>	3D7 <sup>a</sup> EC <sub>50</sub> / EC <sub>90</sub> (μg/mL)	Dd2 <sup>a</sup> EC <sub>50</sub> / EC <sub>90</sub> (μg/mL)	PfENR <sup>b</sup> IC <sub>50</sub> (μM)
triclosan	OH	Cl	H	Cl	H	H	Cl	H	0.4±0.1 / 0.7±0.1	0.9±0.1 / 1.8±0.3	0.034
JPC-2155-A1	OH	H	H	CN	H	OCF <sub>3</sub>	H	H	2.3/5.3	6.1/11.9	2.19
JPC-2161-A-1	OH	Cl	H	Cl	H	Br	CH <sub>3</sub>	H	0.6/1.2	1.3/1.6	1.45
JPC-2165-A1	OH	H	Br	NO <sub>2</sub>	H	H	Cl	H	1.3/2.6	2.8/5.4	0.41
JPC-2204-A1	NH <sub>2</sub>	CH <sub>3</sub>	H	Cl	H	H	CF <sub>3</sub>	H	0.4 / 0.7	1 / 2	>50
JPC-2275-A1	OH	Cl	H	Cl	H		Cl		3.5/6.4	5/7	>20
JPC-2281-A1	OH	Cl	H	Cl	H		Cl	H	9.6/18	9.6/20	21.4
JPC-2327-A1	OH	Cl	H	Cl	H	H	Cl		0.6/1	0.85/1.5	0.280
JPC-2566-A-1	OH	H	H	NO <sub>2</sub>	H	CF <sub>3</sub>	H	H	1/3	1/4	0.174
JPC-2598-A1	OH	Cl	H	Cl	H	Cl	Cl		5/10	4/11	4.070
JPC-2588-A-1	OH	Cl	H	Cl	H	Cl	Cl	I	12.52/24.54	12.30/23.92	>50
JPC-2601-A1	OH	Cl	H	Cl	H		Cl	H			1.4
JPC-2603-A1	OH	Cl	H	Cl	H	H	I	H			0.063
JPC-2604-A1	OH	Cl	H	Cl	H	Cl	Cl	Br			0.099

### 3.2.6 Structural Determination of Miscellaneous Triclosan Derivatives

Other possible PfENR inhibitors evaluated in this study are triclosan derivatives which do not totally resemble the ring A and B structure of triclosan, we have denoted those as miscellaneous analogs (Table 11). This type of analogs was thought to fit in the inhibitor binding pocket in PfENR. Eighty-seven analogues of this type were evaluated and we found that the minimum  $IC_{50}/IC_{90}$  value for the whole cell assay for compound **JPC-2506-A1** (0.04/0.07  $\mu\text{g}/\text{mL}$  for strains 3D7<sup>a</sup> and 0.07/0.16  $\mu\text{g}/\text{mL}$  for strains Dd2<sup>a</sup>) was ten times more potent than triclosan. However, this compound has an  $IC_{50}$  value for the enzymatic assay higher than 50  $\mu\text{M}$ .

On the other hand, the maximum  $IC_{50}/IC_{90}$  value for the whole cell assay was found to be higher than 50/50  $\mu\text{g}/\text{mL}$  for both strains 3D7<sup>a</sup> and Dd2<sup>a</sup> in several compounds in this series. For the enzymatic assay, we found that the maximum  $IC_{50}$  value for most of the compounds in this series was higher than 50  $\mu\text{M}$ , and the minimum was 0.28  $\mu\text{M}$  (approximately ten times less potent than triclosan) for compound **JPC-2195-A1** and a whole cell  $IC_{50}/IC_{90}$  value of 6/12  $\mu\text{g}/\text{mL}$  for strain 3D7<sup>a</sup> and 14/23  $\mu\text{g}/\text{mL}$  for Dd2<sup>a</sup>. This value for the enzymatic assay is not surprising due to the fact that this compound still conserves some characteristics of the triclosan scaffold, such as the chlorophenol ring A required for the inhibitory activity of this type of compounds (Table 11). Other miscellaneous inhibitor which showed considerable inhibitory activity were: compound **JPC-2147-A1** with an  $IC_{50}$  value of 0.57  $\mu\text{M}$ , compound **JPC-2188-A1** with an  $IC_{50}$  value of 3.3  $\mu\text{M}$ , compounds **JPC-2128-A1** with an  $IC_{50}$  of 21.4  $\mu\text{M}$ . In addition compound **JPC-2129-A1** with an  $IC_{50}$  of 17  $\mu\text{M}$  and compound **JPC-2209-A1** with an

IC<sub>50</sub> of 13.8 μM are the most significant considering the variation of the triclosan scaffold that could affect the interactions of this molecule with PfENR-NAD<sup>+</sup> complex.

**Table 11.** Miscellaneous Triclosan Analogs

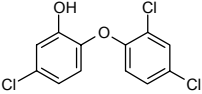
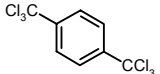
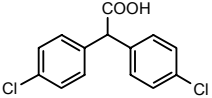
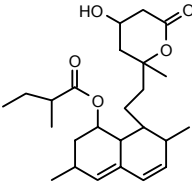
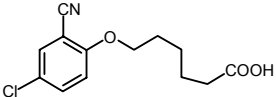
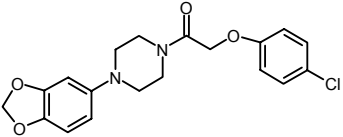
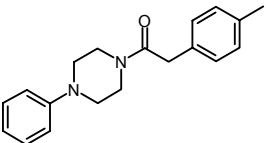
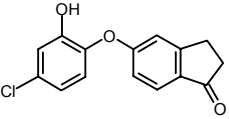
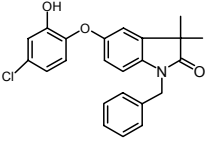
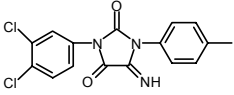
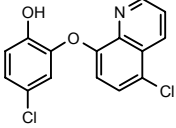
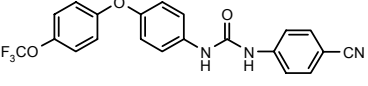
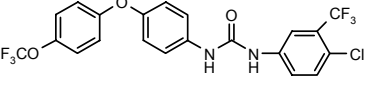
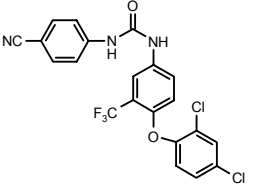
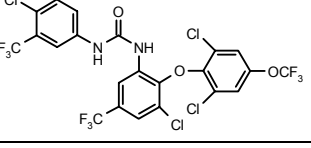
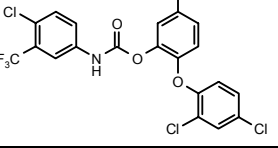
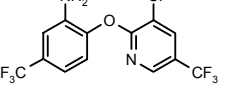
Compound	R	3D7 <sup>a</sup> EC <sub>50</sub> / EC <sub>90</sub> (μg/mL)	Dd2 <sup>a</sup> EC <sub>50</sub> / EC <sub>90</sub> (μg/mL)	PfENR <sup>b</sup> IC <sub>50</sub> (μM)
triclosan		0.4±0.1 / 0.7±0.1	0.9±0.1 / 1.8±0.3	0.034
JPC-2072-A1		0.4 / 2.6	0.3 / 1	>50
JPC-2074-A1		7.7 / 13.6	7 / 12	>50
JPC-2075-A1		30±7 / >50	>50 / >50	>50
JPC-2089-A1		48.6 / >50	48.0 / >50	>50
JPC-2092-B1		40 / >50	35 / >50	>50
JPC-2093-A1		35 / >50	24 / >50	>50

Table 11. Continued

Compound	R	3D7 <sup>a</sup> EC <sub>50</sub> / EC <sub>90</sub> (μg/mL)	Dd2 <sup>a</sup> EC <sub>50</sub> / EC <sub>90</sub> (μg/mL)	PfENR <sup>b</sup> IC <sub>50</sub> (μM)
JPC-2108-A1		1 / 4	0.6 / 1	>50
JPC-2116-A1		13 / 27.5	10 / 21	>50
JPC-2117-A1		6.5 / 17	4.6 / 9	>50
JPC-2124-A1		5/10	1/19	>50
JPC2128-A1		4.6/8.7	4/6	21.4
JPC-2129-A1		10/21	7/18	17
JPC-2147-A1		9/8	19/21	0.570
JPC-2164-A1		12/18	25/42	9.7
JPC-2185-A1		21/48	30/50	17.7
JPC-2188-A1		1 / 2	2 / 4	3.32

Table 11. Continued

JPC-2195-A1		6/ 12	14/ 23	0.28
JPC-2209-A1		2.5/5.5	4.6 / 7	13.8
JPC-2222-A1		4.7/7.4	3.5/6	>50
JPC-2310-A1		2.6/4.6	3.5/6	>50
JPC-2347-A1		0.7/1.4	0.8/1.5	>50
JPC-2365-A1		0.15/0.2	0.14/0.2	>50
JPC-2497-A1		0.3/0.7	0.3/0.6	>50
JPC-2506-A1		0.04/0.07	0.07/0.16	>50
JPC-2546-A1		0.6/0.8	0.6/0.7	>50
JPC-2553-A1		48/>50	43/>50	>50

### 3.3 Discussion

The results described above represent a significant achievement in understanding of the mode of binding of triclosan derivatives to PfENR. Thus, substitutions in positions 1,5 of ring A and 2',4' of ring B as well as the linker (ether atom) position gave us a better visualization of the capacity to design and obtain new potent drugs which target PfENR by modification of triclosan scaffold.

The triclosan binding site resembles that of bacterial FabI from *E. coli* and *M. tuberculosis*, explaining why triclosan and structurally related compounds strongly inhibit PfENR<sup>11</sup>. It has been shown that a single point mutation (A217V) confers triclosan resistance in *E. coli*. In addition, Kapoor et al.<sup>74</sup> have studied the effect of mutations in the binding site of triclosan to PfENR, to characterize the role played by residues like A, N, M and F in triclosan binding generating the following mutations: A217V, A217G, N218A, N218D, M281A, M281T, F368A and F368I, concluding that the mutation of Ala 217 to Val result in unacceptable steric contacts between the side chain of Valine and triclosan, leading to reduced affinity of triclosan for the enzyme, which is the same effect produced by the other mutations. Therefore, to design better inhibitors derived from triclosan scaffold resistance mechanisms used for the parasite have to be taken into consideration.<sup>21,74,76</sup>

Antibacterials like diazaborines (thienodiazaborines or benzodiazaborines) isoniazid target ENR in *E. coli*, *M. tuberculosis* and *P. falciparum* by forming covalent bond between the 2'hydroxyl of the nicotinamide ribose and a boron atom in the drugs to generate a tight, non covalently bound bisubstrate analog.<sup>93</sup>



The position of the aromatic bicyclic ring of the diazaborine, indole naphthyridones, Genz-8575, Genz-10850 and triclosan above the nicotinamide ring forming  $\pi$ - $\pi$  stacking interactions among others inhibitors resembles the model proposed for the binding of the enoyl substrate on the basis of studies in *B. napus* ENR.<sup>94</sup> In the seeking for new antimicrobials that target fatty acid biosynthesis, high-throughput screening to identify inhibitors of *E.coli* ENR have led to the finding of 2-(alkylthio)-4,6 diphenylpyridine-3-carbonitriles “thiopyridines” that were capable of inhibit purified ENR and the cells of *S. aureus* and *B. subtilis* showing to be effective fatty acid biosynthesis inhibitors.<sup>95</sup> In addition new metabolites (iridoid glycoside, pyrrolidinium derivatives, phenylethanoid glycosides, luteolin 7-*O*- $\beta$ -*D*-glucopyranoside with IC<sub>50</sub> values of 2.4  $\mu$ g/mL and chrysoeriol 7-*O*- $\beta$ -*D*-glucopyranoside with IC<sub>50</sub> value of 5.9  $\mu$ g/mL, against the parasite among others metabolites) isolated from *Phlomis brunneogaleata* have been recently tested by Tasademir et al.<sup>96</sup> as possible compounds to treat malaria which have PfENR as a target, showing for compound luteolin 7-*O*- $\beta$ -*D*-glucopyranoside an IC<sub>50</sub> value of 10  $\mu$ g/mL, this compound is suggested to be the first anti-malarial natural product targeting PfENR.<sup>96</sup>

For the triclosan derivatives evaluated in this study replacement of the hydroxyl group at position one of triclosan resulted in the finding of new potent inhibitors (urea series), as is the case with compound **JPC-2201-A1** which resulted in satisfactory inhibitory activity against the parasite (20 times more active than triclosan) However, this compound did not have any effect on PfENR activity. A similar scenario was found when modifications in the linker ether group took place. When complex organic modifications were added to the structure at this ether position the inhibitory capacity of the resulted

analog was affected. Meanwhile, substitutions capable of generating hydrogen bonding as is exemplified by the amino in compound **JPC-2578-A1** (almost as potent as triclosan), are capable of maintaining the interactions at this position stabilizing the binding of these analog to PfENR. Moreover, replacement of chloride groups at position 2' and 4' with groups that have hydrogen bonding characteristics, as is the case of compounds **JPC-2136-A1** (almost 20 times less active than triclosan in both the whole cell and the PfENR assay) with an amino group that targets the enzyme, has low potency against the parasite. This does not happen with the nitro group of compound **JPC-2137-A1** that has shown to be very effective (three times less active than triclosan) against both, the enzyme and the parasite. On the other hand, for compounds where more complex groups were introduced, as in the case of the group of 1H-tetrazol-5-yl compound **JPC-2141-A1**, it was not effective against the parasite (50 times less potent than triclosan) but had a reasonable activity (10 times less potent than triclosan) against the PfENR. Another compound capable of generating hydrogen bonds at this position was resulted from morpholine-4-carboxylic acid group, compound **JPC-2153-A1** which, in fact, had interactions with Ala219 and Asn218 responsible of the hydrogen bond formation at this region of the protein. This compound also had moderate activity (30 times less active than triclosan) against PfENR and low activity (50 times less potent than triclosan) against the parasite. This also occurred with the N-methyl amide of **JPC-2166-A1** which had potent inhibitory activity (10 folds less potent than triclosan) against the enzyme but moderate activity (30 times less effective than triclosan) against the parasite.

The replacement of the chloride group at position 5 of triclosan for groups capable of generating new  $\pi$ - $\pi$  stacking interaction with Tyr267, Try277 or Phe368 (as

was the case for the inhibition in ENRs from other organism, e.i. InhA in *mycobacterium tuberculosis*)<sup>97</sup> led to the determination of the binding characteristics for compound **JPC-2305-A1**. A tolyl group was placed at this position, improving the activity against the parasite as well as the activity against PfENR, which was only five times less than that for triclosan.

The IC<sub>50</sub> values obtained in this study allows correlating the potency of triclosan analogs as inhibitor of PfENR. However, for those analogs that do not target the enzyme, for example most of the urea (substitutions at position one of triclosan) compounds and most of the phenylsulphonamides (substitutions at position two) derivatives but are potent inhibitor of *P.falciparum* in the whole cell assay, to answer the questions about what is the target of these compound within the parasite define the new challenges in this research. Therefore, to investigate in vitro drug interactions of two antimalarials, standard dose-response assays over a range of individual drug concentrations are used. Knowing this information, a graphical representation of growth inhibition data for two compounds, plotted as fractional IC<sub>50</sub> values on an X-Y axis (isobologram) permit the determination of whether the two compounds are synergistic, additive or antagonistic allowing a more clear understanding of the mode of action of these drugs in the parasite.<sup>5</sup>

In general, a low percentage of the inhibitors generated in this study had considerable inhibitory activity against PfENR. However none of these inhibitors shown a better inhibitory activity than triclosan in the enzymatic determination, nevertheless several of these inhibitors were very potent against the parasite, leading us to formulate some hypothesis about the possible targets of those derivatives within the parasite.

There are several studies reporting the mode of action of triclosan in different organisms.<sup>98,99</sup> Inhibition of fatty acid biosynthesis is the most widely accepted.<sup>99</sup> However, it was originally thought that triclosan acted nonspecifically by disrupting cellular membranes<sup>99</sup>. Therefore, it is likely that the triclosan derivatives evaluated in this study have other targets within the intracellular components of the parasite (trophozoite, intra-erythrocytic stage of the life cycle).<sup>93,97-100</sup>

Taking into account the remarkable information obtained with the genome mapping of *P. falciparum*, where it was determined 5,268 predicted proteins, of which, 733 were identified as enzymes, 2/3 of the proteins appear to be unique to this organism and, 551 nuclear-encoded proteins may target the apicoplast and or mitochondrion. Within these proteins are housekeeping enzymes involved in DNA replication and repair, transcription, translation and post-translational modification, cofactor synthesis, protein import, protein turnover, and specific metabolic and transport activities. Moreover, it was also found that the apicoplast has a 35-kb genome that encodes 30 proteins and in addition to fatty acid biosynthesis, other important functions like anabolic synthesis of isoprenoids and hemes take place in this organelle.<sup>6,101-109</sup> Therefore, with this genetic information we can hypothesize about the possible targets that allow an alternative mode of action for the triclosan analogs described in this study which, do not have an effective enzymatic activity against PfENR, however are very potent whole cell growth inhibitors, as is the case of the urea (substitutions at position one of triclosan) compounds and phenylsulphonamides (substitutions at position two) derivatives.

For the *in vivo* determination of the potency of triclosan derivatives described in this study we used the erythrocytic (trophozoite) stage of the parasite. Therefore, from the

metabolism point of view, erythrocytic *P. falciparum* relies principally on anaerobic glycolysis for energy production, with regeneration of  $\text{NAD}^+$  by conversion of pyruvate to lactate.<sup>6,110,111</sup> It is known that genes encoding all of the enzymes necessary for a functional glycolytic pathway (PFK, pentose phosphates pathway, but not fructose biphosphatase) are present in *P. falciparum*, as well as the genes necessary for a complete TCA cycle, including a complete pyruvate dehydrogenase complex (likely to be localized in the apicoplast). In addition to genes encoding all subunits of the catalytic  $F_1$  portion of ATP synthase, and the gene that encodes the proteolipid subunit *c* for the  $F_0$  portion of ATP synthase. It is also known that chorismate is made from erythrose 4-phosphate and phosphoenolpyruvate via the shikimate pathway and that all the life cycle stages of the parasite are incapable of the *de novo* purine synthesis.<sup>6,112-119</sup>

Considering the facts quoted above, it is reasonable to suggest these important metabolic pathways as possible targets for the action of the triclosan derivatives evaluated in this study which are potent inhibitors of *P. falciparum*.

We can also consider the transport system within the parasite as a possible target for these inhibitors. The presence of an elaborate membrane transporter system are lacking in *P. falciparum* genome, particularly, for uptake of organic nutrients, there are low percentage of multispinning membrane proteins, and no amino acid transporter, emphasizing the importance of hemoglobin digestion within the food vacuole as an important source of amino acids for the erythrocytic stages of the parasite, where it is also found transporters for the mobilization of inorganic ions, export of drugs and hydrophobic compounds<sup>6,112,120</sup>. Moreover sodium/proton, calcium/proton exchangers as well as other metal cation transporters were identified. The parasite contains all subunits

of V-type ATPase as well as two proton translocating pyrophosphatases, which could be used to generate a proton motive force, possibly across the parasite plasma membrane as well as across a vacuolar membrane.<sup>6,119,120</sup> The proton pumping pyrophosphatases are not present in mammals, and could form an attractive antimalarial targets.<sup>6</sup>

Dealing with DNA replication, repair and recombination, taking into account the genomic information it is known that the core of eukaryotic nucleotide excision repair is present in *P. falciparum*, although others proteins could not be found, being the same case for proteins involve in the homologous recombination and repair.<sup>6,120</sup> However, there are no known inhibitors of this system in malaria. Therefore, this will be a possible target to study in the search for the mode of action of these triclosan analogs.

For the secretory pathways the parasite contains genes encoding proteins that are important in protein transport in other eukaryotic organisms, there are homologs of important components of the signal recognition particle, the translocon, the signal peptidase complex and many components that allow vesicle assembly, docking and fusion, making this system another reasonable target to consider for the action of these inhibitors.<sup>6,120,121</sup>

In connection with fatty acid biosynthesis, it is known that the surface of bloodstream stage of apicomplexan parasites (*Trypanosome brucei* and *P. falciparum*) contains the glycosyl phosphatidylinositol (GPI) anchor of the parasite variant surface glycoprotein (VSG) that enshrouds the cell surface of the parasite, protecting it from destruction by the host immune system.<sup>92,121,122</sup> This GPI is unusual in that its fatty acyl moiety is exclusively myristate, a 14-carbon saturated fatty acid that is efficiently salvages and processes myristate from the blood stream, but it also makes myristate *de*

*novo* using a reaction pathway known as fatty acid remodeling, where myristate is post-synthetically incorporated into the GPI precursor.<sup>92,113-115,122</sup> Paul et al<sup>96</sup>. Studying *Trypanosome brucei* found that triclosan inhibited multiple steps of the *in vitro* fatty acid remodeling pathway in the same concentration range required to kill *Trypanosome brucei* in culture, also similar concentration of triclosan inhibited myristate exchange, a second biochemically distinct myristoylation pathway. However, it is likely that the fatty acid remodeling and myristate exchange pathways are being nonspecifically inhibited by triclosan perhaps, by perturbation of the membrane structure, it also have been shown that triclosan, being very hydrophobic, was incorporated into bacterial and eukaryotic membranes producing a subtle alteration of the physicochemical properties of artificial lipids bilayers and liposomes. It is suggested that in *T. brucei*, triclosan acts upon cellular membranes, perturbing their physical properties and thereby disrupting the function of some membrane resident enzymes.<sup>93,97,100,122</sup>

Considering the finding of the mode of action of triclosan in *T. brucei*, we can hypothesize the possibility that some of the triclosan derivatives evaluated in this study can have the same mode of action in the *in vivo* evaluation of *P falciparum*.<sup>123</sup>

Another situation faced by antimicrobials and other small molecules to sequestered parasites is the transporting of the inhibitors within the cell which could affect the inhibitory potency of the drug due to its limitation to reach de desire target, one method to avoid this situation for triclosan delivery in *Toxoplasma gondii* (tachyzoites) was to use triclosan conjugated to arginine oligomers. Triclosan released after conjugation to octaarginine via a readily hydrolysable ester linkage inhibits ENR activity, tachyzoites *in vitro*, and tachyzoites in mice. If this is the case for the inhibitors in this

study, one future challenge to face in continuing exploring triclosan analogs will be their delivery into the microorganism (*P. falciparum*). Therefore, to use oligomers of arginine will become a suitable alternative to overcome this problem and ensure that the drug gets into the parasite to further explore and understand its mechanism of action.<sup>120-124</sup>



## CHAPTER IV

### CONCLUSIONS AND FUTURE WORK

Diseases produced by microorganism have been a health problem in every society around the world since ancient times. Infections like malaria, tuberculosis, leishmania, and Chagas disease, among others transmitted by microorganisms, are responsible for millions of deaths annually mainly in developing nations. Therefore, there is an urgent need for the development of antimicrobial agents that are inexpensive and capable of controlling the disease without being harmful to humans. Considering the fact that metabolic pathways like fatty acid biosynthesis are different in these microorganisms compared to mammalian cells we used a known bacterial and apicomplexan fatty acid synthase inhibitor, triclosan, as a scaffold to generate analogs of this molecule. Triclosan is a compound that has some of the characteristics quoted above, however due to its biolability its use in humans as an antimalarial drug is not yet suitable. Therefore, the data presented in this study provides significant information about the structural characteristics and properties of the interactions for several types of triclosan analogs in the search for new antimalarial drugs that target PfENR. Almost 5% of the 520 inhibitors evaluated targeted PfENR, and we were able to establish structural information on the mode of binding for six of those inhibitors.

The information obtained from the crystallographic structures of the analogs gives remarkable information about the type of substituent that can be placed in different positions in ring A and B of triclosan to improve the binding capacity of the resulting analog to PfENR. The correlation on the data obtained for some of the analogs for the *in*

*vivo* (anti parasite) and the *in vitro* (anti PfENR) activity allow us to confirm the inhibition of fatty acid biosynthesis.

The SAR study of these triclosan analogs proved to be an effective strategy to narrow down the effective search for development of antimalarial drugs that specifically target fatty acid biosynthesis. Moreover, the finding of the urea and phenylsulphonamides compounds, which are very potent inhibitors of the erythrocytic (trophozoite) stage of the parasite but do not target PfENR, create a new challenge for the improvement of their inhibitory activity in addition to the determination of the mode of action of these inhibitors in *P. falciparum*.

The triclosan derivatives obtained from modifications in position 5 of ring A and 4' of ring B offers significant information about the kind of modification that can be tolerated for this region in the binding side of PfENR, opening up the possibility of generating new chimera compounds by combination of effective substituents at these positions in the triclosan scaffold.

There is still a long way to go in the fight against malaria and other diseases produced by microorganisms. However, with the establishment of the genome map of these organisms and structural biology studies we can ensure the discovery of a drug capable of controlling this disease will soon be a reality.

Future work in the research of PfENR inhibitors as a strategy to control malaria include the evaluation of the activity of different chemical libraries of compounds to ensure a diversity of possible chemical structures that could bind to PfENR. Laboratory here at Texas A&M as well as pharmaceutical companies like GlaxoSmithKline are currently undergoing projects to screen 500,000 compounds against PfENR<sup>21</sup>. In addition malaria produced by *Plasmodium vivax* is also a threat responsible for many deaths around the world. Therefore, evaluation of the triclosan derivatives obtained in this study as well as structural studies of the *Plasmodium vivax* ENR (PvENR) will be a major priority to better understand the effects of these compounds in other plasmodium species.

In this study we obtained six crystallographic structures of PfENR-NAD<sup>+</sup>-triclosan analogs. However, there are many more of these analogs from which we could get X-ray structures to better understand their mode of binding to PfENR. Therefore, one priority in continuing this research will be to obtain crystal structures of derivatives where substitutions at position 5 and 6 of ring A as well as position 4' of ring B were made, to continue gaining more information about the interactions taking place in the PfENR active site with different triclosan analogs.

## REFERENCES

- (1) RPH Laboratory Medicine **2002**,  
<http://www.rph.wa.gov.au/labs/haem/malaria/history.html>, March **2005**.
- (2) Jeffrey S.; Pia M. The economical and social burden of malaria. *Nature*. **2002**, *415*, 680-685.
- (3) Thomas L.R.; Allan S. Progress and challenges for malaria vaccines. *Nature*. **2002**, *415*, 694-701.
- (4) University of Minnesota, <http://ipmworld.umn.edu/chapters/curtiscf.htm>, February **1996**.
- (5) Fidock D.A., Philip J., Rosenthal S., Croft L., Reto B., and Nwaka S. Antimalarial drug discovery: Efficacy models for compound screening. *Nature. Reviews*. **2004**, *3*, 509-512.
- (6) Gardner M.J., Hall N., Fung E., White O., Berriman M., et al. Genome sequence of the human malaria parasite *Plasmodium falciparum*. *Nature*. **2000**, *419*, 498-511.
- (7) Campbell, J. & Cronan, J. Bacterial fatty acid biosynthesis: targets for antibacterial drug discovery. *Annu Rev Microbiol*. **2001**, *55*, 305-32.
- (8) Gornicki, P. Apicoplast fatty acid biosynthesis as a target for medical intervention in apicomplexan parasites. *Int J Parasitol*. **2003**, *33*, 885-96.
- (9) McLeod, R.; Muench, S.; Rafferty, J.; Kyle, D.; Mui, E.; Kirisits, M.; Mack, D.; Roberts, C.; Samuel, B.; Lyons, R.; Dorris, M.; Milhous, W. & Rice, D. Triclosan inhibits the growth of *Plasmodium falciparum* and *Toxoplasma gondii* by inhibition of apicomplexan Fab I. *Int J Parasitol*. **2001**, *31*, 109-13.
- (10) Wiesner, J. Seeber, F. The plastid-derived organelle of protozoan human parasites as a target of established and emerging drugs. *Expert Opin. Ther. Targets*. **2005**, *9*, 23-44.
- (11) Perozzo, R.; Kuo, M.; Sidhu, A.; Valiyaveetil, J.; Bittman, R.; Jacobs, J.; Fidock, D. & Sacchettini, J.C., Structural elucidation of the specificity of the antibacterial agent triclosan for malarial enoyl acyl carrier protein reductase. *J Biol Chem*. **2002**, *277*, 13106-14.
- (12) Levy, C.; Roujeinikova, A.; Sedelnikova, S.; Baker, P.; Stuitje, A.; Slabas, A.; Rice, D. & Rafferty, J. Molecular basis of triclosan activity. *Nature*. **1999**, *398*, 383-4.
- (13) Lily McClure & Josh Cargill, **2003**, <http://www.sirinet.net>, March **2005**.
- (14) Surolia, N. & Surolia, A. Triclosan offers protection against blood stages of malaria by inhibiting enoyl-ACP reductase of *Plasmodium falciparum*. *Nat Med*. **2001**, *7*, 167-73.

- (15) Wang L.Q.; Falany C.N.; James M.O. Triclosan as a Substrate and Inhibitor of 3'-Phosphoadenosine 5'-Phosphosulfotransferase and UDP-Glucuronosyl Transferase in human liver fractions. *Drug Metabolism and Disposition*. **2004**, *32*, 1162-1169.
- (16) Sharma S., Ramya T.N., Surolia A., Surolia N. Triclosan as a systemic antibacterial agent in a mouse model of acute bacterial challenge. *Antimicrob. Agents. Chemother.* **2003**, *47*, 3859-3866.
- (17) The World Health Report: Reducing risks, promoting healthy life. *World Health Organization*, <http://www.who.int/whr/2002/en/index.html>, **2002**.
- (18) Warrell, D.A. & Gilles, H.M Essential Malariology, *Arnold*, **2002**, 55-72.
- (19) Gidelines for malaria prevention in sub-Saharan Africa, [http://www.netdoctor.co.uk/travel/malaria\\_prevention/subsaharan\\_africa.htm](http://www.netdoctor.co.uk/travel/malaria_prevention/subsaharan_africa.htm) **1998-2005**, March **2005**.
- (20) Lokeshwar M.R.; Malaria in children, an overview, <http://www.pediatriconcall.com/for-doctor/diseasesandcondition/malaria.asp>, **2000**, March **2005**.
- (21) Zhiquiang J.L., Lee P. J., Waters N. C and Prigge S. T. Fatty acid synthesis as a target for antimalarial drug discovery. *Combinatorial chemistry and high throughput screening*. **2005**, *8*, 15-26.
- (22) Ralph, S.; D'Ombra, M. & McFadden, G. The apicoplast as an antimalarial drug target. *Drug Resist Updat.* **2001**, *4*, 145-51.
- (23) Ryall, K.; Harper, J. & Keeling, P. Plastid-derived Type II fatty acid biosynthetic enzymes in chromists. *Gene*. **2003**, *313*, 139-48.
- (24) Wilson, R.; Rangachari, K.; Saldanha, J.; Rickman, L.; Buxton, R. & Eccleston, J. Parasite plastids: Maintenance and functions. *Philos Trans R Soc Lond B Biol Sci.* **2003**, *358*, 155-62; discussion 162-4.
- (25) Voet D.; Voet J.G.; Biochemistry second edition. *John Wiley and Sons Inc.* **1995**, 680-688.
- (26) Waller, R. & McFadden, G. The apicoplast: a review of the derived plastid of apicomplexan parasites. *Curr Issues Mol Biol.* **2000**, *7* 57-79.
- (27) Gornicki, P. Apicoplast fatty acid biosynthesis as a target for medical intervention in apicomplexan parasites. *Int. J. Parasitol.* **2003**, *33*, 885-896.
- (28) Rangan, V.S, Smith S. Fatty acid synthesis in eukaryotes. *Biochemistry of lipids, lipoproteins and membranes*. Vence D.E, Elsevier Science, Amsterdam **2002**, 151-179.
- (29) Heath R.J, White S.W, Rock C.O. Inhibition of fatty acid synthesis as antimicrobial chemotherapeutics. *Appl. Microbiol. Biotechnol.* **2002**, *58*, 695-703.
- (30) Campbel J.W cronan J.E. Bacterial fatty acid biosynthesis: targets for antibacterial drug discovery. *Annu. Rev. Microbial*, **2001**, *55*, 305-332.
- (31) Heath R.J, Rock C.O. Fatty acid biosynthesis as a target for novel antibacterials. *Curr. Opin. Investig. Drugs.* **2004**, *5*, 146-153.
- (32) Waller R. F, Keeling P.J, Donald R.G. Nuclear-encoded proteins target to plastid in *Toxoplasma gondii* and *Plasmodium falciparum*. *Proc. Natl. Acad. Sci. USA*, **1998**, *95*, 12352-12357.

- (33) Waller, R.; Ralph, S.; Reed, M.; Su, V.; Douglas, J.; Minnikin, D.; Cowman, A.; Besra, G. & McFadden, G. A type II pathway for fatty acid biosynthesis presents drug targets in *Plasmodium falciparum*. *Antimicrob Agents Chemother.* **2003**, *47*, 297-301.
- (34) Soldati, D. The apicoplast as a potential therapeutic target in and other apicomplexan parasites. *Parasitol Today.* **1999**, *15*, 5-7.
- (35) Surolia, A.; Ramya, T.; Ramya, V. & Surolia, N. 'FAS't Inhibition of malaria. *Biochem J.* **2004**, *383*, 401-12.
- (36) Foth B. J., McFadden, G. I. The apicoplast: a plastid in *Plasmodium falciparum* and other Apicomplexan parasites. *Int. Rev. Cytol.* **2003**, *224*, 57.
- (37) Jelenska J., Sirikhachornkit A., Haselkorn R., and Gornicki P. The carboxyltransferase activity of the apicoplast acetyl-CoA carboxylase of *Toxoplasma gondii* is the target of aryloxyphenoxypropionate inhibitors. *J Biol Chem.* **2002**, *277*, 23208.
- (38) Konishi T., Yamada K., and Sasaki Y. Acetyl-CoA carboxylase in higher plants: most plants other than gramineae have both the prokaryotic and the eukaryotic forms of this enzyme. *Plant Cell Physiol.* **1996**, *37*, 117.
- (39) Konishi T., and Sasaki Y. Compartmentalization of two forms of acetyl-CoA carboxylase in plants and the origin of their tolerance toward herbicides. *Proc Natl Acad Sci U S A.* **1994**, *91*, 3598.
- (40) Waller R.F., Ralph S. A., Reed M. B., Su V., Douglas J. D., Minnikin D.E., Cowman A. F., Besra G. S., and McFadden, G. I. A type II pathway for fatty acid biosynthesis presents drug targets in *Plasmodium falciparum*. *Antimicrob Agents Chemother.* **2003**, *47*, 297.
- (41) Zagnitko O., Jelenska J., Tevzadze G., Haselkon R. and Gornicki P. An isoleucine/leucine residue in the carboxyltransferase domain of acetyl-CoA carboxylase is critical for interaction with aryloxyphenoxypropionate and cyclohexanedione inhibitors. *Proc Natl Acad Sci U S A.* **2001**, *98*, 6617.
- (42) Zhang H., Yang Z., Shen Y., and Tong L. Crystal structure of the carboxyltransferase domain of Acetyl-Coenzyme A Carboxylase. *Science.* **2003**, *299*, 2064.
- (43) Zhang H., Tweel B., and Tong L. Molecular basis for the inhibition of the carboxyltransferase domain of acetyl-coenzyme-A carboxylase by haloxyfop and diclofop. *Proc. Natl. Acad. Sci. USA.* **2004**, *101*, 5910.
- (44) Waller, R. F., Reed M. B., Cowman A. F and McFadden, G. I. Protein trafficking to the plastid of *Plasmodium falciparum* is via the secretory pathway. *EMBO Journal.* **2000**, *19*, 1794.
- (45) Waller R. F., Keeling P. J., Donald R. G., Striepen, B., Handman E., Lang-Unnasch N., Cowman A. F., Besra G. S., Roos D. S and McFadden, G. I. Nuclear-encoded proteins target to the plastid in *Toxoplasma gondii* and *Plasmodium falciparum*. *Proc Natl Acad Sci U S A.* **1998**, *95*, 12352.
- (46) Elovson J., and Vagelos, P., R. Acyl carrier protein. X. acyl carrier protein synthetase. *J Biol Chem.* **1968**, *243*, 3603.
- (47) Brenner S. The molecular evolution of genes and proteins: a tale of two serines. *Nature.* **1988**, *334*, 528.

- (48) Prigge S. T., He X., Gerena L., Waters N. C., and Reynolds K. A. Oxygen and hydrogen isotope effects in an active site tyrosine to phenylalanine mutant of peptidylglycine alpha-hydroxylating monooxygenase: mechanistic implications. *Biochemistry*. **2003**, *42*, 1160.
- (49) Serre L., Verbree E. C., Dauter Z., Stuitje A. R., and Derewenda, Z. S. The *Escherichia coli* malonyl-CoA:acyl carrier protein transacylase at 1.5-Å resolution. Crystal structure of a fatty acid synthase component. *J Biol Chem*. **1995**, *270*, 12961.
- (50) Kremer L., Namppoothiri K. M., Lesjean S., Dver L. G., Graham S., Betts J., Brennan P. J., Minnikin D. E., Loch C., and Besra G. S. Biochemical characterization of acyl carrier protein (AcpM) and malonyl-CoA:AcpM transacylase (mtFabD), two major components of *Mycobacterium tuberculosis* fatty acid synthase II. *J Biol Chem*. **2001**, *276*, 27967.
- (51) Zhang. Y., and Cronan J. E. Jr. Transcriptional analysis of essential genes of the *Escherichia coli* fatty acid biosynthesis gene cluster by functional replacement with the analogous *Salmonella typhimurium* gene cluster. *J Bacteriol*. **1998**, *180*, 3295.
- (52) Waller R. F., Keeling P. J., Donald R. G., Striepen, B., Handman E., Lang-Unnasch N., Cowman A. F., Besra G. S., Roos D. S and McFadden, G. I. Nuclear-encoded proteins target to the plastid in *Toxoplasma gondii* and *Plasmodium falciparum*. *Proc Natl Acad Sci U S A*. **1998**, *95*, 12352.
- (53) Prigge S. T., He X., Gerena L., Waters N. C., and Reynolds K. A. Oxygen and hydrogen isotope effects in an active site tyrosine to phenylalanine mutant of peptidylglycine alpha-hydroxylating monooxygenase: mechanistic implications. *Biochemistry*. **2003**, *42*, 1160.
- (54) Waller R.F., Ralph S. A., Reed M. B., Su V., Douglas J. D., Minnikin D.E., Cowman A. F., Besra G. S., and McFadden, G. I. A type II pathway for fatty acid biosynthesis presents drug targets in *Plasmodium falciparum*. *Antimicrob Agents Chemother*. **2003**, *47*, 297.
- (55) Tsay J. T., Rock C. O., and Jackowski S. Overproduction of beta-ketoacyl-acyl carrier protein synthase I imparts thiolactomycin resistance to *Escherichia coli* K-12. *J Bacteriol*. **1992**, *174*, 508.
- (56) Jones S. M., Urch J. E., Brun R., Harwood J. L., Berry C., and Gilbert I. H. Analogues of thiolactomycin as potential anti-malarial and anti-trypanosomal agents. *Bioorg Med Chem*. **2004**, *12*, 683.
- (57) Daines R. A., Pendrak I., Sham K., Van Aller G. S., konstantinidis A. K., Lonsdale J. T., Janson C. A., and Head M.S. First X-ray cocrystal structure of a bacterial FabH condensing enzyme and a small molecule inhibitor achieved using rational design and homology modeling. *J Med Chem*. **2003**, *46*, 5.
- (58) Campbell J. W., and Cronan J. E. Jr. Bacterial fatty acid biosynthesis: targets for antibacterial drug discovery. *Annu Rev Microbiol*. **2001**, *55*, 305.
- (59) Jornvall H., Persson B., Krook M., Atrians S., and Ghosh D. Short-chain dehydrogenases/reductases (SDR). *Biochemistry*. **1995**, *34*, 6003-13.
- (60) Oppermann U., Filling C., Hult M., Shafqat N., Kallberg Y., Person B., Lindh M., and Jornvall H. Short-chain dehydrogenases/reductases (SDR): the 2002 update *Chemico-Biological Interaction*. **2003**, *247*, 143-144.

- (61) Pillai S., Rajagopal C., Kapoor M., Kumar G., Gupta A., and Surolia N. Functional characterization of beta-ketoacyl-ACP reductase (FabG) from *Plasmodium falciparum*. *Biochemical and Biophysical Research Communications*. **2003**, 303, 387.
- (62) Wright H., Cofactors in fatty acid biosynthesis-active site organizers and drug targets. *Structure (Camb)*. **2004**, 12, 358.
- (63) Price A. C., Zhang Y. M., Rock C. O., and White S. W., Structure of beta-ketoacyl-[acyl carrier protein] reductase from *Escherichia coli*: negative cooperativity and its structural basis. *Biochemistry*. **2001**, 40, 12772.
- (64) Heath, R.J.; Rubin, J. R.; Holland, D. R.;Zhang, E.; Snow, M. E.; Rock, C. O.; Mechanism of triclosan inhibition of bacterial fatty acid synthesis. *J. Biol. Chem.* **1999**, 274, 11110-11114.
- (65) Sharma S. K., Kapoor M., Ramya T. N., Kumar S., Sharma S., Surolia N. and Surolia A., Identification, characterization, and inhibition of *Plasmodium falciparum* beta-hydroxyacyl-acyl carrier protein dehydratase (FabZ). *Journal of Biological Chemistry*. **2003** , 278, 45661.
- (66) Mohan S., Kelly T. M., Eveland S.S., Raetz C. R., and Anderson M. S., An *Escherichia coli* gene (FabZ) encoding (3R)-hydroxymyristoyl acyl carrier protein dehydrase. Relation to fabA and suppression of mutations in lipid A biosynthesis. *Journal of Biological Chemistry* **1994**, 269, 32896.
- (67) Brock D.J., Kass L. R., and Bloch K., Beta-hydroxydecanoyl thioester dehydrase. II. Mode of action. *Journal of Biological Chemistry*. **1967**, 242, 4432.
- (68) Leesong M., Henderson B. S., Gillig J. R., Schwab J. M., and Smith J. L., Structure of a dehydratase-isomerase from the bacterial pathway for biosynthesis of unsaturated fatty acids: two catalytic activities in one active site. *Structure*. **1996**, 4, 253.
- (69) Lakshmi Swarna M. P., Kumar S., Kapoor M., Surolia N., Surolia A., and Suguna K., Crystallization and preliminary crystallographic analysis of beta-hydroxyacyl ACP dehydratase (FabZ) from *Plasmodium falciparum*. *Acta Crystallographica section D: Biological Crystallography*. **2004**, 60, 120.
- (70) Bergler H., Wallner P., Ebeling A., Leitinger B., Fuchsbichler S., Aschauer H., Kollenz G., Hogenauer G., and Turnowsky F. Protein EnvM is the NADH-dependent enoyl-ACP reductase (FabI) of *Escherichia coli*. *J Biol Chem*. **1994**, 269, 5493.
- (71) Levy C. W., Roujeinikova A., Sedelnikova S., Baker P. J., Stuitje A. R., Alabas A. R., Rice D. W., and Rafferty J. B., Molecular basis of triclosan activity. *Nature*. **1999**, 398, 983.
- (72) Qiu X., Janson C. A., Court R. I., Smyth M. G., Payne D. J., and Abdel-Meguid S. S. Molecular basis for triclosan activity involves a flipping loop in the active site. *Protein Sci*. **1999**, 8, 2529.
- (73) Seefeld, M.; Miller, W.; Newlander, K.; Burgess, W.; DeWolf, J.; Elkins, P.; Head, M.; Jakas, D.; Janson, C.; Keller, P.; Manley, P.; Moore, T.; Payne, D.; Pearson, S.; Polizzi, B.; Qiu, X.; Rittenhouse, S.; Uzinskas, I.; Wallis, N. & Huffman, W. Indole naphthyridinones as inhibitors of bacterial enoyl-ACP reductases FabI and FabK. *J Med Chem*. **2003**, 46, 1627-35.



- (74) Kapoor M., Gopalakrishnapai J., Surolia N., Suralia A. Mutational analysis of the triclosan-binding region of enoyl-ACP (acyl-carrier protein) reductase from *Plasmodium falciparum*. *Biochem J.* **2004**, *381*, 735-41.
- (75) Ciba Specialty Chemicals, what is triclosan? **2000-2005**, <http://www.cibasc.com/ind-pc-triclosaninfo-general.htm>, March **2005**.
- (76) Rawat, R.; Whitty, A. & Tonge, P. The isoniazid-NAD adduct is a slow, tight-binding inhibitor of InhA, the *Mycobacterium tuberculosis* enoyl reductase: adduct affinity and drug resistance. *Proc Natl Acad Sci U S A.* **2003**, *100*, 13881-6.
- (77) Wang L.Q.; Falany C.N.; James M.O. Triclosan as a Substrate and Inhibitor of 3'-Phosphoadenosine 5'-Phosphosulfotransferase and UDP-Glucuronosyl Transferase in Human Liver Fractions. *Drug Metabolism and Disposition.* **2004**, *32*, 1162-1169.
- (78) Samuel B.U., Hearn B., Mack D. Delivery of antimicrobials into parasites. *Proc. Natl. Acad. Sci. USA*, **2003**, *100*, 14281-14286.
- (79) Sharma S., Ramya T.N., Surolia A., Surolia N. Triclosan as a systemic antibacterial agent in a mouse model of acute bacterial challenge. *Antimicrob. Agents. Chemother.* **2003**, *47*, 3859-3866.
- (80) Roa S.P., Surolia A., Surolia N. Triclosan: a shot in the arm for antimalarial chemotherapy. *Mol. Cell. Biochem.* **2003**, *253*, 55-63.
- (81) Vallalain J., Mateo C. R., Aranda F. J., Shapiros s., Micol V. Membranotropic effects of the antibacterial agent triclosa. *Arch. Biochem. Biophys.* **2001**, *390*, 128-136.
- (82) Lygre H., Moe G., Skalevik R., Holmsen H. Interaction of triclosan with eukaryotic membrane lipids. *Eur. J. Oral Sci.* **2003**, *111*, 216-222.
- (83) Wang L.Q., Falany C. N., James M. O. Triclosan as a substrate and inhibitor of PAPS-sulfotransferase and UDP-glucuronosyl transferase in human liver fractions. *Drug Metab. Dispos.* **2004**, *32*, 1162-1169.
- (84) Paul K.S., Bacchi C. J., Englund P. T. Multiple triclosan targets in *Trypanosoma bruce*. *Eukaryot. Cell.* **2004**, *3*, 855-861.
- (85) Liu B., Wang Y., Fillgrove K. L., Anderson V. E. Triclosan inhibits enoyl-reductase of type I fatty acid synthase *in vitro* and is cytotoxic to MCF-7 and SKBr-3 breast cancer cells. *Cancer Chemother Pharmacol.* **2002**, *49*, 187-93.
- (86) Copeland R.A. Enzymes a practical introduction to structure, mechanism, and data analysis. *Wiley-VCH*, second edition. **2000**, 267-303.
- (87) Rozwarski D.A., Grant G.A., Barton D.H., Jacobs W. R., and Sacchettini J.C. Modification of the NADH of the Isoniazid Target (InhA) from *Mycobacterium tuberculosis*. *Science.* **1998**, *279*, 98-102.
- (88) Pidugu, L.; Kapoor, M.; Surolia, N.; Surolia, A. & Suguna, K. Structural basis for the variation in triclosan affinity to enoyl reductases. *J Mol Biol.* **2004**, *343*, 147-55.
- (89) Russell, A. Whither triclosan? *J Antimicrob Chemother.* **2004**, *53*, 693-5.
- (90) Schweizer, H. Triclosan: a widely used biocide and its link to antibiotics. *FEMS Microbiol Lett.* **2000**, *202*, 1-7.

- (91) Muench, S.; Rafferty, J.; McLeod, R.; Rice, D. & Prigge, S. Expression, purification and crystallization of the *Plasmodium falciparum* enoyl reductase. *Acta Crystallogr D Biol Crystallogr.* **2003**, *59*, 1246-8.
- (92) Regos J., and Hitz H.R. Investigation on the mode of action of triclosan, a broad spectrum antimicrobial agent. *Zentbl. Bakteriolog. Orig. A.*, **1974**, *226*, 390-401.
- (93) Baldock C., de Boer G., Raffery J.B., Stuitje A.R., and Rice D.W. Mechanism of action of diazaborines. *Biochemical Pharmacology.* **1998**, *55*, 1541-1549.
- (94) Levy C.W., Baldock C., Wallace A.J., Sedelnikova S.E, Viner R.C., Slabas A.R., Rice D.W., and Raffery J.B., A Study of the structure-activity relationship for diazaborine inhibition of *E. coli* Enoyl –ACP reductase. *J. Mol Biol.* **2001**, 171-180.
- (95) Ling L.L., Xian j., Ali S., Geng B., Orgueira H., Ashwell M.A., Xiang Y., and Moir D.T. Identification and characterization of inhibitors of bacterial Enoyl-Acyl carrier protein reductase. *Antimicrobial Agents and Chemotheraphy.* **2004**, *48*, 1541-1547.
- (96) Tasdemir D., Gner N.D., Perozzo R., Brun R., Donmez A.A, Calis I., and Ruedi P. Anti protozoal and plasmodial FabI enzyme inhibiting metabolites of *Scrophularia lepidota* roots. *Phytochemistry.* **2005**, *66*, 355-362.
- (97) Kuo MR, Morbidoni HR, Alland D, Sneddon SF, Gourlie BB, Staveski MM, Leonard M, Gregory JS, Janjigian AD, Yee C, Musser JM, Kreiswirth B, Iwamoto H, Perozzo R, Jacobs WR Jr, Sacchettini JC, Fidock DA. Targeting tuberculosis and malaria through inhibition of enoyl reductase. *The Journal of Biological Chemistry.* **2003**, *278*, 20851-29859.
- (98) Paul K.S., Jiang D., Morita Y.S., Englund P.T. Fatty acid synthesis in African trypanosomes: a solution to the myristate mystery. *TRENDS in Parasitology.* **2001**, *17*, 381-387.
- (99) Paul K.S., Bacchhi C.J., Englund P.T. Multiple triclosan targets in *Trypanosome brucei*. *Eukaryotic Cell.* **2004**, *3*, 855-861.
- (100) Ferguson, M. A. The structure, biosynthesis and functions of glycosylphosphatidylinositol anchors, and the contributions of trypanosome research. *J. Cell Sci.* **1999**, *112*, 2799-2809.
- (101) Sherman , I.W. In *Malaria parasite biology, pathogenesis, and protection.* (ed. Sherman, I.W) ASM, Washington DC. **1998**, 135-143.
- (102) Clarke, J. L., Scopes, D. A., Sodeinde, O. & Mason, P. J. Glucose-6-phosphate dehydrogenase-6-phosphogluconolactonase. A novel bifunctional enzyme in malaria parasites. *Eur. J. Biochem.* **2001**, *268*, 2013-2019.
- (103) Lygre, H., G. Moe, R. Skalevik, and H. Holmsen. Interaction of triclosan with eukaryotic membrane lipids. *Eur. J. Oral Sci.* **2003**, *111*, 216-222.
- (104) Meincke, B. E., R. G. Kranz, and D. L. Lynch. Effect of irgasan on bacterial growth and its adsorption into the cell wall. *Microbios* **1980**, *28*, 133-147.
- (105) Villalain, J., C. R. Mateo, F. J. Aranda, S. Shapiro, and V. Micol. Membranotropic effects of the antibacterial agent Triclosan. *Arch. Biochem. Biophys.* **2001**, *390*, 128-136.
- (106) Paper: Baldock C., Raffery J.B, Sedelnikova S.E., Baker P. J., Stuitje A.R., and Rice D.W. A mechanism of drug action revealed by structural studies of enoyl reductase, *Science.* **1996**, *274*, 2107-2110.

- (107) Kirmizibekmez H., Calis I., Perozzo R., Brun R., Donmez A.A., Linden A., Ruedi P., Tasdemir D. Inhibiting activities of the secondary metabolites of *Phlomis brunneogaleata* against parasitic protozoa and plasmodial enoyl-ACP reductase, a crucial enzyme in fatty acid biosynthesis. *Planta Med.* **2004**, *70*, 711-717.
- (108) Tasdemir D., Brun R., Perozzo R., and Donmez A.A. Evaluation of antiprotozoal and plasmodial enoyl-ACP reductase inhibition potential of Turkish medicinal plants. *Phytotherapy Research.* **2005**, *19*, 162-166.
- (109) Tasdemir D., Guner N.D., Perozzo R., Brun R., Donmez A.A., Calis I., Ruedi P. Anti-protozoal plasmodial FabI enzyme inhibiting metabolites of *Scrophularia lepidota* roots. *Phytochemistry.* **2005**, *66*, 355-362.
- (110) Roberts C. W., Mcleod R., Rice D.W., Ginger M., Chance M.L., Goad L.J. Fatty acid and sterol metabolism: potential antimicrobial targets in apicomplexan and trypanosomatid parasitic protozoa. *Molecular and Biochemical Parasitology.* **2003**, *126*, 129-142.
- (111) Buckwitz, D., Jacobasch, G., Gerth, C., Holzhutter, H.G., and Thamm, R.A. Kinetic model of phosphofructokinase from *Plasmodium berghei*. Influence of ATP and fructose -6-phosphate. *Mol.Biochem. Parasitol.* **1998**, *27*, 225-232,
- (112) Kirmizibekmez H., Calis I., Perozzo R., Brun R., Donmez A.A., Linden A., Ruedi P., Tasdemir D. Inhibiting activities of the secondary metabolites of *Phomis brunneogaleata* against parasitic protozoa and plasmodial enoyl-ACP reductase, a crucial enzyme in fatty acid biosynthesis. *Planta Med.*, **2004**, *70*, 711-717.
- (113) Miclet, E. *et al.* NMR spectroscopic analysis of the first two steps of the pentose-phosphate pathway elucidates the role of 6-phosphogluconolactonase. *J. Biol. Chem.* **2001**, *276*, 34840-34846.
- (114) McConkey, G. A. Targeting the shikimate pathway in the malaria parasite *Plasmodium falciparum*. *Antimicrob. Agents Chemother.* **43**, **1999**, 175-177.
- (115) Roberts, F. *et al.* Evidence for the shikimate pathway in apicomplexan parasites. *Nature.* **1998**, *393*, 801-805.
- (116) Roberts, C. W. *et al.* The shikimate pathway and its branches in apicomplexan parasites. *J. Infect. Dis.* **2002**, *185*, (Suppl. 1), S25-S36.
- (117) Paulsen, I. T., Nguyen, L., Sliwinski, M. K., Rabus, R. & Saier, M. H. Jr. Microbial genome analyses: comparative transport capabilities in eighteen prokaryotes. *J. Mol. Biol.* **2000**, *301*, 75-100.
- (118) Dyer, M., Wong, I. H., Jackson, M., Huynh, P. & Mikkelsen, R. Isolation and sequence analysis of a cDNA encoding an adenine nucleotide translocator from *Plasmodium falciparum*. *Biochim. Biophys. Acta.* **1994**, *1186*, 133-136.
- (119) McIntosh, M. T., Drozdowicz, Y. M., Laroiya, K., Rea, P. A. & Vaidya, A. B. Two classes of plant-like vacuolar-type H<sup>+</sup>-pyrophosphatases in malaria parasites. *Mol. Biochem. Parasitol.* **2001**, *114*, 183-195.
- (120) Samuel B.U., Hearn B., Mack D., Wender P., Rothbard J., Kirisits M.J., Mui e., Wernimont S., Rice D.W., Prigge S.T Law A.B McLeod R. Delivery of antimicrobials into parasites. *PNAS.* **2003**, *25*, 14281-14286.
- (121) Fidock, A. D. *et al.* Mutations in the *P. falciparum* digestive vacuole transmembrane protein PfCRT and evidence for their role in chloroquine resistance. *Mol. Cell.* **2000**, *6*, 861-871.

- (122) Ferguson, M. A., and G. A. M. Cross. Myristylation of the membrane form of a *Trypanosoma brucei* variant surface glycoprotein. *J. Biol. Chem.* **1984**, 259, 3011-3015.
- (123) Rosenthal P.J. Antimalarial chemotherapy, mechanisms of action, resistance, and new directions in drug discovery. *Humana Press. Inc.* **2001** 15- 23, 87-100, 265-287.
- (124) Payne D.J. The potential of bacterial fatty acid biosynthetic enzymes as a source of novel antibacterial agents. *Drugs News Perspect.* **2004**, 17, 187-194.

**VITA**  
**Edinson Lucumi Moreno**

Permanent Address: 6285 Souder st. Philadelphia PA. 19149  
E-mail: ediluc@rocketmail.com

**EDUCATION**

MS, Biochemistry Texas A&M University College Station, Tx. December 2005  
Thesis: Structural Determination of Triclosan Derivatives as Inhibitors of  
*Plasmodium falciparum* Enoyl Reductase (PfENR) (Prof. Jim Sacchettini)

MS, Assay of Traditional Medicine, Universidad de Barcelona, Barcelona, Spain,  
2000. Thesis: Alkaloids Formation in Cell Suspension Cultures of  
*Tabernaemontana* Species after Feeding of Tryptamine and Loganin (Prof. Rob  
Verpoorte)

BS Chemistry, Universidad del Valle, Cali-Colombia, 1997  
Thesis: Screening for Secondary Metabolites with Anti malarial Activity of some  
Colombian Native Plants

**HONORS AND AWARDS**

Recipient of the 1999 scholarship to pursue a Master in “Assay of Traditional  
Medicine” whitening the METRA net, sponsored by the ALFA program from the  
European Community.

**SELECTED PUBLICATIONS**

- Joel S. Freundlich, John W. Anderson, Dimitri Sarantakis, Hong-Ming Shieh, Min Yu, Juan-Carlos Valderramos, **Edinson Lucumi**, Mack Kuo, William R. Jacobs, Jr, David A. Fidock, Guy A. Schiehser, David P. Jacobus and James C. Sacchettini., Synthesis, biological activity, and X-ray crystal structural analysis of diaryl ether inhibitors of malarial enoyl acyl carrier protein reductase. Part 1: 4'-Substituted triclosan derivatives. *Bioorganic & Medicinal Chemistry Letters*. Vol. 15, 23, 5247-5252, **2005**.
- **E. Lucumi**, A. Vera, D. Hallard, R van der Heijden and R. Verpoorte., Alkaloids Formation in Cell Suspension Cultures of *Tabernaemontana elegans* after Feeding of Tryptamine and Loganin or Secologanin, *Plant cell organ and tissue culture*, 68:293-299, **2002**.

**LANGUAGES**

Fluent in Spanish and English